Loss of the Histone Demethylase Phf8 Is Compatible With Development but Confers Resilience to Anxiety and Depression

Loss of the histone demethylase Phf8 is compatible with development but confers resilience to anxiety and depression

A dissertation presented

by

Ryan Michael Walsh

to

The Division of Medical Sciences

in partial fulfillment of the requirements

for the degree of

Doctor of Philosophy

In the subject of

Cell and Developmental Biology

Harvard University

Cambridge, Massachusetts

December 2015

Dissertation Advisor: Dr. Konrad Hochedlinger Author: Ryan Michael Walsh

Loss of the histone demethylase Phf8 is compatible with development but confers resilience to anxiety and depression

Abstract

Phf8 is a histone demethylase associated with human developmental disorders and cancer. Early studies of Phf8 in humans indicated that inactivating mutations in the gene were linked to syndromic intellectual disability with cleft lip and palate (Siderius syndrome). However, Phf8's functional role in regulating mammalian development and behavior has not been demonstrated. In this thesis I present my findings on a knockout mouse model of *Phf8*, which I have generated and characterized to interrogate Phf8's function in these processes in an *in vivo* mammalian system. Unexpectedly, I did not detect any gross physiological defects nor intellectual disability, but instead report here that mice null for *Phf8* are resilient to anxiety and depression. I further characterized the molecular nature of Phf8's role regulating mammalian behavior by performing RNA-seq on regions in the brain key to mediating anxiety disorders and depression. Here I find evidence that Phf8 directly regulates multiple serotonin receptors in the prefrontal cortex, which have a long standing link to anxiety disorders and depression, suggesting a likely mechanism for resiliency.

In addition to its proposed function in behavior and development, multiple studies have implicated Phf8 cancer. It has been suggested that Phf8 can behave as an oncogene, notably in

the case of T-ALL, where it cooperates with the Notch pathway and is required to drive tumor proliferation *in vitro* and in xenograft models. Within this thesis I will also present my findings on Phf8's function in the context of an *in vivo* model of T-ALL. I do not observe a requirement for Phf8 in T-ALL nor does its loss seem to at all impair the progression of T-ALL driven by a constitutively active Notch1. However, I do observe a subtle defect in T-cell development, which is likely consistent with its function in effecting Notch signaling. The data within this thesis represent the first characterization of a mammalian knockout model of *Phf8* and describe a novel role for this gene in the regulation of anxiety and depression.

TABLE OF CONTENTS

Chapter 1

Introduction

Histone modification and transcriptional regulation

Transcription in eukaryotes is controlled by the interplay between DNA and DNA-associated proteins, which together comprise the chromatin of a cell. The nucleosome, the basic structural subunit of chromatin, is formed by 146bp of DNA wrapped around the outside of a barrel-like histone octamer made up of an H3:H4 tetramer and two H2A:H2B dimers (Luger *et al*. 1997). The nucleosome, however, has functions beyond DNA-packaging as its structure and positioning is of prime importance to transcriptional regulation. One of the key mechanisms responsible for this transcriptional regulation stems from post-translational modifications covalently attached to the histones themselves (Li *et al 2007)*.

The four core histones all contain a compacted globular domain and an unstructured N-terminal tail, the latter of which is decorated with an array of post-translational modifications (Jenuwein & Allis 2001). Interestingly, these modifications are associated with specific functions, which can vary depending on their nature. Acetylation of lysine residues, for example, was the first of these post-translational modifications whose function was appreciated. Histone lysine acetylation leads to a relaxing of chromatin structure, likely facilitating access by transcription factors (Wade *et al*. 1997). Additionally, several histone residues (e.g. H3K9ac) serve as binding sites in the recruitment of co-activating factors (Dhalluin *et al*. 1999; Hassan *et al*. 2007). Accordingly, histone lysine acetylation tends to be associated with transcriptional activation (Li *et al*. 2007).

Methylation of lysine residues, on the other hand, can be associated with differing functions, depending on the specific lysine residue and the status of the surrounding residues. Presented here is a brief summary of the associated functions of such methyl-modifications relevant to this thesis; these include methylation of H3K4, H3K27, H3K9, and H4K20 (for a review of additional modifications see Li *et al*. 2007 and Kouzarides 2007). The divergent functions associated with histone lysine methylation can largely be attributed to the fact that these methylated residues serve as binding sites for diverse groups of chromodomain and plant homeodomain (PHD) finger containing proteins, so called "chromatin readers." One such modification, H3K4 trimethylation (H3K4me3), is typically associated with active promoters, as it acts as a binding site for transcriptional coactivator complexes containing histone acetyltransferase (Pary-Grant *et al*. 2005) and nucleosome remodeling (Li *et al*. 2006) activity. Conversely, methylation of H3K27, H3K9 and H4K20 are associated with gene repression. H3K27me3, for example, has an established role in the repression of transcription, at least in part through the direct recruitment of the polycomb repressor complex 1 (PRC1) (Fischle *et al*. 2003), which represses transcription likely through the compaction of chromatin and inhibition of chromatin remodeling complexes (Shao *et al*. 1999; Francis *et al*. 2001). H3K9 methylation is also associated with repression, with the di- and trimethylated forms serving as binding sites for heterochromatin protein 1 (HP1) (Bannister *et al*. 2001; Lachner *et al*. 2001), which allows for the oligomerization/compaction and silencing of heterochromatic regions (Nielsen *et al*. 2001). Though less extensively studied, H4K20me1/2 are also associated with the repression of transcription, likely through the recruitment of the chromatin-compacting factor L3mbtl1 (Trojer *et al*. 2007). Finally, it is of note that multiple modifications may often coexist at the

same loci, a well-characterized example being the co-occupancy of lineage-specific genes by H3K4me3 and H3K27me3 in undifferentiated cells (Bernstein *et al*. 2006; Mikkelsen *et al*. 2007). These so-called "bivalent" loci are repressed in undifferentiated cells and thought to be poised for activation once a differentiation program is initiated.

Regulation of histone modifications by histone demethylases

Several distinct families of proteins make up the histone acetyltransferases, deacetylases, methyltransferases and demethylases, which are the most recently described of this group. The first histone demethylase was discovered in 2004 when LSD1 was demonstrated to have demethylase activity with specificity for H3K4me1/2 as substrates (Shi *et al*. 2004). Demethylation by LSD1 is carried out by its amine-oxidase domain, which, due to the chemistry required for this reaction, is limited to demethylating only mono and dimethylated lysine groups. Several years after the discovery of LSD1, an additional class of demethylases was described, which contain a dioxygenase *jumonji C* (*JmjC*) domain (Tsukada *et al*. 2006; Klose *et al*. 2006; Whetstine *et al*. 2006). Unlike the amino-oxidase domain of LSD1, the *JmjC* domain has the capacity to demethylate tri-, di- and monomethylated histones, although additional, likely structural, constraints may limit this activity in many of the *JmjC* demethylases (Shi & Whetstine 2007). The mammalian *JmjC* family of histone demethylases contains 29 different proteins, which vary considerably in their substrate selectivity (Table 1.1) (Kooistra *et al*. 2012; Hojfeldt *et al*. 2013). Since their discovery, many members of this family of proteins have been linked to both mammalian development and disease (Nottke *et al*. 2009), although research into their precise roles in these processes remains ongoing.

Table 1.1 *JmjC* domain containing proteins. Shown are known *jmjC* domain containing proteins and their substrate specificity. Only validated histone substrates are listed. More closely related demethylases are grouped coded by color (alternating blue and white). Adapted from Kooistra *et al*. 2012 and Hojfeldt *et al*. 2013.

Gene Symbol	Histone Substrates	Additional Notes
Phf8	H3K9me1/2, H3K27me2, H4K20me1	
Kdm7a	H3K9me1/2, H3K27me1/2	
Phf2	H3K9me2	Requires Arid5b for catalytic activity
Kdm2a	H3K36me1/2	
Kdm2b	H3K4me3, H3K36me1/2	
Jmjd8	Not Determined	
Jmjd6	H3R2, H4R3	
Jmjd4	Not Determined	
Kdm8	H3K36me2	
Hspbap1	Not Determined	
Hif1an	Not Determined	
Jmjd7	Not Determined	
Hr	Not Determined	Non-canonical jmjC domain, may lack activity
Kdm3b	H3K9me1/2	
Kdm3a	H3K9me1/2	
Jmjd3	H3K27me2/3	
Utx	H3K27me2/3	
Uty	H3K27me2/3	Poor activity in vitro
Kdm4a	H3K9me2/3, H3K36me2/3, H1.4K26me2/3	
Kdm4c	H3K9me2/3, H3K36me2/3, H1.4K26me2/3	
Kdm4b	H3K9me2/3, H3K36me2/3, H1.4K26me2/3	
Kdm4d	H3K9me2/3, H3K36me2/3, H1.4K26me2/3	
Kdm5b	H3K4me2/3	
Kdm5c	H3K4me2/3	
Kdm5d	H3K4me2/3	
Kdm5a	H3K4me2/3	
Jarid2	Not Detected	Non-canonical jmjC domain, may lack activity
Mina	Not Detected	
NO66	H3K4me2/3, H3K36me2/3	

Functions and features of the histone demethylase Phf8

PHF8 was first described as a gene mutated in a set of patients with familial X-linked intellectual disability and cleft lip/palate (Laumonnier *et al*. 2005). Subsequent studies identified two additional mutations in the gene linked to intellectual disability (Abidi *et al*. 2007; Koivisto *et al*. 2007), suggesting a causative role. PHF8 has only two recognizable functional domains, a PHD finger, involved in mediating protein-protein interactions and a *JmjC* domain responsible for the catalysis of histone lysine demethylation. Intriguingly, all of the disorder associated mutations described for *PHF8* have been predicted to disrupt the function of the *JmjC* domain, suggesting that loss of demethylation activity is of key importance to the etiology of the disease.

Though the *JmjC* domain has the capacity to use trimethyl-lysine as a substrate, the *JmjC* domain of PHF8 has been shown to only have activity toward demethylating mono- and dimethyl lysine residues (Leonarz *et al*. 2010; Kleine-Kohlbrecher *et al*. 2010; Feng *et al*. 2010). The crystal structure of PHF8 indicates that this is due to a structural difference between the *JmjC* domain of Phf8 and that of tri-demethylases, which sterically prevents a third methyl from entering the active site (Horton *et al*. 2009). Interestingly, PHF8 has a rather broad substrate specificity compared to other demethylases, showing activity toward H3K9me1/2, H3K27me2, and H4K20me1 depending on whether histones or nucleosomes are used as a substrate (Leonarz *et al*. 2010; Kleine-Kohlbrecher *et al*. 2010; Feng *et al*. 2010). One report additionally demonstrated specificity for H3K36me2 (Leonarz *et al*. 2010); however this result has not been observed in follow-up studies (Kleine-Kohlbrecher *et al*. 2010; Feng *et al*. 2010). With the exception of H3K36me2, each of these modifications is associated with gene repression,

indicating that PHF8 acts predominantly as a coactivator of gene expression. Over-expression of PHF8 in cell culture has additionally been shown to cause global decreases in each of these modifications; interestingly, however, the substrate targeted varies based on the cell type analyzed (Liu *et al*. 2010; Leonarz *et al*. 2010; Kleine-Kohlbrecher *et al*. 2010; Feng *et al*. 2010). Thus, it is likely that PHF8's substrate specificity is context or cell type specific, perhaps depending on its interactions with additional proteins.

One such protein capable of interacting and modifying the function of PHF8 is, in fact, histone H3 itself. More specifically, PHF8 is capable of binding directly to H3K4me3 through its PHD finger (Horton *et al*. 2010); this is intriguing as it indicates that PHF8 functions as a chromatin reader in addition to being a chromatin modifier. Direct binding to H3K4me3 not only serves as a major mechanism for PHF8's recruitment to chromatin (Kleine-Kohlbrecher *et al*. 2010; Feng *et al*. 2010; Fortschegger 2010), but also alters the activity of the enzyme itself. PHF8 has a relatively poor activity toward demethylating H3K9me2 on peptide substrates, however, a striking increase – roughly 12 fold – in demethylation of H3K9me2 is observed when these peptides contain both H3K4me3 and H3K9me2 (Horton *et al*. 2010). Consequently, mutations to the PHD domain ablate its ability to activate transcription (Feng *et al*. 2010).

The primary cellular function of PHF8 appears to be the regulation of both cell growth and division. With respect to cell growth, PHF8 binds directly to ribosomal DNA, likely through recruitment by H3K4me3, and promotes transcriptional activation by catalyzing the removal of H3K9me1/2 (Feng *et al*. 2010; Zhu *et al*. 2010). PHF8 further functions to regulate cell cycle progression by being directly recruited to E2F1 target sites, where it demethylates HK20me1, serving as a coactivator for genes required for cell cycle progression (Liu *et al*. 2010). This

activity is regulated in a cell cycle dependent manner whereby Cdk1-mediated phosphorylation leads to Phf8's dissociation from the chromatin and M-phase progression (Liu *et al*. 2010). Knockdown of PHF8 in cell culture leads to a reduction in the transcription of both rRNA and E2F1 targets, causing a slight accumulation of cells in the G1 & M phases of the cell cycle and a subtle decrease in cellular division rates (Liu *et al*. 2010; Feng *et al*. 2010).

At a genome wide level, PHF8 has a rather large number of targets aside from rDNA and genes involved in cell-cycle progression. Depending on the cell type analyzed, ChIP-seq and ChIP-ChIP data suggest that PHF8 targets between 7,000 and 14,000 loci (Kleine-Kohlbrecher *et al*. 2010; Liu *et al*. 2010; Fortschegger *et al*. 2010; Qi *et al*. 2010; Wang *et al*. 2014). PHF8 is found primarily enriched around the transcription start site, though, enrichment is also seen within gene bodies and in intergenic regions (Kleine-Kohlbrecher *et al* 2010; Qi *et al*. 2010; Liu *et al*. 2010; Fortschegger *et al*. 2010). Of note, PHF8 binding sites show extensive overlap with H3K4me3, likely due to direct binding by the PHD domain. However, binding at non-H3K4me3 loci also occurs with a frequency of 5% to 20% depending on the cell type (Kleine-Kohlbrecher *et al*. 2010; Fortshegger *et al*. 2010; Liu *et al*. 2010), suggesting additional mechanisms by which PHF8 is recruited to chromatin.

In spite of PHF8's extensive list of genic target loci, knockdown of PHF8 leads to very subtle changes in gene expression, with only between 5% and 7% of PHF8-bound transcripts becoming misregulated (Fortschegger *et al*. 2010; Wang *et al*.2014). The majority – roughly two thrids – of these misregulated genes become downregulated following PHF8's knockdown *in vitro*. Surprisingly, however, analysis of PHF8 binding among the misregulated genes shows relatively equal enrichment at promoters of down- and upregulated genes, with around 60%

being bound by PHF8 in either case (Fortschegger *et al*. 2010; Wang *et al*. 2014). The fact that strength of PHF8 binding at a locus is not a good indicator of whether or not it will be down- or upregulated following PHF8 loss is surprising given PHF8's substrate specificity and suggests that PHF8 may have additional functions as a transcriptional repressor. In keeping with this notion, PHF8 co-occupies promoters with the silencing factor REST, though a direct interaction has not yet been demonstrated (Wang *et al*. 2014). Additionally, PHF8 is found in complexes with the repressive H3K4me1/2 demethylase LSD1 (Yatim *et al*. 2012), further indicating it may act as a transcriptional repressor.

In summary, the molecular studies of PHF8 to date indicate a number of interesting features. PHF8's ability to bind H3K4me3 not only provides a mechanism of recruitment, but also allosterically activates its demethylase activity, allowing it to adjust to the local chromatin structure at target loci. PHF8's preference toward H3K9me1/2, H4K20me1 and H3K27me2 and a number of functional experiments in cell culture support its role in transcriptional activation, although it also appears to have a context-dependent repressive function. The relatively small changes in gene expression observed on PHF8 loss suggest that despite the large number of genomic targets, PHF8 plays only a modest role in gene regulation.

Phf8's role in development

Initial insights into PHF8's function during development came from human genetics studies linking it to intellectual disability and cleft lip/palate (Laumonnier *et al*. 2005; Abidi *et al*. 2007; Koivisto *et al*. 2007). The first animal study describing a mutation of *PHF8* was a loss of function mutation for the gene *F29B9.2* in *C. elegans* (Kleine-Kohlbrecher *et al*. 2010). *F29B9.2*

displays *in vitro* demethylation activity toward H3K9me2 and H3K27me2 and represents one of two sequences in *C. elegans* homologous to Phf8's family of proteins, which includes Phf8, Phf2, and Kdm7a (Shi & Whetstine 2007). RNAi mediated knockdown of *F29B9.2* leads to locomotion defects, which are rescued by re-expressing *F29B9.2* from a pan-neuronal promoter (Kleine-Kohlbrecher *et al*. 2010). This phenotype indicated a role for *F29B9.2* in controlling *C. elegans* behavior, however it is not clear which member of Phf8's family this models as all three are expressed in the brain/neurons and have H3K9me2/H3K27me2 demethylation activity (Kleine-Kohlbrecher *et al*. 2010; Qiu *et al*. 2010; Huang *et al*. 2010; Baba *et al*. 2011; Hasenpusch-Theil *et al*. 1999).

Additional evidence suggesting that Phf8 has a non-redundant role in development has been provided from morpholino oligonucleotide (MO) knockdown experiments in zebrafish. Interestingly, MO-mediated knockdown of the single Phf8 homolog in zebrafish, zPHF8, leads to both craniofacial defects and additional complications in the central nervous system (CNS) (Qi *et al*. 2010). Specifically, zPHF8 morphants do not develop a lower jaw and have under developed pharyngeal arches, potentially analogous to the cleft palates observed in human patients. Moreover, zPHF8 morphants display increased apoptosis within the CNS during development, further supporting a possible role in neural development. These phenotypes were linked to dysregulation of the transcription factor *msxb*, whose mRNA was able to partially rescue the craniofacial and CNS defects in morphants. While these results certainly implicate PHF8 in animal development, additional genetic studies are required to determine PHF8's role specifically in mammalian development and in regulating more complex behaviors.

Functions of PHF8 in cancer

Emerging roles of Phf8 in tumorigenesis

Apart from its involvement in craniofacial development and the central nervous system, PHF8 appears to be associated with multiple types of cancer. For example, PHF8 has been implicated in prostate cancer, T-cell acute lymphoblastic leukemia (T-ALL), acute promyelocytic leukemia (APL), esophageal squamous cell carcinoma, non-small cell lung cancer (Bjorkman *et al*. 2012; Yatim *et al*. 2012; Arteaga *et al*. 2013; Sun *et al*.2013; Shen *et al*. 2014). PHF8's role in governing cell growth and division would provide a plausible mechanism by which it contributes to malignant growth. Although this does indeed appear to be the case in prostate cancer and esophageal squamous cell carcinoma, PHF8's function in other forms of cancer has proven to be more complicated. In APL, for example, PHF8 seems to mitigate tumor resistance upon treatment with all-*trans* retinoic acid *in vitro* and *in vivo* by promoting activation of RARα target genes and granulocyte differentiation (Arteaga *et al*. 2013), suggesting that PHF8 actually behaves as a tumor suppressor here. This example, however, is rather unique, with PHF8 behaving as an oncogene in all other cancers it has been linked to thus far. While much remains unknown about its role in driving cancer, the best lines of evidence in support of PHF8's oncogenic potential have come from studies of its role in prostate cancer and T-ALL.

Phf8 regulates extracellular matrix and motility in prostate cancer

The first evidence to suggest that PHF8 has a function in cancer came from an siRNA screen of epigenetic factors in prostate cancer cell lines (Bjorkman *et al*. 2012). PHF8 was the

only validated demethylase that reduced proliferative capacity of the cancer cell lines *in vitro* and was found to be significantly over-expressed in primary tumors when compared to normal prostate tissue. Additionally, it was later demonstrated that PHF8 knockdown in these cell lines significantly reduces, but does not completely ablate, their ability to form tumors in an *in vivo* xenograft model (Ma *et al*. 2015).

Interestingly, PHF8 may have multiple functions in prostate cancer. Expression of PHF8 in primary prostate tumors is correlated with the expression of multiple genes involved in cytoskeletal regulation and cell motility (Bjorkman *et al*. 2012). Accordingly, PHF8 knockdown in prostate cancer cell lines results in reduced motility and colony forming potential in 3D culture (Bjorkman *et* al. 2012). This finding could indicate that Phf8 is involved in controlling invasion and metastasis, however further studies will be needed to determine the nature of this regulation *in vitro* as well as its validity *in vivo*. It remains unclear how PHF8 knockdown contributes to the reduced growth rates observed in prostate cancer cell lines. For example, one study observed extensive apoptosis following PHF8 knockdown (Ma *et al*. 2015) while another study detected a slight reduction in the fraction of cells in S-phase but without a significant increase in apoptosis (Bjorkman *et al*. 2012), similar to what has been reported for PHF8 knockdown in untransformed cell lines (Liu *et al*. 2010; Feng *et al*. 2010). Though additional clarification is needed, these lines of evidence were some of the first to link PHF8 to the development of cancer.

Phf8 cooperates with Notch1 to drive T-ALL

T-ALL is a highly aggressive hematological cancer propagated by the expansion of immature T-cell lymphoblasts (Grabher *et al*. 2006). Activity of the Notch pathway is central to

the development of the disease in mice and humans; activating mutations in *NOTCH1* are found in over 50% of human patients and expression of constitutively active *Notch1* in the bone marrow is sufficient to cause T-ALL in mice (Weng *et al* 2004; Pear *et al*. 1996). Under normal, homeostatic conditions, activation of the Notch pathway plays a central role in T-cell development, being required for T-cell specification, proliferation and survival in the thymus (Yashiro-Ohtani *et al*. 2010). In T-ALL, hyper-activation of this pathway leads to an aberrant expansion of CD4/CD8 double positive T-cell progenitors within the thymus, which rapidly spreads to the peripheral blood and tissues (Grabher *et al*. 2006). Notch's oncogenic activity is driven in large part through its intracellular domain (ICN), which is freed from the plasma membrane and translocates to the nucleus upon activation (Kopan & Ilagan 2009). In the nucleus, ICN cooperates with a co-activator complex, which includes MAML and CSL to trigger direct transcriptional activation of target genes (Kopan & Ilagan 2009). In an attempt to identify additional cofactors important for Notch target gene activation and tumorigenesis, Yatim and colleagues (2012) immunoprecipitated the ICN-MAML-CSL complex from human T-ALL cell lines. Among the ICN interacting partners identified in this study were several chromatin-modifying proteins, including PHF8.

Importantly, PHF8 was found to be recruited to key NOTCH1 target genes where it was required for H3K9me1/2 and H3K27me2 demethylation and efficient activation of transcription (Yatim *et al*. 2012). Knockdown of PHF8 in these cell lines reduced the expression levels of multiple NOTCH target genes. Notably, this silencing phenotype was rescued by re-expression of full-length PHF8, but not by a catalytically dead mutant, nor full-length PHF8 in the presence of a NOTCH inhibitor. This indicates that PHF8's demethylase activity is critical for activating

NOTCH targets and that it is capable of responding to NOTCH signaling within the cell. PHF8's role in affecting NOTCH signaling during T-ALL was further demonstrated by showing that knockdown of PHF8 with a single shRNA reduces the proliferation rates of T-ALL lines *in vitro* and renders them incapable of forming tumors in a xenograft model. These results not only suggested that Phf8 may play a crucial role in the tumorgenicity of T-ALL, but also identified ICN as one of only a handful of non-general transcription factors known to be capable of recruiting PHF8 to specific loci. Whether or not Phf8 can contribute to T-ALL in a non-xenograft *in vivo* model, however, remains an open question. These observations also raise the interesting possibility that Phf8 may be required for normal thymocyte development, given its apparent role in Notch signaling and the fact that it is highly expressed within the thymus (Suppl. Fig. 1).

Pathways involved in anxiety, depression and resilience in mammals

---

Prevalence and features of anxiety and depression

Anxiety disorders and depression represent very serious and debilitating conditions; depression is the leading cause of years lost to disability worldwide, while anxiety disorders rank fifth (Vos *et al*. 2012). Annually, 18% and 7% of US adults suffer from anxiety disorders and depression, respectively (Kessler *et al*. 2005; SAMHSA, 2013). One major factor contributing to these statistics is the lack of effective treatments. The response of patients to available antidepressant medications is poor, an estimated remission rate as low as 30% (Trivedi *et al*. 2006). Response rates in the treatment of anxiety disorders are generally higher, however, there remain between 15% and 40% of patients for which current treatments are unable to

provide an alleviation of symptoms (Bystritsky 2006). These shortcomings emphasize the importance of research into the mechanisms and causes of these syndromes in order to identify new targets and develop new treatments.

Anxiety disorders, which include posttraumatic stress disorder (PTSD), panic disorder, social anxiety disorder and general anxiety disorder, are characterized by unwarranted fear in benign situations (Shin & Liberzon 2010), while the hallmarks of depression include a negative world- and self-view, increased sensitivity to negative psychological feedback, and an inability to experience pleasure (Willner *et al*. 2013). Though anxiety and depression represent distinct psychiatric disorders with differing clinical manifestations, they occur with a staggering degree of comorbidity – by some estimates as high as 90% (Kessler *et al*. 1994; Gorman 1996). Additionally, there is a significant overlap between both the neural circuitry involved in controlling these disorders and the types of effective treatments (Ressler & Mayberg 2007).

Neural circuits controlling anxiety and depression

Our understanding of the multitude of inputs that contribute to the development of anxiety disorders and depression is derived from fMRI studies in human patients as well as genetic animal models. Together, these studies have helped define the corticolimbic neural networks involved in development and potentiation of each of these disorders, which will be summarized here. In the case of anxiety, the signaling circuits are closely linked to those that control fear (Davis *et al*. 2010). The *amygdala*, the fear center of the brain, integrates sensory information with additional inputs and cross-talk from forebrain structures, most notably, the *prefrontal cortex* and *hippocampus* (Tovote *et al*. 2015). When activated, the amygdala outputs

to the hypothalamus, activating the *hypothalamus-pituitary-adrenal* axis, which ends in the systemic release of the stress-associated hormone cortisol/corticosterone (Willner *et al*. 2013). In a healthy individual, this circuit functions to elicit a fear in response to threatening stimuli. However, in anxiety disorder patients, a misregulation of this circuit leads to a sustained activation of the amygdala resulting in a fear-like response in the absence of a real threat (Davis *et al*. 2010). Interestingly, the same regions also participate in the signaling network of depression, which further includes the *ventral tegmental area* and the *nucleus accumbens*, the reward center of the brain. The nucleus accumbens is the largest component of the *ventral striatum,* which integrates signals from the prefrontal cortex, hippocampus, and ventral tegmental and its output is responsible for reward anticipation and seeking positive outcomes (Willner *et al*. 2013). In cases of depression, this activity of the nucleus accumbens appears dampened in response to rewarding stimuli (Pizzagalli *et al*. 2009; Robinson *et al*. 2012). Conversely, the amygdala is hyperactive in depressed patients, activity which is linked to the heightened response to negative stimuli (Sheline *et al.*2001; Siegle *et al*. 2002).

Molecular pathways contributing to anxiety and depression

An additional similarity between anxiety disorders and depression is that they both seem to result from a maladaptive response to stressful life events (Heim & Nemeroff 1999). When faced with such a stressor, some individuals are capable of successfully coping while others develop either an anxiety disorder or depression. The understanding of the mechanisms which mediate this coping response, referred to as resiliency (Charney 2004; Rutter 2006), could be of prime importance in identifying future treatments. Resiliency is influenced by both

environmental and genetic factors, the identification of which is an area of active research. In rodents and humans, resiliency appears to be an adaptive process associated with molecular changes in key regions of the brain (Krishnan *et al*. 2007). Studies on human patients, which are typically limited to circulating factors (i.e. hormones), have elucidated a number of molecular pathways implicated in this process. However, the majority of these findings are associations, still awaiting confirmation in animal models.

Considerable effort has been put into identifying genetic causes and contributors to anxiety and depression. Though the field has been hindered by inconsistencies between studies from both candidate gene approaches and genome wide association studies (Cohen-Woods *et al*. 2013), a few promising molecular pathways have emerged. These pathways, which will be summarized below, include glucocorticoid signaling, neuropeptide Y (NPY) signaling, BDNF signaling, and, notably, the serotonin signaling pathway (Cohen-Woods *et al*. 2013; Flint & Kendler 2014; Gatt *et al*. 2014).

Serotonin signaling in anxiety and depression and anxiety disorders

The serotonin signaling pathway has long been linked to anxiety and depression as selective serotonin reuptake inhibitors (SSRIs), which act to potentiate serotonin signaling at the synapse, are the most commonly prescribed treatment for both anxiety disorders and depression (Vaswani *et al*. 2003). More recently, multiple genes in this pathway have been linked to depression through analysis of common genetic variants in genome-wide association studies (GWAS), including the serotonin transporter *SLC6A4* (Furlong *et al*. 1998; Anguelova *et al*. 2003; Lasky-Su *et al*. 2005; Lopez-Leon *et al*. 2008; Clarke *et al*. 2010) along with the

serotonin receptors *HTR1A* (Lopez-Leon *et al*. 2008; Kishi *et al*. 2009; Kishi *et al*. 2013), *HTR2A* (Anguelova *et al*. 2003; Lopez-Leon *et al*. 2008; Jin *et al*. 2013) and *HTR1B* (Lopez-Leon *et al*. 2008). On the molecular side, the study of post-mortem tissues from depressed suicide victims has indicated a decrease in serotogenergic projections to the prefrontal cortex (Austin *et al*. 2002). Additionally, patients suffering from depression or panic disorder display significantly reduced levels of the 5-HT1A receptor (the gene product of *Htr1a*) in the prefrontal cortex (Drevets *et al*. 2000; Lopez-Figueroa *et al*. 2004; Moses-Kolko *et al*. 2008; Neumeister *et al*. 2004). Similar results have been observed for 5-HT2A (*HTR2A)* (Attar-Levy *et al*. 1999; Yatham *et al*. 2000; Lopez-Figueroa *et al*. 2004; Mintun *et al*. 2004). However, some conflicting results with respect to 5-HT2A binding potential have been reported (Meyer *et al*. 2003; Bhagwagar *et al*. 2006), possibly owing to medications the patients were taking at the time (Savits & Drevets 2013). Finally, expression of the 5-HT1B receptor, though less extensively characterized in these contexts, is reduced in the ventral striatum/nucleus accumbens and pallidum of patients suffering from depression (Murrough *et al*. 2013). Though conclusions on the functional nature of the role of serotonin signaling in anxiety and depression cannot be drawn from these data alone, they argue that the prefrontal cortex and hippocampus likely have blunted serotonin signaling in the context of these diseases.

Studies in animal models of anxiety and depression have shed additional light on the function of the serotonin transporter and receptors in these disorders. First, mice deficient for either *Slc6a4* or *Htr1a* display increased signs of anxiety and depression across a panel of assays (Lira *et al*. 2003; Zhuang *et al*. 1999). Importantly, restoration of the 5-Ht1a receptor solely in the excitatory neurons of the cortex and hippocampus of the *Htr1a* knockout mouse is

sufficient to rescue the anxiety and depression phenotypes (Gross *et al*. 2002), suggesting that serotonin signaling specifically in these regions is responsible for the disorder. Additionally, overexpression of *Htr1a* produces the opposite phenotype, conferring resilience to anxiety and depression in mice (Kusserow *et al.*2004). Conversely, loss of either *Htr1b* or *Htr2a* reportedly confers resilience (Zhuang *et al*. 1999; Weisstaub *et al*. 2006). Though these results may appear contradictory to the human observations, receptor-specific agonists for 5-Ht1b and 5-Ht2a can also cause resiliency in rodents (Onaivi *et al*. 1995; Ripoll *et al*. 2005; Ripoll *et al*. 2006), indicating that precise levels of receptor signaling are important in depression and anxiety and that the hyperactivity of either of these receptors also has the potential to impart resiliency. Although the underlying mechanisms are not fully understood, a wealth of genetic and pharmacologic evidence from both humans and rodents has implicated serotonin signaling and these serotonin receptors in anxiety disorders and depression.

Additional molecular mechanisms regulating anxiety disorders, depression and resiliency

Though they will not be the focus of this thesis, a number of additional pathways and mechanisms have been linked to anxiety, depression and resiliency, which will be briefly summarized here. One such pathway, the *hypothalamic-pituitary-adrenal* (HPA) axis, lies at the center of the body's stress response (Herman *et al*. 1997). A major output of the HPA axis is the release of multiple glucocorticoid hormones, a few of which have been directly linked to anxiety disorders and depression. For example, examination of cortisol releasing hormone, cortisol, and dehydroepiandrosterone in human plasma and cerebrospinal fluid has revealed a correlation between each of these hormones and posttraumatic stress disorder (PTSD) or

depression (Bremner *et al*. 1997; Baker *et al*. 1999; Yehunda *et al.* 2006a; Stetler & Miller 2011). Aside from the HPA-released hormones, low plasma levels of testosterone have been reported in male patients suffering from either PTSD (Mulchahey *et al*. 2001) or major depressive disorder (Pope *et al*. 2003). Further, men suffering from treatment-resistant depression supplemented with testosterone displayed an alleviation of symptoms (Pope *et al*. 2003), suggesting a protective role for this hormone. Finally, there is evidence to suggest that the peptide-neurotransmitter NPY may also contribute to both depression and anxiety disorders. It has been demonstrated that patients with treatment-resistant major depression display reduced NPY levels in cerebrospinal fluid (Heilig *et al*. 2004). Further, combat exposed veterans with PTSD show reduced levels of NPY when compared to those did not develop PTSD, indicating that NPY may be actively involved in conferring resilience here (Yehuda *et al*. 2006b).

Animal models of resiliency

A functional characterization of the pathways involved in anxiety disorrdres, depression and, importantly, resiliency holds the potential for the development of novel treatments. Animal models have provided us with a number of insights into the molecular nature of these processes, functionally defining roles for a number of novel proteins acting here. Of the more significant of these is BDNF, which has also been associated with major depression by one genome wide association study (Verhagen *et al*. 2010), but not in independent studies (Lopez-Leon *et al*. 2008, Gyekis *et al*. 2013). In mice, BDNF signaling to the nucleus accumbens from the ventral tegmental area is found to be increased specifically in animals susceptible to anxiety and depression when compared to a subset of animals, which were found to be spontaneously

resilient (Krishnan *et al*. 2007). Moreover, knockdown of BDNF in the VTA leads to the acquisition of resiliency in mice, highlighting the importance of BDNF signaling from the VTA to the nucleus accumbens in these disorders (Krishnan *et al*. 2007). Differing expression patterns within the nucleus accumbens itself have also been shown to contribute to resiliency (Vialou *et al*. 2010; Wilkinson *et al*. 2011). For example, forced expression of the transcription factor ΔFosB or it's transcriptional target GluR2 specifically in the nucleus accumbens is sufficient to push susceptible mice toward resiliency (Vialou *et al*. 2010).

A role in resiliency has been attributed to neurons in the prefrontal cortex as we;;, where increased neuronal activity was observed specifically in resilient animals (Krishnan *et al*. 2007; Adamec *et al*. 2012). This finding has been functionally linked to resiliency via direct optogenetic activation of the neurons in the prefrontal cortex, which is capable of reducing depression-associated behaviors (Covington *et al*. 2010). In spite of all of these findings, however, our understanding of the complex processes that play into anxiety disorders, depression and, importantly, resiliency is far from complete. Expanding our knowledge of the pathways involved in these disorders could be fundamental in improving available treatment options.

Chapter 2

The role of Phf8 in murine behavior and development

Contributing Authors

Ryan M. Walsh, Erica Y. Shen, Anthony Anselmo, Yan Jiang, John Chen, Ruslan Sadreyev, Schahram Akbarian and Konrad Hochedlinger.

Attributions

Behavioral experiments were done by Erica Shen in the lab of Schahram Akbarian. Yan Jiang assisted with the dissections for RNA-seq. RNA library preparation and RNA-seq was performed by the Tufts Genomics core (TUCF). Anthony Anselmo performed the bioinformatics analysis of the RNA-seq data in the lab of Ruslan Sadreyev. The MRI was performed and analyzed by John Chen. I designed and performed all other experiments.

Abstract

Phf8 is an X-linked histone demethylase capable of catalyzing the demethylation H3K9, H3K27 and H4K20. Mutations of *PHF8* have been found in patients with X-linked mental retardation and cleft lip/palate. Transient suppression of Phf8 expression in zebrafish reportedly causes craniofacial and central nervous system abnormalities during development. However, the functional role of Phf8 in mammalian development and physiology remains unexplored. Here, we examined the biology of Phf8 in developing and adult mice by generating the first mammalian knockout model. Unexpectedly, *Phf8* deficient mice do not display obvious developmental defects, are born at Mendelian ratios and survive to adulthood. While we failed to detect signs of intellectual disability, we uncovered a striking resilience to anxiety and depression upon loss of *Phf8*. Expression analysis of mutant mice revealed a misregulation of serotonin signaling within the prefrontal cortex. Moreover, we show that Phf8 directly binds to regulatory regions of the serotonin receptor genes *Htr1a*, *Htr1b* and *Htr2a* in the neocortex, providing a molecular explanation for the observed behavioral phenotype. Our results clarify the functional role of Phf8 in mammalian development and adult behavior and establish a direct link between Phf8 expression and serotonin receptor regulation.

Introduction

Phf8 has been predominantly studied as a transcriptional activator through its ability to demethylate the repressive histone modifications H3K9me1/2, H3K27me2 and H4K20me1

(Kleine-Kohlbrecher *et al*. 2010; Feng *et al*. 2010; Loenarz *et al*. 2010). More recent data indicate that Phf8 may also repress transcription of certain target genes, although the underlying mechanisms remain unknown (Wang *et al*. 2014). In addition to its role as a histone demethylase, Phf8 functions as a chromatin reader by directly binding H3K4me3 through a pocket in its PHD domain, enabling recruitment to chromatin (Feng *et al*. 2010; Kleine-Kohlbrecher *et al*. 2010).

Mutations in *PHF8* have previously been identified in a subset of patients with X-linked intellectual disability, which is often accompanied by cleft lip/palate (Laumonnier *et al*. 2005), suggesting a causative role. Molecularly, Phf8 directly binds to ribosomal DNA and E2F1 targets in HeLa and U2OS cells (Feng *et al*. 2010; Fortschegger *et al*. 2010; Chen *et al*. 2010; Liu *et al*. 2010), facilitating their activation. Accordingly, knockdown of Phf8 in these cell lines results in a cellular growth defect. However, it remains unclear whether defects in cellular proliferation also underlie the observed behavioral symptoms in patients. Notably, suppression of a homolog of the PHF family of demethylases reportedly leads to behavioral abnormalities in *C. elegans* (Kleine-Kohlbrecher *et al*. 2010). Moreover, morpholino-mediated knockdown of Phf8 in zebrafish results in the development of brain and craniofacial abnormalities, in part through direct regulation of the *msxb* gene, which is functionally involved in craniofacial development (Qi *et al*. 2010).

Phf8's role in mammalian development and behavior, however remains unexplored. Moreover, studies on Phf8 in cultured mammalian cells have thus far been confined to shRNA-mediated approaches, which may exhibit off-target effects not observed in a knockout (Welstead *et al*. 2012). To overcome these limitations and investigate the biological role of Phf8

in a mammalian organism, we generated and analyzed the first *Phf8* knockout (KO) mouse model.

Results

Generation of a Phf8 knockout allele

To generate a knockout (KO) allele, we introduced *loxP* sites flanking exons 7 and 8 of the *Phf8* locus by conventional targeting in embryonic stem cells (ESCs). We chose those exons as they encompass roughly half of the catalytic JmjC domain, including a highly conserved histidine residue essential for the demethylation function of Phf8 (Qi *et al*. 2010) (Fig. 2.1a). Moreover, Cre-mediated deletion of these exons is expected to cause a frameshift mutation and thus a nonfunctional protein. Briefly, the *Phf8* targeting construct was electroporated into V6.5 ESCs, exposed to drug selection, and correctly targeted clones were subsequently identified by Southern blot analysis. Verified clones were then electroporated with a plasmid transiently expressing Cre recombinase to generate *Phf8* KO ESCs (Fig. 2.1b).

We confirmed loss of Phf8 in these cells by Western blot analysis and RNA-sequencing (Fig. 2.1c&d). Notably, examination of H3K9me1/2, K3K27me2 and K4K20me1 levels in Phf8 KO and control ESCs using Western blot analysis failed to show significant differences, indicating that loss of *Phf8* does not lead to a global misregulation of these covalent modifications (Fig. 2.1e).

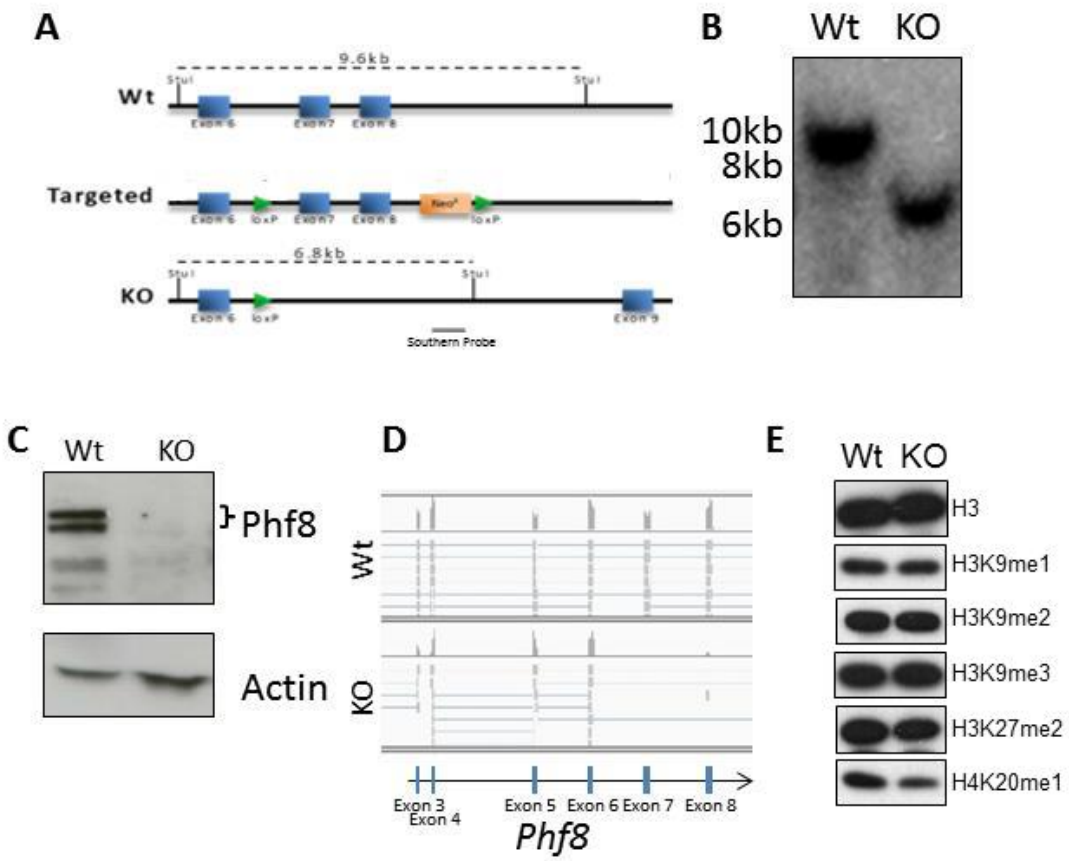

Figure 2.1 Generation of a *Phf8* null allele. A) Diagram of genomic *Phf8* around exons 7 and 8 for wt (top), targeted (middle) and KO (bottom) alleles. B) Southern blot of *Phf8* KO genomic DNA, note the appearance of the 6.8kb band indicated in A. C) Western blot of Phf8 from wt and KO ESCs. D) RNA-seq tracks from *Phf8* KO and wt ESCs, note missing exons 7 and 8 in the KO. E) Western blot showing no difference in global histone methylation levels in the *Phf8* KO.

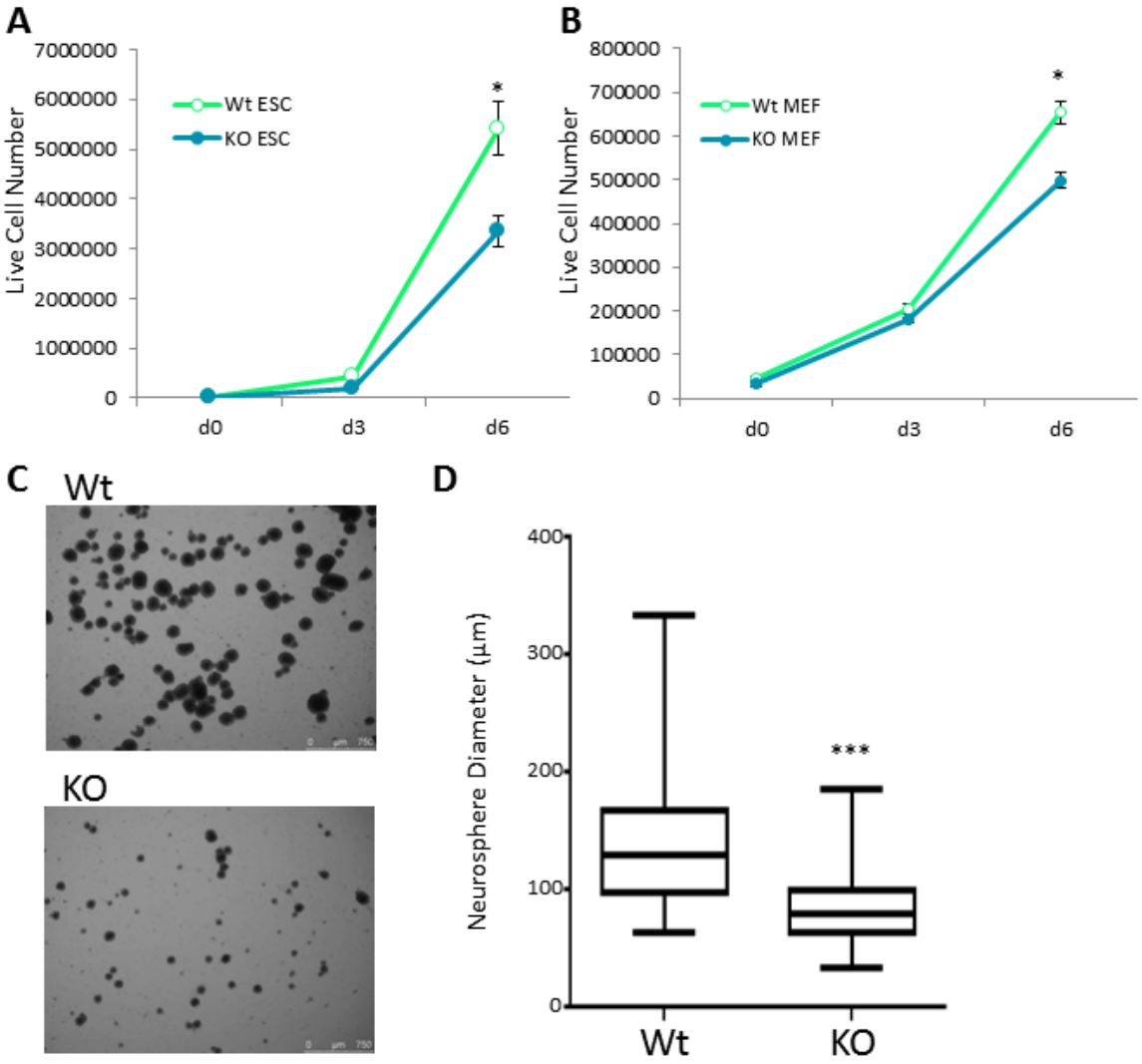

Figure 2.2 Reduced proliferation in both differentiated and undifferentiated primary cells null for *Phf8*. A) Growth curve for *Phf8* wt and KO ESCs. B) Growth curve for *Phf8* wt and KO MEFs. C) Representative images of *Phf8* wt and KO neurospheres grown for 1 week from single cell suspensions. D) Quantification of neurosphere diameter after 1 week of growth from a single cell suspension. *=p<0.05, ***=p<0.001

Loss of Phf8 impairs cell growth in cultured stem, progenitor and differentiated cells

Knockdown of Phf8 reportedly causes growth defects in transformed cell lines. To assess whether this phenotype is also seen in primary cells lacking the endogenous *Phf8* gene, we determined growth rates of *Phf8*-deficient embryonic fibroblasts (MEFs), neural progenitor cells (NPCs) and ESCs. Deletion of *Phf8* impaired the proliferation potential of MEFs, NPCs and ESCs compared to wild type controls, suggesting that this histone demethylase regulates growth potential in vitro in multiple primary cell types regardless of differentiation stage and tissue origin (Fig. 2.2a-d). It is worth mentioning that despite the subtle proliferation defect, Phf8-/- NPCs and ESCs were capable of continuous self-renewal in the presence of appropriate cytokines (data not shown).

To identify possible downstream regulators of Phf8 that may cause the observed proliferation defect, we performed RNA-sequencing of Phf8-deficient and wild type NPCs and ESCs. Surprisingly, loss of *Phf8* did not lead to major expression differences between *Phf8* KO and WT ESCs and NPCs, and unbiased hierarchical clustering was unable to separate samples by genotype (Fig. 2.3a). However, a closer inspection of differentially expressed genes revealed a slight downregulation of multiple cell cycle regulators, including *Rbl1, Ccnb2* and *Aurka* (Fig. 2.3b&c), thus providing a potential explanation for the observed growth deficit.

Phf8 KO mice are viable and do not show developmental defects or clefting

Given the reported brain and craniofacial defects in Phf8 knockdown zebrafish embryos and the association between *PHF8* mutations and cleft/palate in patients, we next asked whether *Phf8* KO mice are born at sub-Mendelian ratios due to developmental defects or

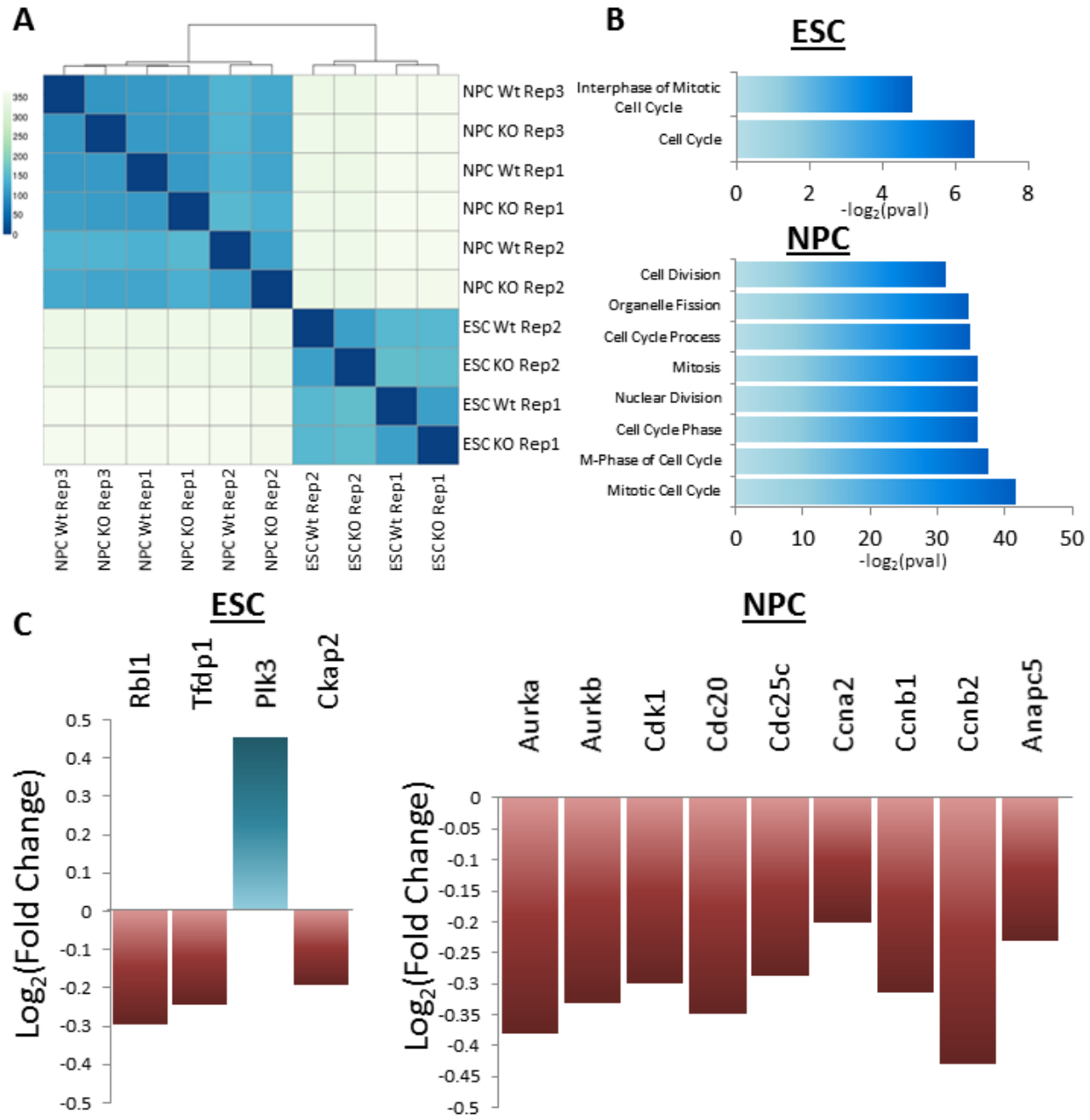

Figure 2.3 RNA-seq identifies only subtle defects related to cell cycle in *Phf8* KO ESCs and NPCs. A) Unbiased hierarchical clustering of *Phf8* wt and KO ESCs and NPCs. B) Enriched GO terms among differentially expressed gene sets for ESCs and NPCs. C) Genes related to cell cycle and growth misregulated in the *Phf8* KO ESCs (left) and NPCs (right), only very subtle differences were observed.

A

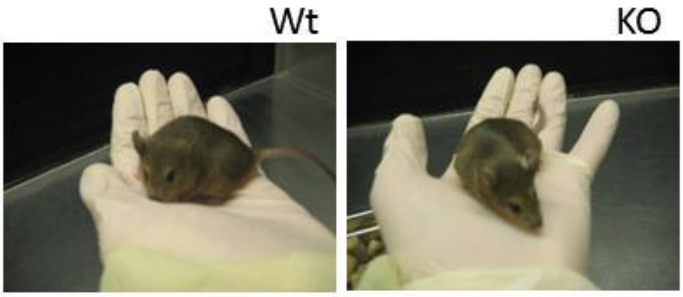

B

$Phf8^{+/-}$ x $Phf8^{+/Y}$

Genotype	$Phf8^{+/+}$ $Phf8^{+/Y}$	$Phf8^{KO/+}$	$Phf8^{KO/Y}$
Total	84	46	41
% Observed	49.1	26.9	24
% Expected	50	25	25

C

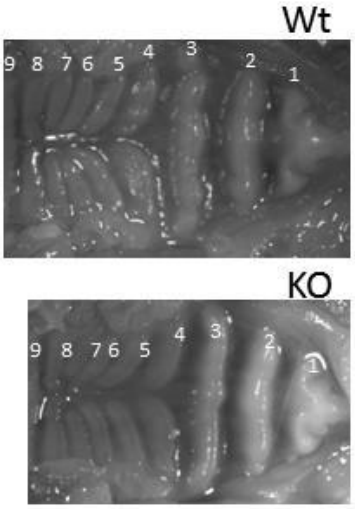

D

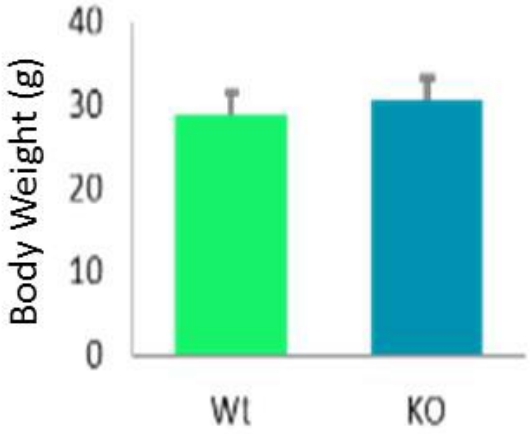

Figure 2.4 No gross physiologic defects observed in *Phf8* KO mice. A) *Phf8* wt (left) and KO (right) mice are indistinguishable from each other. B) Summary of the distribution of genetypes observed from live births in a cross between a $Phf8^{+/-}$ dam and a $Phf8^{+/Y}$ sire. *Phf8* KO mice are born at the expected Mendelian ratios. C) Representative images of the palates from *Phf8* wt (n=3) and KO (n=5) mice. D) No difference in body weight seen between adult (2 month old) *Phf8* wt and KO (n=3) mice.

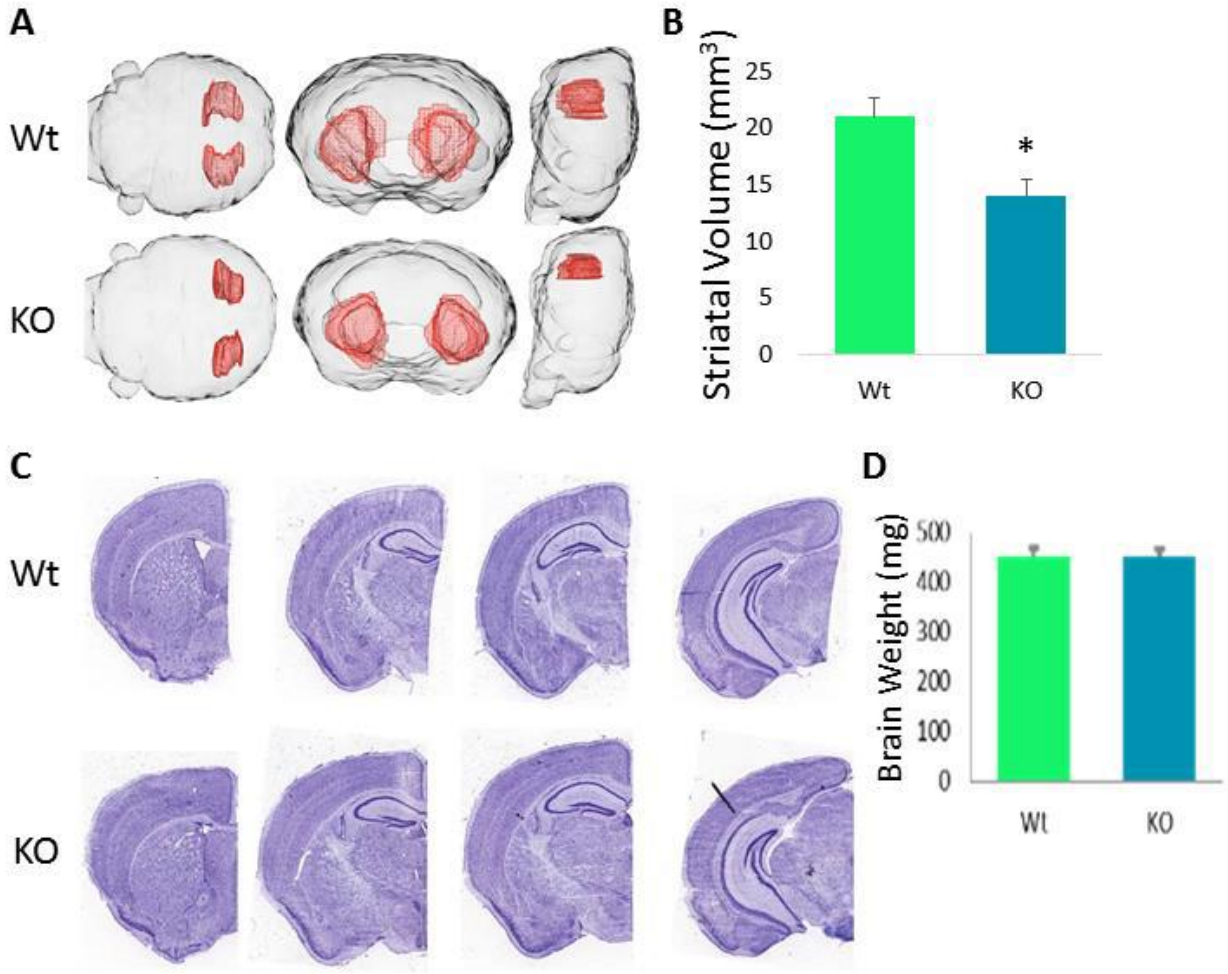

Figure 2.5 Neuroarchitecture of the *Phf8* KO mice. A) Representative 3D reconstruction of MRI images taken from *Phf8* wt and KO mice (n=3), striatum is shown in red. B) Quantification of striatal volume observed by MRI. C) Representative Nissl stains of sections through the brain of *Phf8* wt (top) and KO (bottom), no significant differences observed. D) Weights of brains from *Phf8* wt and KO mice, no difference is seen. *=p<0.05.

clefting. However, *Phf8* KO mice were recovered at the expected Mendelian ratios and survived to adulthood (Fig. 2.4a&b), demonstrating that Phf8 is not required for embryonic development or postnatal survival. Moreover, we failed to detect obvious craniofacial abnormalities including cleft palate in *Phf8* KO mice (Fig. 2.4c), suggesting either species-specific differences between zebrafish, mice and humans, compensation by other molecules or an incompletely penetrant phenotype.

We were also unable to detect any gross physiologic abnormalities or differences in the weight of adult *Phf8* KO mice compared to WT controls (Fig. 2.4d), which is in contrast to the growth deficit of cultured *Phf8* null cells. However, a closer examination of the brain revealed a subtle yet significant reduction in the volume of the striatum (Fig. 2.5a&b) even though total brain size and architecture appeared normal (Fig. 2.5c&d). Of note, behavioral abnormalities have been associated with defects of the striatum, which prompted us to evaluate potential behavioral phenotypes in *Phf8* KO mice.

Behavioral assessment of Phf8 KO mice

We subjected *Phf8* KO mice to a battery of behavioral assays to determine whether they mirror the intellectual deficits observed in *PHF8* deficient patients (Table 2.1). Briefly, we utilized the radial arm maze assay as an assessment of working memory and the contextual fear conditioning assay as a measure of learning, either of which would be expected to be disrupted in a mouse model of intellectual disability (Demas *et al*. 1996; Mineur *et al*. 2002; Moretti *et al*. 2006; Bianchi *et al*. 2010). Surprisingly, neither assay detected any signs of intellectual disability

in mice lacking *Phf8* (Fig. 2.6a&b), suggesting that the loss of *Phf8* in this mouse background is not sufficient to cause intellectual disability.

Phf8 deficient mice are more resilient to anxiety and depression

We next evaluated whether *Phf8* KO mice exhibit aberrant behavior in response to stress-inducing stimuli. Towards this end, we subjected *Phf8* KO animals to an open field test, which measures the preference of animals to spend time in the center or periphery of an open chamber, a readout for anxiety (Fig. 2.7a; Heredia *et al*. 2014). This assay showed that *Phf8* KO mice were more active than controls within the first 15 minutes of the assessment and they spent more time in the center of the chamber, suggesting reduced anxiety (Fig. 2.7b&c). To measure anxious behavior with an independent assay, we next performed an elevated plus maze test (Walf & Frye 2007). In this assay, mice are placed at the center of an elevated four-armed maze with two open and two covered arms; the amount of time a mouse spends in the covered versus the open arms provides a readout of the animal's anxiety (Fig. 2.7d). We find that mice *Phf8* mutant mice spend significantly less time in the closed arms and more time in the open arms, which supports the notion that loss of *Phf8* leads to a decrease in anxiety (Fig. 2.7e&f). Although we failed to detect a significant difference between the *Phf8* KO and WT mice using a third anxiety test, the light-dark box assay (Fig. 2.7g&h; Kulesskaya & Voikar 2014), our results suggest an unexpected involvement of *Phf8* in conferring resiliency to anxiety in certain anxiogenic situations.

Anxiety and depression are regulated by overlapping pathways (Ressler & Mayberg 2007) and both conditions show a significant degree of comorbidity (Kessler *et al*. 2005). We

Table 2.1 Behavioral Assessment of Phf8 KO mice. Summary of all behavioral experiments performed on the *Phf8* KO mice.

Assay	Behavior Assessed	# of mice	Phenotype in KO animal	Figure
Forced Swim	Depression-like	WT n=17 KO n=16	↑ Latency to immobile ↓ time immobile	Fig. 2.8b&c
Tail Suspension	Depression-like	WT n=17 KO n=16	Not Detected	Fig. 2.8d&e
Social Defeat	Depression-like	WT n=7 KO n=9	↑ Time in interaction zone	Fig. 2.8g&h
Open Field Locomotion	Anxiety-like	WT n=17 KO n=16	↑ Activity in new environment	Fig. 2.7b
Center Entry	Anxiety-like	WT n=17 KO n=16	↑ Entries into center ↑ Time in center	Fig. 2.7c
Elevated Plus Maze	Anxiety-like	WT n=17 KO n=16	↑ Time in open arms	Fig. 2.7e&f
Light/Dark Box	Anxiety-like	WT n=17 KO n=16	Not Detected	Fig. 2.7g&h
Radial Arm Maze	Working Memory	WT n=12 KO n=13	Not Detected	Fig. 2.6a
Contextual Fear Conditioning	Associative Learning	WT n=30 KO n=30	Not Detected	Fig. 2.6b

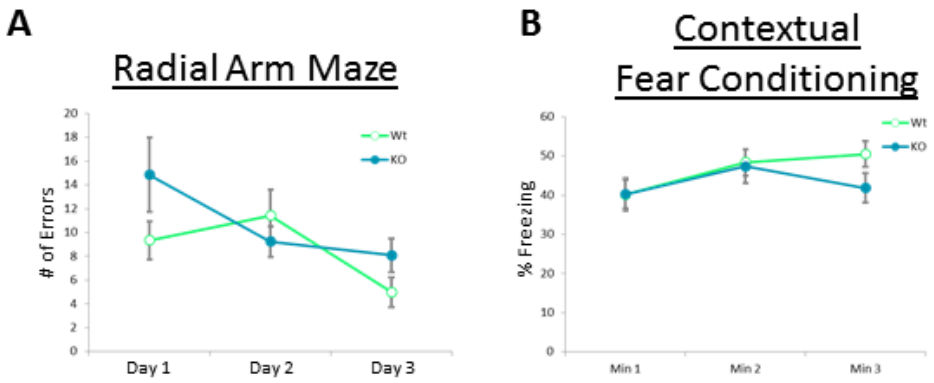

Figure 2.6 *Phf8* null mice do not display signs of intellectual disability. A) Number of errors (multiple entries into the same arm) made in the radial arm maze test. B) Freezing behavior observed during testing phase of contextual fear conditioning, no significant difference is seen.

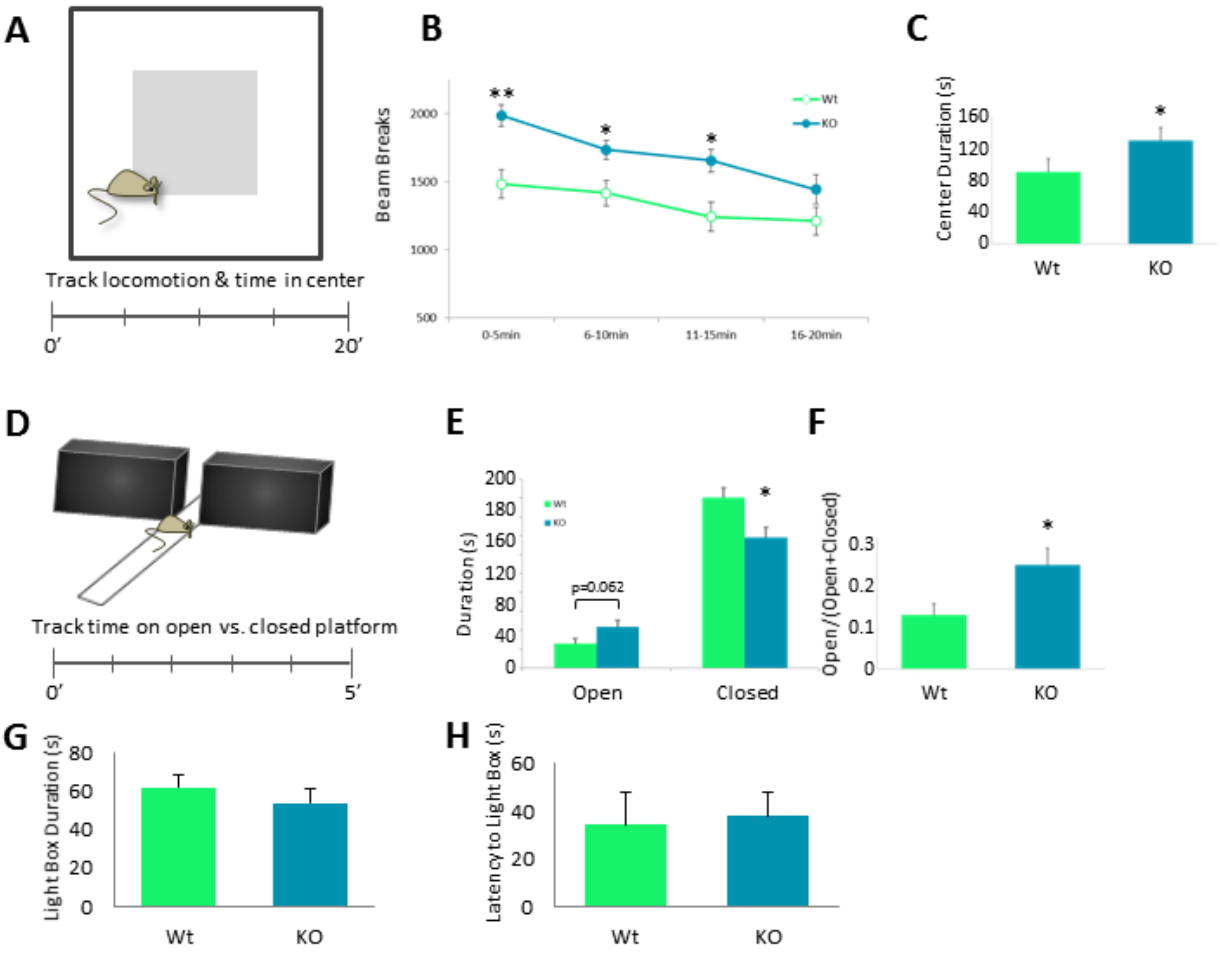

Figure 2.7 Loss of *Phf8* confers resilience to anxiety. A) Diagram of open field test. Mice are placed in an open, lit chamber and locomotion and time spent in the center are monitored for 20min. B) Locomotion as quantified by sensor beam breaks within the open field chamber. C) Time spent in the center by *Phf8* wt & KO mice. D) Diagram of the elevated plus maze. Mice are placed in the center of an elevated maze containing 2 open and 2 enclosed arm; time spent on each is monitored for 5min. E) Quantification of the duration in each arm during the elevated plus maze assay. F) Quantification of the fraction time spent in the open arms over the total time. G) Quantification of the results of the Light/Dark box assay, the total time spent in the anxiogenic light box is shown. H) Latency to first entry to the light box in the Light/Dark box assay is shown. *=p<0.05.

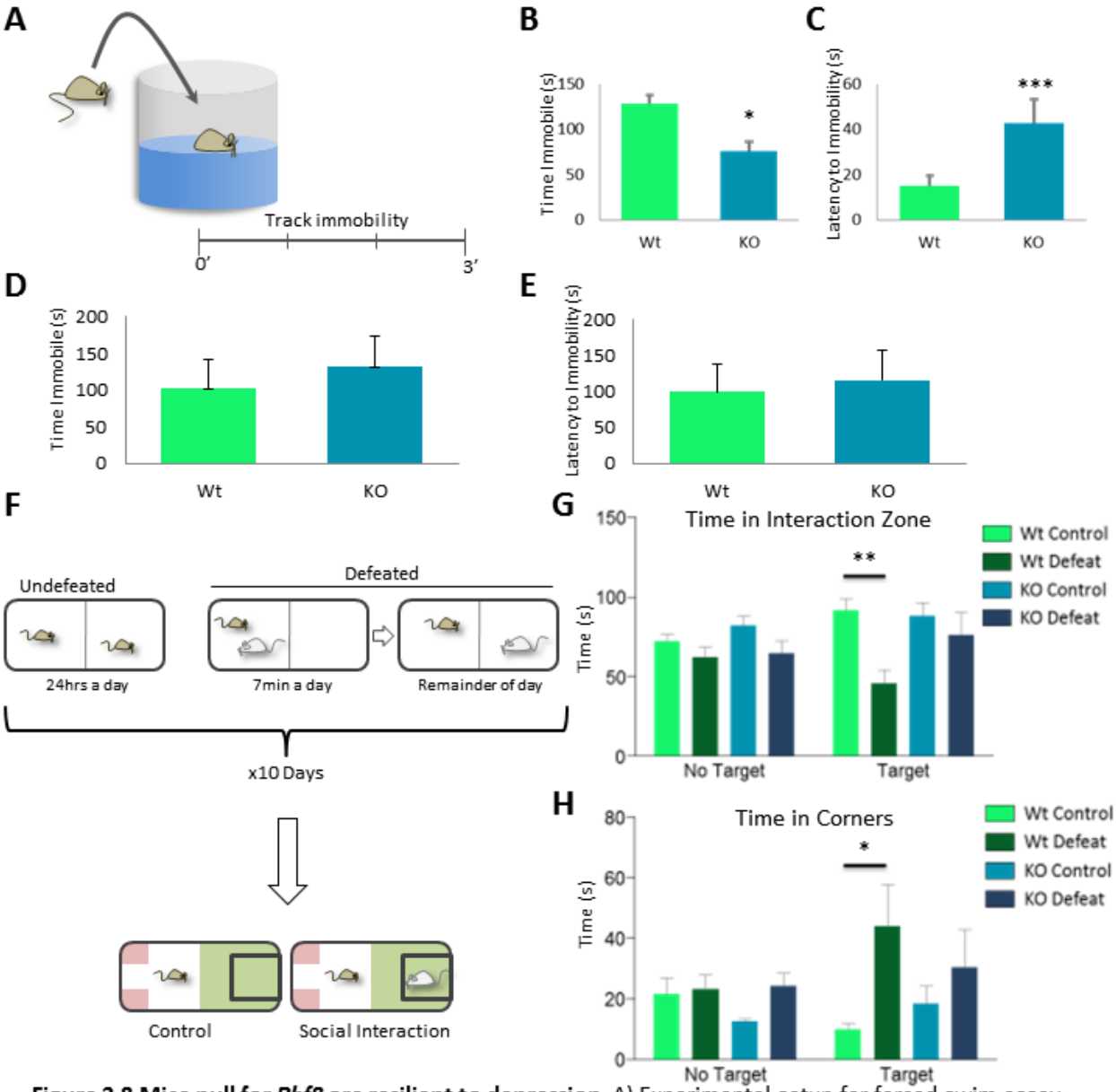

Figure 2.8 Mice null for *Phf8* are resilient to depression. A) Experimental setup for forced swim assay. Mice are placed in a platformless beaker of water and monitored for 3 min. B) Time spent immobile in forced swim assay. C) Latency to first immobility in forced swim assay. D) Experimental design of social defeat assay. Mice are subject to social defeat over a 10 day training period then placed with a novel mouse and time spent in the interaction zone (green) versus opposite corners (red) is quantified. E) Time spent in interaction zone for social defeat assay. Control=no social defeat during training phase, No target=no novel mouse in experimental phase, Target=novel mouse in experimental phase. F) Time spent in corners during social defeat. G) Time immobile in a tail suspension assay in which mice are suspended by the tail with tape and monitored for immobility over a 5min period. H) Latency to first immobility for tail suspension assay. *=p<0.05, **=p<0.01.

therefore tested whether *Phf*8 KO mice also exhibit a depressive phenotype. We first employed a forced swim assay where the mouse is placed into a water-filled beaker in order to measure immobility time and the latency before the animal first begins to swim, which correlate with depressive behavior (Fig. 2.8a; Castagne *et al*. 2011). In keeping with the reduced anxiety phenotype, we observed that *Phf8* KO mice spend significantly less time immobile than their WT counterparts (Fig. 2.8b). Moreover, *Phf8 KO* animals display a striking increase in latency before the first period of immobility (Fig. 2.8c). However, we noticed that *Phf8* KO mice did not show significant differences compared to controls in immobility time using the alternative tail suspension assay (Fig. 2.8d&e; Castagne *et al*. 2011). Thus, to further characterize Phf8's role in depression, we subjected *Phf8* KO mice to a social defeat paradigm, which represents yet another, robust measurement of depressive behavior (Avgustinovich *et al*. 2005). In brief, experimental mice are subject to social defeat by exposure to a more aggressive mouse over a 10-day training period. Subsequently, experimental mice are placed into a new cage containing a novel mouse. The amount of time the experimental mouse spends in an "interaction zone" around the novel mouse versus in the opposite, serving as a readout for social avoidance and hence depression (Fig. 2.8f). Defeated wild type mice showed evidence of social avoidance, as detected by less time spent in the interaction zone and more time in the corners when compared to an undefeated wild type animal (Fig. 2.8g&h). In contrast, *Phf8* KO mice did not display any signs of avoidance behavior following social defeat, spending a comparable amount of time in the interaction zone and corners as undefeated *Phf8* KO and wild type animals. Together these data suggest that *Phf8* KO mice have a remarkable resiliency to anxiety and depression using several independent stress-inducing paradigms.

Loss of Phf8 leads to molecular defects in the prefrontal cortex

To understand the molecular and cellular basis for the observed phenotype, we first determined Phf8 expression patterns in the brain, which remain poorly characterized. In adult mice, Phf8 protein is broadly expressed across forebrain neurons of the neocortex, with strongest expression detectable in layer V, the CA1 and CA3 regions of the hippocampus, and throughout the ventral striatum (Fig. 2.9a-d). Considering that altered gene expression in each of these structures has previously been linked to specifically to resiliency to depression (Covington *et al*. 2010; Vialou *et al*. 2010; Taliaz *et al*. 2011), we began our molecular analysis by performing RNA-sequencing on the ventral striatum and prefrontal cortex of Phf8 KO and WT animals. Unlike global expression analysis of ESC and NPC samples, which failed to show a separation of *Phf8* KO and wild type samples (Fig. 2.3a), we find that the transcriptomes of prefrontal cortex and ventral striatum samples cluster by genotype using unsupervised clustering (Fig. 2.10a). A comparison of differentially expressed genes between *Phf8* KO and control samples revealed 73 upregulated and 169 downregulated genes within the prefrontal cortex, and 79 upregulated and 17 downregulated genes within the ventral striatum with a FDR <0.05 (Fig. 2.10b).

To assess whether any particular biological processes are associated with the dysregulated genes in *Phf8* KO cells, we next applied gene ontology (GO) analysis on the up- and downregulated gene sets (>1.4 fold change; FDR<0.05; Fig. 2.11a&b). We found that “hormone binding”, “amine receptor activity” and “serotonin receptor activity” were the top

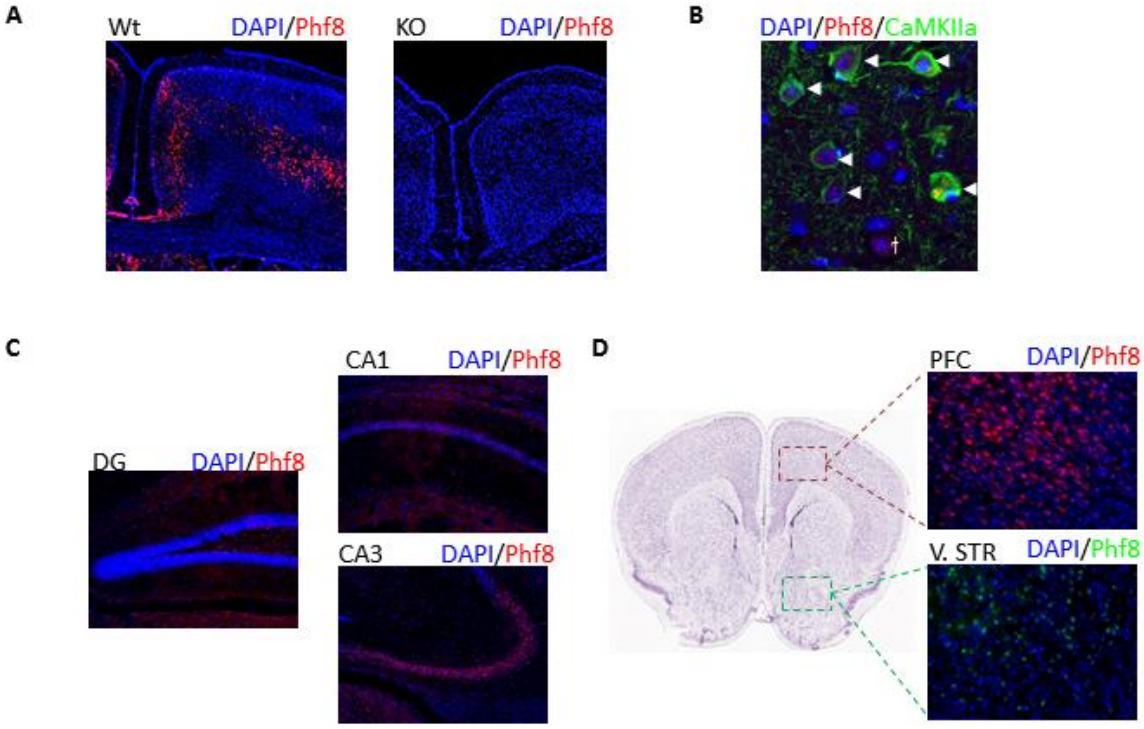

Figure 2.9 Expression of Phf8 in structures linked to anxiety and depression. A) Phf8 expression (red) in the neocortex. Though also detectable in layer II/III, Phf8 is most strongly expressed in layer V. B) Phf8 (red) in expressed in CaMKIIa+ (green) excitatory projection neurons in layer V (arrows), as well as a smaller subset of CaMKIIa- cells (†). C) Phf8 expression in the dorsal hippocampus is primarily in CA3 (bottom right), it is also weakly expressed in CA1 (top right), but absent from the dentate gyrus (left). D) Phf8 is expressed throughout the prefrontal cortex (top) and ventral striatum/nucleus accumbens (bottom).

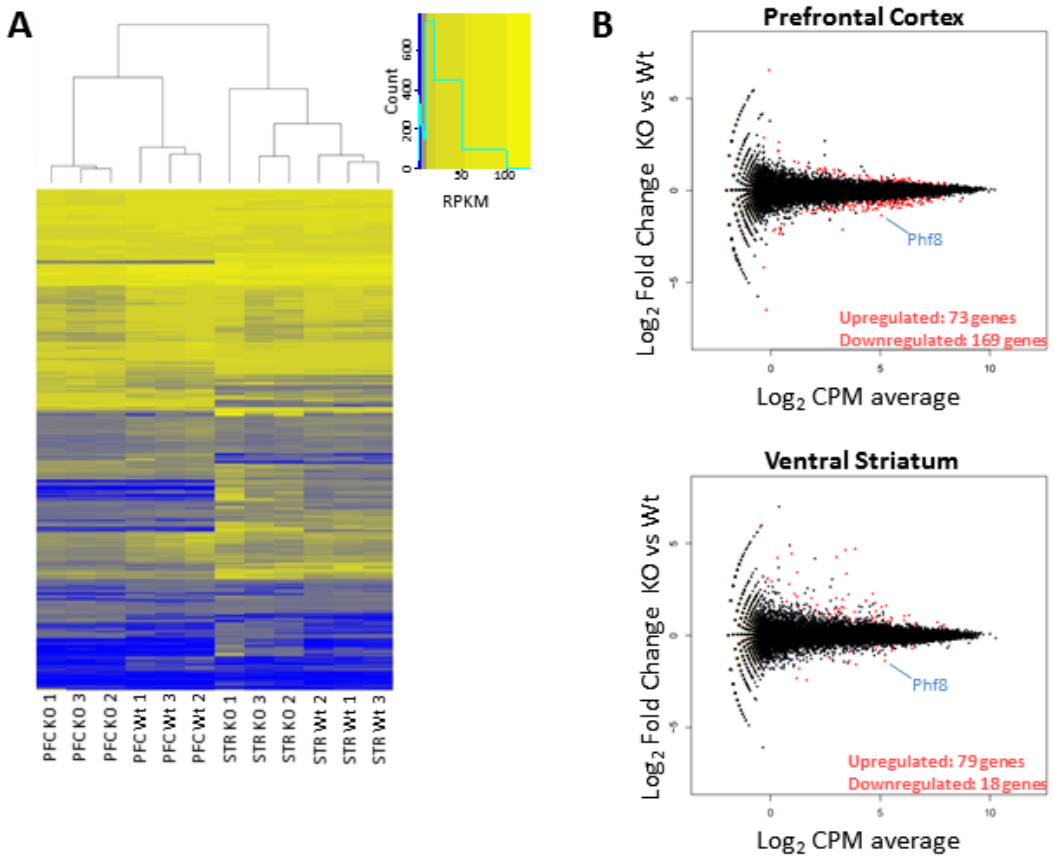

Figure 2.10 RNA-seq on the prefrontal cortex and ventral striatum identifies subtle transcriptional differences in *Phf8* KO mice. A) Unbiased hierarchical clustering and heatmap for differentially expressed genes between *Phf8* wt and KO prefrontal cortex and ventral striatum. B) Mean Average plots comparing *Phf8* wt and KO RNA-seq data from prefrontal cortex (top) and ventral striatum (bottom). Differentially expressed genes ($p<0.05$, FDR<0.05) between wt and KO for each sample set are shown in red.

enriched categories when considering upregulated genes in the prefrontal cortex (Fig. 2.11a), which is in agreement with the notion that serotonin signaling has an important role in modulating anxiety and depression (Ressler & Nemeroff 2000). We detected fewer GO categories when analyzing differentially expressed genes in the striatum. Moreover, a number of top differentially expressed genes between *Phf8* KO and WT samples could not be validated, notably *Oxt* and *Avp*, suggesting contamination from the hypothalamus (Fig. 2.12a&b). Given the cleaner expression data of the prefrontal cortex and the well-established link between serotonin signaling and depression, we decided to focus on the molecular mechanisms by which Phf8 may perturb serotonin signaling in the remainder of this study.

Phf8 *directly regulates serotonin receptors in the neocortex*

Inspection of differentially expressed genes in the prefrontal cortex of *Phf8* KO mice revealed upregulation of multiple serotonin receptors including *Htr1b, Htr2a* and *Htr1a,* which have previously been linked to anxiety and depressive phenotypes in rodents (Fig. 2.13a) (Zhuang *et al*. 1999; Onaivi *et al*. 1995; Ripoll *et al*. 2005; Ripoll *et al*. 2006). We confirmed upregulation of this serotonin receptor family in an additional cohort of Phf8 KO mice using RT-qPCR (Fig. 2.13b), indicating that lack of *Phf8* leads to a subtle yet significant misregulation of serotonin receptor signaling.

We next sought to determine how Phf8 may cause the upregulation of these serotonin receptors. Given that Phf8 has specificity for repressive histone modifications, direct targets are expected to be downregulated in the absence of Phf8. We therefore considered the possibility that Phf8 may target a repressor of serotonin receptor expression. Towards this end, we

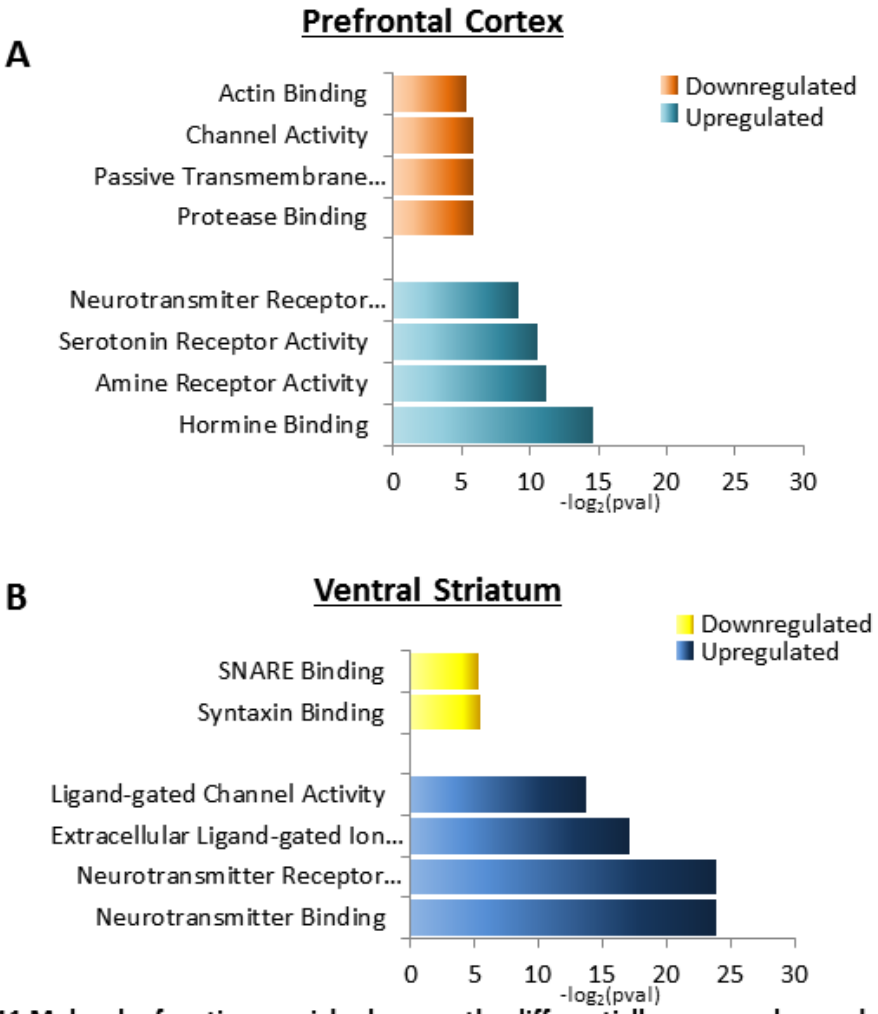

Figure 2.11 Molecular functions enriched among the differentially expressed genes between *Phf8* KO and wt mice. A) GO Molecular Function analysis of the differentially expressed upregulated and downregulated gene sets from the prefrontal cortex (1.4 fold cutoff, FDR<0.05). B) GO Molecular function for differentially expressed genes in the ventral striatum (1.4 fold cutoff, FDR<0.05).

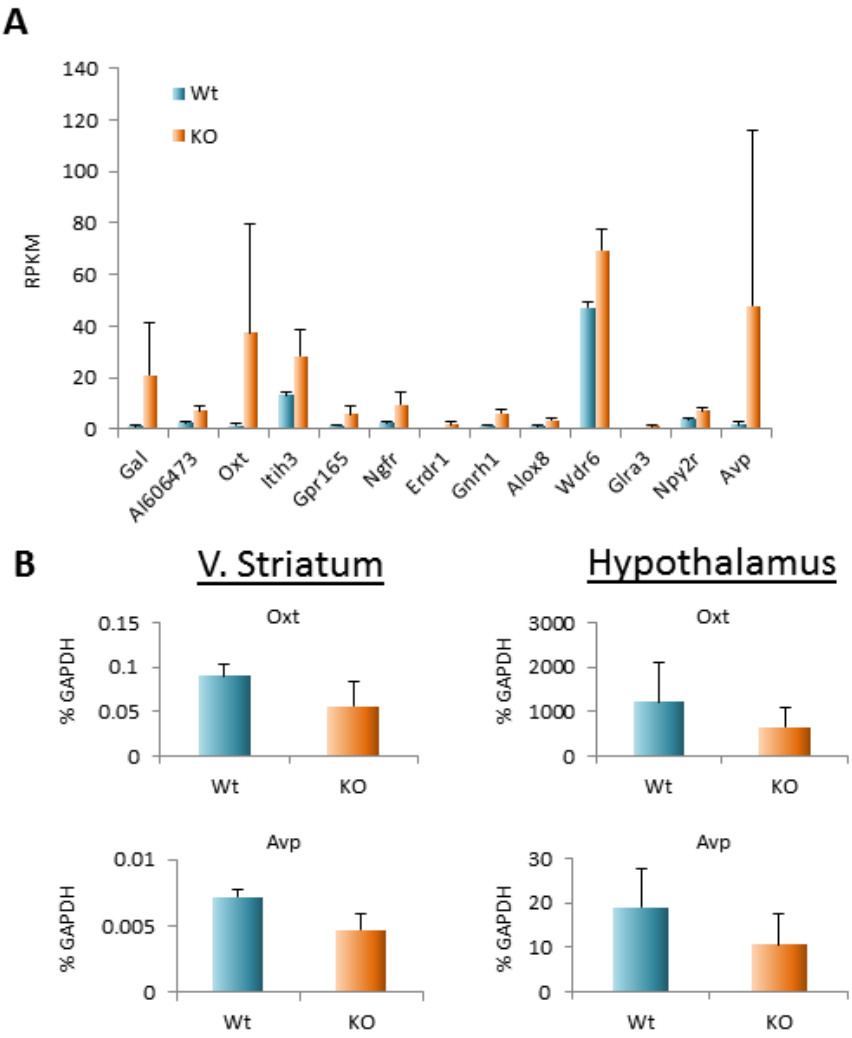

Figure 2.12 Variable gene expression in the ventral striatum. A) RPKM values for the most significantly (ranked by p-value) upregulated genes from the ventral striatum. B) RT-qPCR for two hypothalamic genes, *Oxt* & *Avp*, linked to anxiety and upregulated in the RNA-seq data from the *Phf8* KO. No increase in expression was detected for either of these genes in the ventral striata from a new set of mice nor in the hypothalamus, where these genes are normally expressed (wt n=3, KO n=5). Thus indicating a likely hypothalamic contamination of the original *Phf8* KO ventral striata owning to the reduced striatal size in the KO.

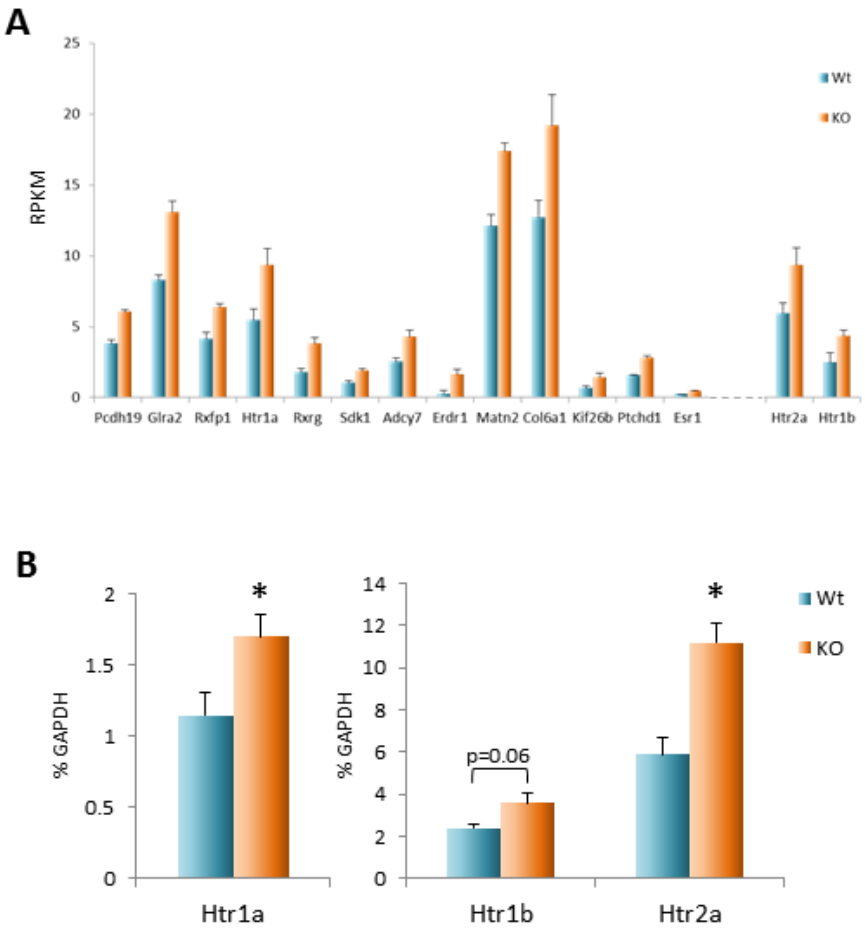

Figure 2.13 Loss of *Phf8* leads to increased expression of multiple serotonin receptors in the prefrontal cortex. A) RPKM values for the most significantly (ranked by p-value) upregulated genes from the prefrontal cortex. Note the presence of the 3 serotonin receptors *Htr1a, Htr1b* and *Htr2a*. B) RT-qPCR analysis of *Htr1a, Htr1b* and *Htr2a* expression in the prefrontal cortices of a new set of mice (wt n=3, KO n=5). A statistically significant increase in expression of a similar magnitude seen in the RNA-seq data is observed. *=p<0.05.

surveyed the expression levels of transcription factors that are predicted or known to bind to the promoter and enhancer elements of the *Htr1a* locus (Albert 2012). However, none of these candidate factors were differentially expressed between *Phf8* KO and control mice (Fig. 2.14a), suggesting that *Htr1a* upregulation is unlikely to be the consequence of repression of a repressor.

To explore whether Phf8 may be directly recruited to serotonin receptor loci to repress their expression, as has been observed for a subset of Phf8 targets (Fortschegger *et al*. 2010; Wang *et al*. 2014), we performed chromatin immunoprecipitation (ChIP) followed by quantitative PCR on the neocortices of Phf8 KO and wild type mice. We designed primers recognizing the promoters and putative enhancers of *Htr1a, Htr1b* and *Htr2b*, which were defined as conserved cerebral DNaseI hypersensitive sites upstream of the transcriptional start sites. Remarkably, we observed a significant enrichment of Phf8 binding at the promoters of all three receptors as well as at putative enhancers of *Htr1b* and *Htr2a*. However, no enrichment was found at the promoter region of the unrelated pluripotency factor *Utf1* (Fig. 2.14b). Altogether, these data suggest that Phf8 recruitment to the serotonin receptor loci serves to repress their transcription, likely in combination with corepressors.

Discussion

Previously, multiple studies observed a reduced growth rate for cell lines on knockdown of Phf8 and further demonstrated a direct role for Phf8 regulating genes involved in cell cycle progression and cell growth (Feng *et al*. 2010; Fortschegger *et al*. 2010; Chen *et al*. 2010; Liu *et*

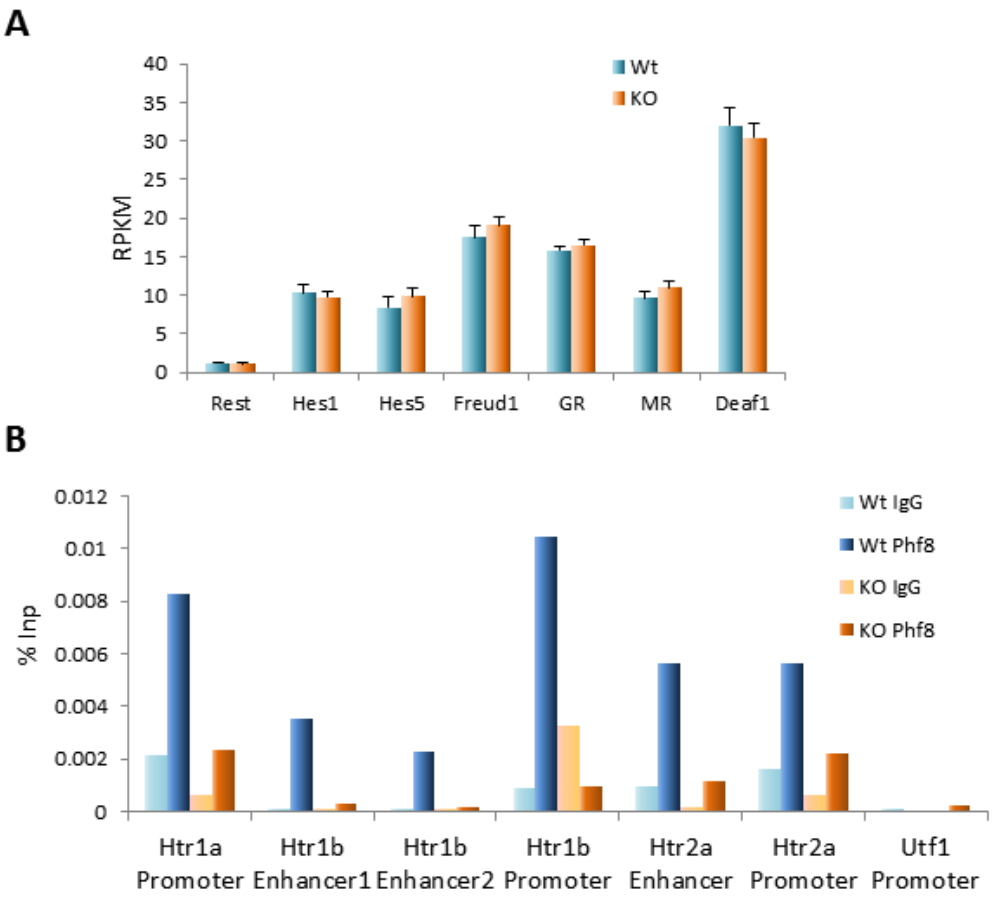

Figure 2.14 Phf8 directly regulates the serotonin receptors *Htr1a, Htr1b* and *Htr2a* in the prefrontal cortex. A) RPKM expression values for known transcriptional regulators of *Htr1a* from RNA-seq of *Phf8* wt and KO prefrontal cortices. No difference in expression was observed between *Phf8* wt and KO samples. B) ChIP-qPCR on the neocortex with primers located in conserved regions either ~200bp upstream of the TSS (Promoter) or within 1kb (Enhancer) for the serotonin receptors. Phf8 is detected at all three serotonin receptors but not and the promoter of the pluripotency factor *Utf1*.

al. 2010). We have shown here that this phenomenon is also observed in primary ESCs, NPCs and MEFs that have a genetic deletion of *Phf8*. Though this function of Phf8 appears to be broadly reproducible in multiple types of cultured cells, it does not seem to have direct consequences for a developing animal. With the exception of the striatum, *Phf8* KO mice are identical to their WT littermates in terms of size, indicating that this function of Phf8 is almost entirely compensated for during development. Further, though we can detect both RNA and protein from Phf8 in cultured NPCs, *in vivo* in adults, NPCs do not express high levels of this protein (see Fig. 2.9c). It is more likely that Phf8's primary function in the adult brain is in regulating gene expression in one of the populations of post-mitotic neurons where it is more abundantly expressed.

Our behavioral analysis did not indicate that *Phf8* KO mice have deficits in either memory or learning, which we would have expected given the human condition associated with *PHF8* mutations. It is difficult to say whether this was due to compensation in the strain we analyzed that was somehow absent in the human families studied or just due to intrinsic differences that exist between the mechanisms controlling learning behavior between mice and humans. However, it should be noted that the reported level of intellectual disability for *PHF8* mutation in humans was variable, with some individuals showing only very mild disability. This would suggest that there are additional genetic or environmental factors that contribute to the development of this disorder. Though these factors are currently unknown, perhaps future studies with this *Phf8* KO model may be able to uncover them.

We did, however, observe a striking behavioral deference between the *Phf8* KO and WT mice in resiliency to anxiety and depression. Though unexpected, we were able to observe

resiliency in the *Phf8* KO mice toward anxiety and depression through multiple independent behavioral paradigms (Table 2.1). Though this phenotype has not been reported in human patients with inactivating mutations in *PHF8*, possibly due to the additional intellectual disability phenotype present in humans, it nonetheless provided us with an intriguing possibility to gain insight into both Phf8's function and the regulation of resiliency.

The expression pattern of Phf8 in the adult brain provided us with a first insight into its possible functions. Here, we observed that Phf8 is abundantly expressed in multiple structures of the forebrain, including the prefrontal cortex, ventral striatum and hippocampus, which are known to contribute to resiliency toward anxiety and depression (Zhuang *et al*. 1999; Onaivi *et al*. 1995; Ripoll *et al*. 2005; Ripoll *et al*. 2006). Phf8 expression in the cortex is primarily within CaMKIIa^{+} excitatory neurons of layer V, though it is additionally expressed in a smaller subset of CaMKIIa- cells. Notably, layer V is also where the 5-Ht1a receptor is primarily expressed within the neocortex making it is likely that Phf8 is acting specifically in these cells to regulate the expression level of this receptor. Phf8 also shows an intriguing pattern of expression within the hippocampal formation; dorsally Phf8 is undetectable in the dentate gyrus, very strongly expressed in the CA3 region and again off or weakly expressed in the CA1 region. Of note, Phf8's expression patter is the reverse of the 5-Ht1a receptor's expression pattern in the dorsal hippocampus (Tanaka *et al*. 2012).

Phf8's apparent role in negatively regulating these serotonin receptors would seem counter-intuitive considering its histone substrate specificity. However, several lines of evidence suggest that it should not be entirely unexpected that Phf8 may act to facilitate gene repression. As discussed previously, evidence for this has been observed by multiple groups in

cell lines, where knockdown of Phf8 leads to an increase in the expression levels of a significant number Phf8's direct targets (Fortschegger *et al*. 2010; Wang *et al*. 2014). Furthermore, Phf8 has been found in complexes with the H3K3 mono- and di-demethylase Lsd1. Though so far these Phf8-Lsd1 containing complexes have only been shown to act as coactivators (Yatim *et al*. 2012), it is not inconceivable that in certain contexts the H3K4 demethylase activity of Lsd1 in association with Phf8 may act to repress transcription. Finally, the closely related histone demethylase Phf2, which shares Phf8's specificity toward H3K9me2 (Baba *et al*. 2011), has been demonstrated to act as a repressor in some contexts by recruiting the H3K9 methyltransferase Suv39h1 (Shi *et al*. 2014).

The role which serotonin signaling plays in anxiety and depression is complex and an area of active research, however, there are multiple lines of evidence that suggest the increase in serotonin receptors we observe is likely involved in the resiliency phenotype of the *Phf8* KO mice. SSRIs, which act to enhance serotonin signaling by inhibiting its reuptake, are among the most commonly prescribed antidepressants and antianxiety medications (Vaswani *et al*. 2003). In addition, multiple laboratories have reported a reduced 5-HT binding potential of the 5-HT1A receptor in the prefrontal cortex and hippocampus and of 5-HT2A in the prefrontal cortex in patients of depression (Savitz & Drevets 2012). Further, *HTR1B* mRNA was found reduced within prefrontal cortex and hippocampus of post-mortem tissue from suicide victims (Anisman *et al*. 2008). In addition, functional data from numerous animal models suggests a strong link between the expression levels of serotonin receptors and anxiety and depression. First, mice null for *Htr1a* display increased anxiety and depression in an array of assays (Zhuang *et al*. 1999) with overexpression of the receptor producing the opposite phenotype (Kusserow *et*

*al.*2004). Although the 5-Ht1a*,* 5-Ht1b and 5-Ht2a receptors have differing or even opposing effects on cortical neurons, it has additionally been demonstrated that a similar anxiolytic effect is seen in rodents treated with either 5-Ht1a, 5-Ht1b or 5-Ht2a agonists (Blier & Ward 2003; Onaivi *et al*. 1995; Ripoll *et al*. 2005; Ripoll *et al*. 2006), again suggesting that increasing the activation of this receptor can lead to a reduction of anxiety in animal models. It should, however, be noted that complete loss of *Htr1b* or *Htr2a* is also anxiolytic in mice (Zhuang *et al*. 1999; Weisstaub *et al*. 2006). With these observations in mind, we propose a model in which Phf8 acts to modulate the expression of these receptors in the cortex through direct repression, and in its absence their subtle but significant increase in expression confers resiliency to anxiety and depression in mice (Fig 2.15).

Anxiety disorders and depression represent very serious and debilitating conditions and patient response to treatment is often incomplete (Trivedi *et al*. 2006). A more complete understanding of the mechanisms governing anxiety and depression will be critical for improving their treatment in the future. It is not currently clear if inhibiting PHF8 in humans would produce results similar to those we observed in the mouse. However, we detected multiple peaks for human PHF8 at the *HTR1A* and *HTR1B* loci using publically available ChIP-seq data from undifferentiated human ESCs (Ram *et al*. 2011), suggesting that these targets are conserved. Though caution should be taken in considering Phf8 as a therapeutic target given the human genetic evidence linking *PHF8* loss to intellectual disability, it is formally possible that this enzyme could be inhibited in healthy adults without the same consequences, thereby providing a potential avenue of improved treatment.

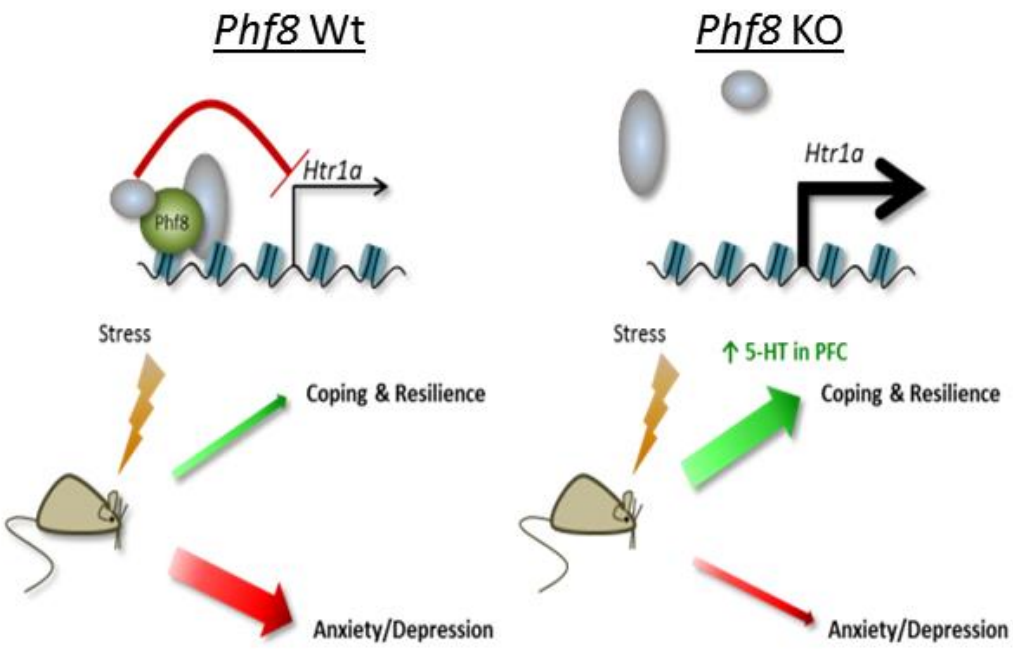

Figure 2.15 Model for Phf8's role in serotonin receptor regulation and resiliency. A) In the wt mouse (left) Phf8 binds upstream of the serotonin receptors and represses them, likely through association with additional factors. When Phf8 is absent, this repression is relieved, leading to moderate increases in the expression of *Htr1a, Htr1b* and *Htr2a*. This misregulation of serotonin signaling likely explains the observed shift toward a successful coping response and resiliency in mice null for *Phf8*.

Methods

Generation of the knockout mouse

A targeting construct containing exons 7 and 8 flanked by *loxP* sites and a neomycin resistance cassette was electroporated into V6.5 ESCs. Electroporated ESCs were selected with G418, picked, and clonally expanded. Integration of the targeting construct was confirmed by Southern blot. Positive clones were electroporated again with a CMV-Cre expression vector, picked, and clonally expanded again. Loop out of exon's 7 & 8 was confirmed by Southern blot and positive clones were injected into E3.5 BDF1 blastocyts and transferred into the uteri of surrogate Swiss Webster mice.

Western Blot

Whole cell extract was run on either 10% or 15% SDS-PAGE gels at 150V until separated and transferred at 4^{o}C for either 1hr at 80V (histones) or overnight at 20V (Phf8) onto a PVDF membrane. Membranes were blocked in 5% milk PBS-T (1X PBS, 0.1% Tween-20) for 30min at RT then incubated with primary antibodies for 1hr in block at RT. Membranes were washed in PBS-T, and incubated in the appropriate horseradish-peroxidase-conjugated secondary for 45min at RT. Membranes were then washed again and visualized using ECL reagents (Pierce). Primary antibodys: Phf8 Abcam ab36068, H3 abcam ab1791, H3K9me1 Abcam ab8896, H3K9me2 Abcam ab1220, H3K9me3 Abcam ab8898, H3K27me2 Millipore 07-452, H4 Abcam ab17036, H4K20me1 Abcam ab9051, beta Actin-HRP Abcam ab20272.

Southern Blot

20ug of genomic DNA collected from ESCs was digested overnight at 37^{o}C with 500U/ul of StuI (New England Biolabs) then electophoresed on a 0.8% agarose gel at 70V until separated (6-8hrs). The gel was depurinated in 0.5N HCl for 25min at RT and quenched in transfer buffer (1.5M NaCl, 0.5M NaOH) for 45min at RT. Samples were transferred to a Hybond-XL membrane (GE Healthcare) via a downward transfer for 14-16hr. The membrane was washed for 15min at RT in 2X SSC then blocked for an hour at 65^{o}C in Hyb buffer (0.5M NaP_i, 7% SDS, 1mM EDTA). Probes (See Supplemental Table 1 for probe primer sequences) were labeled with Prime-IT II Random Primer Labeling Kit (Agilent) and added to membranes in 30ml of fresh Hyb buffer, hybridization was run overnight. Membranes were washed 2X with wash buffer (40mM NaP_i, 0.1% SDS) for 15min and 30min prior to exposure.

Growth curve and neurosphere formation assay

For MEFs and ESCs equal numbers of cells were plated into triplicate wells of a six well plate, 20,000cells/well for MEFs and 5,000cells/well for ESCs. Wells containing ESCs were gelatinized with 0.2% gelatin to support attachment. Cells were stained with trypan blue and trypan blue negative cells were counted every 3 days.

For neurosphere formation assays, undifferentiated NPCs ($CD24^{-}EGFR^{+}$) were sorted and plated at low density to avoid clumping, 10cells/ul, in low attachment 6-well or 24-well plates. New neurospheres were allowed to grow for 1 week and imaged in brightfield. Sphere diameters were measured in NIS Elements software (Nikon), the shortest possible diameter was recorded for all spheres.

Behavioral analysis

Open field locomotion was monitored in a 40x40x40cm clear plastic arena using a photocell-beam-based detecting system (OmniTech Electronics. Inc). Animals were introduced into the corner of the chamber and allowed free exploration for 20min individually under standard lighting conditions. Beam breaks were recorded every 5min as was the total distance traveled and the duration in the center.

The elevated plus maze (Med Associates Inc) contained a 6x6cm center square, two open and two closed arms at 35x6cm each. Closed arms were enclosed with black walls measuring 20cm in height. Mice were placed in the center square facing one of the closed arms to begin the assessment. Time spent in each arm was scored by the EthoVision video tracking system (Noldus, Wageningen, The Netherlands).

The light/dark box test was performed in an open field with a black box insert measuring 20cm L x 20cm W x 40cm H, which divided the arena into a light and dark component connected by a small hole. Mice were introduced into the dark chamber and allowed free exploration for 10min. Duration spent in each chamber was tracked during this time.

For the forced swim assay, animals were placed in a 4L Pyrex beaker 13cm diameter and 24cm high filled with 17cm of 22^{o}C water. Activity of the animals was tracked for 5 minutes and latency to first freeze as well as time spent immobile was assessed by EthoVision.

In the tail suspension test, mice were suspended by the tail with duct tape and videotaped for 5 minutes. Latency to first freezing and time spent immobile was evaluated with EthoVision software, animals displaying tail climbing behavior were excluded from the analysis.

In the contextual fear conditioning assay, mice were placed in a fear conditioning chamber measuring 30.5x24.1x21cm (Med Associates, Inc.) for a 7min training session. During this time 3 shocks were delivered and the percentage of time freezing before the first shock (baseline) and after each shock was measured. After 24hrs, mice were returned to the chamber for a 3min retrieval testing and percentage of time freezing was measured.

For the radial arm maze test, mice were placed in the center of an 8 armed apparatus, each arm measuring 5x50cm with 30cm high walls. Mice were assessed for 4 consecutive days and each day the test was continued until all eight arms had been visited at least once. A mistake was defined as a repeated entry into an already visited arm. Total mistakes during a session were measured.

For the social defeat assay, mice were subjected to 7min social defeat by a novel CD1 aggressor daily for 10 days, during which time they were housed together across a plexiglass divider allowing for sensory contact. Control mice were housed in cages separated from other control mice and were rotated to a different cage daily. After 10 days with of social defeat, experimental and control mice were placed in an arena 44x44cm containing a novel CD1 mouse within a Plexiglas/wire mesh enclosure measuring 10x6cm against one wall of the arena. Time spent in the 14x26cm interaction zone around the enclosure and time spent in the opposite corners was quantified using EthoVision software.

Immunofluorescence

Animals were anesthetized with avertin prior to transcardial perfusion with 20ml cold 4% PFA in PBS. Brains were dissected and post-fixed 14-16hrs in 4% PFA PBS following which they were

cryoprotected in 30% sucrose PBS. Cryoprotected brains were frozen in OCT on dry ice and 30 micron floating sections were cut using a Leica cryostat. Floating sections were washed in PBS 0.3% triton 15min at RT then blocked in 0.3% triton, 10% normal donkey serum, PBS for 2hr at RT. Sections were incubated with primary antibodies overnight at 4^{o}C in PBS 0.3% triton. Sections were washed 3X 15min in PBS and incubated with Alexa488, Alexa546 or Alexa647 conjugated secondary antibodies in PBS for 2hr at RT. Sections were washed 3X 15min in PBS with DAPI added to the second wash and mounted in Prolong Gold Antifade (Life Technologies) for imaging. Primary antibodies: Phf8 Abcam ab191386, CaMKIIa Cell Signaling 50049, NeuN Millipore ABN90.

Bioinformatic analysis of RNA-seq data

Data was aligned with the splace-aware alignment program STAR ((http://bioinformatics.oxfordjournals.org/content/early/2012/10/25/bioinformatics.bts635) to map the sequencing reads to a mouse reference genome (assembly mm10/GRCm38). Gene expression counts were calculated using the program HTSeq (http://www-huber.embl.de/users/anders/HTSeq/doc/overview.html) based on a current Ensembl annotation file for mm10/GRCm38 (release 75). We then used the R package "edgeR" (https://bioconductor.org/packages/release/bioc/html/edgeR.html) to make differential gene expression calls from these counts according to the following criteria: Gene expression was considered to be UP-regulated if log2 FC > +1 or DOWN-regulated if the log2 FC < -1 (FC= fold-change of CPM) with respect to the conditions being compared at an arbitrary false discovery

rate (FDR) value < 0.05. GO analysis was performed using DAVID (https://david.ncifcrf.gov/) for "GO Molecular Function."

Hierarchical clustering

Heatmaps/dendrograms of the 12 samples were constructed using RPKM expression values of all genes for PFC and STR samples which registered an FDR <0.05 for differential expression. Heatmaps were created using the "heatmap.2 function from the gplots package for R" (http://www.inside-r.org/packages/cran/gplots/docs/heatmap.2) in conjunction with the hierarchical clustering option 'ward.D2.'

RNA preparation for sequencing and RT-qPCR

RNA from ESCs, NPCs, the prefrontal cortex or the ventral striatum was purified using an RNeasy kit (Qiagen) and including the optional DNase digest step. For sequencing, quality of RNA was assessed using an Agilent RNA 6000 Nano kit. For library preparation, Illumina TruSeq RNA Sample Prep Kit was used with 1ug of sample RNA. Library quality was again assessed with the BioAnalyzer Agilent High Sensitivity DNA kit. Bar-coded libraries were then pooled at equimolar concentration and sequenced on an Illumina HiSeq 2000.

For RT-PCR, 500ng of purified RNA was used for an RT reaction with the Transcriptor First strand cDNA synthesis kit (Roche). cDNA reactions were heat inactivated, diluted 1:10-1:50 and analyzed by qPCR on a Roche LightCycler 480 with a Brilliant III Ultra-Fast SYBR Green kit (Agilent). See Supplemental Table 1 for primer sequences.

Chromatin Immunoprecipitation

The cortex was dissected from adult mice (~2months old) homogenized to a single cell suspension using a dounce homogenizer in ice cold PBS. The suspension was filtered and treated with 1.5mM EGS (ethylene glycolbis(succinimidylsuccinate)) for 25min at RT in PBS, crosslinking was continued with the addition of 1% formaldehyde for 10min at RT. Crosslinking was quenched by adding 0.125M glycine 10min RT. Samples were washed with PBS and lysed in 50mM Tris-HCl pH 8.0, 1% SDS, 4mM EDTA with protease inhibitor cocktail (Roche complete mini) on ice for 20min. Lysed samples were sonnicated 10min total sonication time, in a bioruptor with pulses of 30 seconds on, 30 seconds off then cleared by spinning at max in a tabletop centrifuge for 10 minutes at 4^{o}C. Samples were diluted 5X with dilution buffer (165mM NaCl, 0.01% SDS, 1.1% Triton-X, 1.2mM EDTA, 16.7mM Tris-HCl pH8.0). Samples were precleared with 20ul streptavidin-agarose beads for 2hr at 4^{o}C. 10% was removed for input and the remainder incubated with 5ug of primary antibody (Phf8 Abcam ab36068 or Rb IgG abcam) overnight at 4^{o}C. 8ul of protein-G Dynabeads (Life Technologies) were added to each sample and incubated 2hr at 4^{o}C. Beads were collected on a magnet and washed 1X with dilution buffer, 2X with low salt buffer (150mM NaCl, 0.5% Sodium deoxycholate, 0.1% SDS, 1% IGEPAL, 1mM EDTA, 50mM Tris-HCl pH 8.0), 4X with high salt buffer (500mM NaCl, 0.5% Sodium deoxycholate, 0.1% SDS, 1% IGEPAL, 1mM EDTA, 50mM Tris-HCl pH 8.0), and twice with TE. All wash buffers contained complete mini protease inhibitor (Roche). Samples were eluted with 2 rounds of constant vortexing for 10min in 50ul elution buffer (1% SDS, 100mM sodium bicarbonate) then brought to a final concentration of 0.3M NaCl and incubated overnight at 65^{o}C. Samples were brought to final concentration of 50mM Tris-HCl pH 6.8, 10mM EDTA and

treated with proteinase K for 1hr at 55^{o}C then purified with a PCR purification kit (Qiagen). Samples were eluted in water and diluted 1:3 for analysis in qPCR with a Brilliant III Ultra-Fast SYBR Green kit (Agilent) on a Roche LightCycler 480. See Supplemental Table 1 for primer sequences.

Chapter 3

Loss of *Phf8* confers subtle hematopoietic defects without affecting progression of T-ALL in mice

Contributing Authors

Ryan M. Walsh, Benjamin A. Schwarz, Adlen Foudi, Hanno R. Hock, and Konrad Hochedlinger

Attributions

I designed and generated the knockout mice used in this study, made the virus, infected the bone marrow, performed the transplants for the T-ALL experiments and performed all subsequent analyses of these mice. Adlen Foudi and Ben Schwarz provided advice on the analysis of the peripheral blood, marrow, and thymus for the analysis of the knockout and competitive transplant mice. Adlen Foudi performed the analysis of the bone marrow and assisted with the analysis of the thymus of the knockout mice. I performed the competitive transplants and subsequent analysis with assistance from Ben Schwarz.

Abstract

Though it was initially described as a gene mutated in cases of intellectual disability with cleft lip/palate, more recent studies suggest that Phf8 may have additional functions in the hematopoietic system, which are misregulated in cancer. In human T-cell acute lymphoblastic leukemia (T-ALL) cell lines, PHF8 has been shown to interact directly with intracellular NOTCH1, being required for the activation of Notch target genes (Yatim *et al*. 2012). Importantly, knockdown of PHF8 here leads to a loss of expression of Notch targets, reduced proliferation and loss of tumorgenicity (Yatim *et al*. 2012). However, it is unclear how Phf8 functions during normal hematopoiesis; given this link to Notch signaling and the fact that Phf8 is highly expressed in the thymus, a role in T-cell development seems likely. Interestingly, Phf8 has also been implicated in regulation of hematopoietic stem cells (HSCs). Knockdown of Phf8 in HSCs reportedly compromises their ability to reconstitute a mouse's bone marrow. Here, we revisited these knockdown-based studies by characterizing our *Phf8* KO mouse in the context of T-ALL and hematopoiesis. Unexpectedly, we find that deletion of *Phf8* does not affect progression of T-ALL nor normal hematopoiesis. However, analysis of mice receiving competitive transplant marrow from *Phf8* WT and KO mice reveals a subtle defect in T-cell development and progenitor expansion *in vivo*.

Introduction

A growing body of evidence suggests that the histone demethylase Phf8 functions as an oncogene in multiple tissues (Bjorkman *et al*. 2012; Yatim *et al*. 2012; Sun *et al*. 2013; Shen *et al*. 2014; Zhu *et al*. 2015). This was first described for prostate cancer (Bjorkman *et al*. 2012), and subsequently extended to cancers of the hematopoietic system, including T-ALL (Yatim *et al*. 2012). Specifically, human PHF8 has been identified as a coactivator for the ICN1-CSL-MAML complex and in T-ALL cell lines, is required for the activation of a number of critical Notch effector genes, including *IL-7R, HEY1* and DTX1 (Yatim *et al*. 2012). Importantly, knockdown of PHF8 in these cell lines leads to an impairment of cell expansion *in vitro*, and a failure to form tumors in xenograft transplants (Yatim *et al*. 2012).

In addition to this link to tumorigenesis, an independent study suggested that Phf8 may also be involved in hematopoiesis. Specifically, knockdown of Phf8 in the LSK ($Lin^-Sca1^+cKit^+$) $CD150^+$ fraction of murine bone marrow, a population enriched for HSCs, decreased their ability to contribute to bone marrow in transplanted chimeras following a brief *in vitro* culture (Cellot *et al*. 2013). It remains unclear, however, whether Phf8 plays any role during normal steady state hematopoiesis in the absence of *in vitro* culture. We therefore analyzed our *Phf8* KO mice in the contexts of cancer and hematopoiesis.

Results

Genetic deletion of Phf8 does not alter progression of T-ALL in the mouse

Considering that *in vitro* data suggests that PHF8 is critical for mediating propagation of Notch-driven T-ALL, we set to interrogate the response of the *Phf8* KO mice to an established mouse model of T-ALL. Briefly, bone marrow was collected from *Phf8* KO or WT mice, lineage depleted and infected with a retrovirus carrying either an empty backbone (EV) control or a portion of the *Notch1* gene lacking the majority of the extracellular domain (*NotchΔE*) (Pear *et al*. 1996). Subsequently, infected marrow was mixed with healthy rescue marrow and transplanted into a lethally irradiated host for to induce T-ALL (Fig 3.1a). Truncated *Notch1ΔE* phenocopies activating mutations found in human T-ALL patients and is a potent driver of T-ALL, capable of inducing leukemia in transplanted mice within 3 weeks and lethality within 3 months (King *et al*. 2013).

Unexpectedly, loss of *Phf8* did not impede the development of T-ALL in host mice receiving *NotchΔE* marrow, as indicated by the presence of CD4+CD8+ double positive lymphoblasts in peripheral blood at 1 month post-transplant (Fig. 3.1b, upper panels). These peripheral lymphoblasts expressed GFP (Fig. 3.1b, bottom panels), indicating expression of the transgene, and did not express Phf8 (Fig. 3.1c). In both *Phf8* WT and *Phf8* KO host mice, infiltrating lymphoblasts can be observed in the liver and lung of leukemic mice at the time of euthanasia (Fig. 3.1d). Of note, survival curves for either primary or secondary T-ALL transplants did not suggest that any difference exists in the progression of T-ALL derived between *Phf8* KO

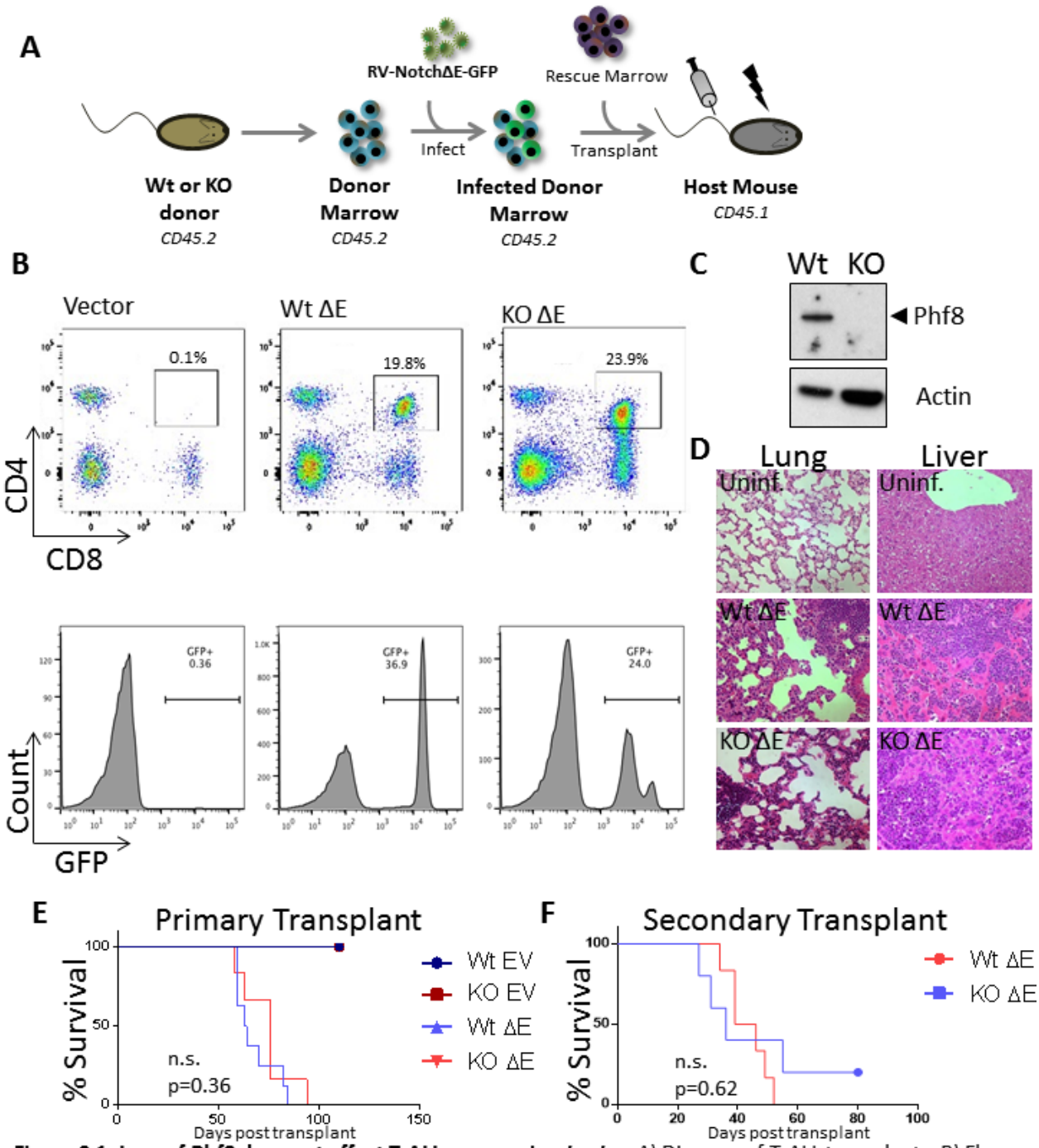

Figure 3.1. Loss of Phf8 does not effect T-ALL progression *in vivo*. A) Diagram of T-ALL transplants. B) Flow analysis of CD4/CD8 double positive (top) cells in peripheral blood of *NotchΔE* infected bone marrow chimeras. GFP indicates expression of transgene (bottom). C) Western confirming loss of Phf8 in peripheral blood in leukemic BM chimeras. D) H&E stains of Phf8 KO and Wt lung and liver collected from morbid animals showing infiltrating lymphoblasts. E&F) Kaplan-Meier survival curve for primary (E) and secondary (F) transplants of *NotchΔE* infected bone marrow.

and WT mice (Fig. 3.1e&f). These results indicate that loss of *Phf8* neither stops nor slows the progression of T-ALL in the context of a constitutively active Notch mouse model.

Phf8 KO mice have unaltered stead-state hematopoiesis

Given previous observations linking Phf8 to the regulation of HSCs, we began our analysis by examining the fractions of HSCs and multipotent progenitors (MPPs) in the bone marrow of *Phf8* KO mice under homeostatic conditions. Unexpectedly, we failed to detect any differences in either the percentages of HSCs or MPPs present in the marrow of *Phf8* KO mice when compared to littermates (Fig. 3.2a&b). We also did not detect any defects in B-cell numbers or the development of erythrocytes and granulocytes in *Phf8* KO marrow (Fig. 3.3a-d).

We next expanded this analysis to the thymus to track T-cell development. Given that *Phf8* is abundantly expressed in the thymus (Suppl. Fig. 1) and the previous reports of Phf8's function in affecting Notch signaling, a critical regulator of T-cell specification and development (Tanigaki & Honjo 2007), we expected loss of *Phf8* to cause a T-cell defect. Examination of the CD4/CD8 expressing cells in the thymus of *Phf8* KO mice did not immediately point to any clear deficits in T-cell development (Fig. 3.4a&b). Likewise, deeper analysis of the development of the $CD4^-$ $CD8^-$ double negative population did not indicate any observable T-cell defect (Fig. 3.4c). Knockout of *Notch1* in the bone marrow causes a breakdown in T-cell specification and ectopic B-cell development in the thymus (Wilson *et al*. 2001). We therefore additionally assayed for the presence of B-cell development in the thymus. However, no sign of ectopic B-cell development was also detected (Fig. 3.4d). Thus, loss of *Phf8* does not appear to lead to any obvious defects in hematopoiesis or thymocyte development under homeostatic conditions.

Subtle defects in hematopoiesis and T-cell development of Phf8 KO mice in a competitive setting

With the divergence between our observations and previous reports based on Phf8 knockdown *in vitro*, we decided to delve further into the hematopoiesis of these mice. To this end, we performed a competitive transplant in which whole bone marrow from either *Phf8* WT or KO mice were mixed 1:1 with competitor marrow and transplanted into a lethally irradiated host mouse (Fig 3.5a). Engraftment efficiencies were first assessed at 4 weeks post-transplant, at which point we were able to confirm equal engraftment between *Phf8* WT and *Phf8* KO mice (Fig. 3.5b). Surprisingly, at 8 weeks post-transplant an increase in the percentage of host-derived granulocytes could be observed in the *Phf8* KO mice when compared to WT controls (Fig. 3.5c), potentially indicating an expansion of HSCs in the marrow of the KO mice. This trend continued until 16 weeks post-transplant (Fig. 3.5d), at which point we ran an analysis of HSCs in the marrow of transplant mice to determine the nature of the KO's HSC phenotype.

At 16 weeks post-transplant, we were able to observe an increase in the proportion of donor derived LSK cells, a population enriched for HSCs and MPPs, in the *Phf8* KO chimeras. However, further subdivision of this population with more stringent HSC-specific markers did not show any difference between *Phf8* KO and WT chimeras. Specifically, we did not observe a difference in chimerism between *Phf8* KO and WT in the LSK $CD150^{+}CD48^{-}$ fraction (Fig. 3.5e), which is a population significantly enriched for *bona fide* HSCs. These results suggest that our previously noted difference in peripheral granulocytes is likely do to an expansion of an early LSK progenitor population in the *Phf8* KO chimeras and not an expansion of HSCs.

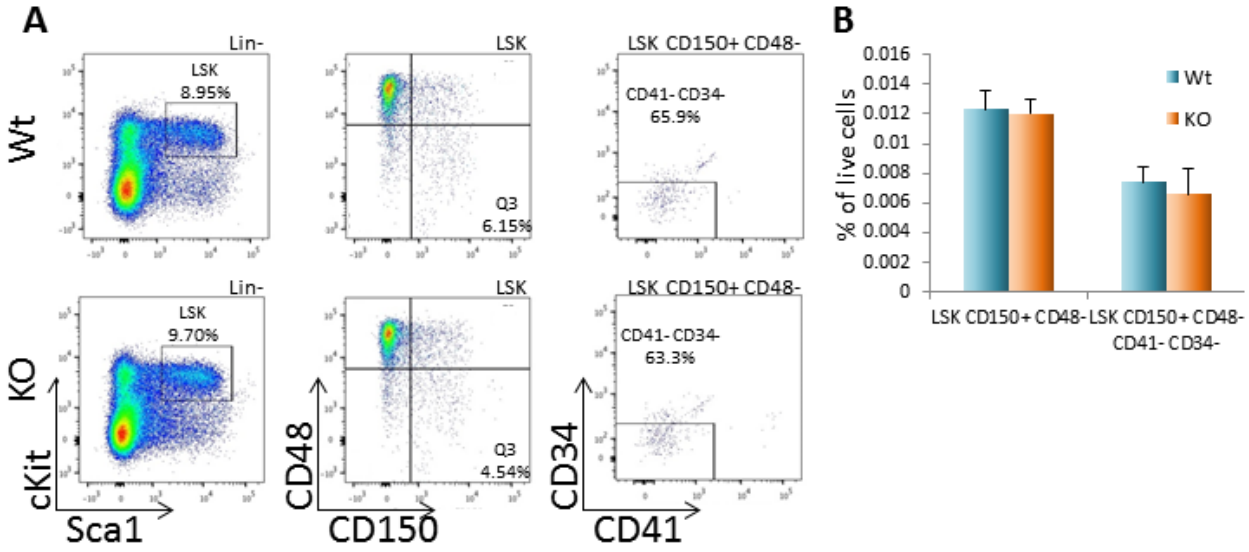

Figure 3.2 Loss of *Phf8* does not effect HSCs under homeostatic conditions. A) HSC stain on marrow collected from *Phf8* wt and KO mice, the most HSC enriched population, LSK CD150+CD48-CD41-CD34-, shows no difference between wt and KO marrow. Lin=CD3e, B220, Gr1, Mac1, Ter119. B) Quantification of data shown in A, populations as a percentage of live cells are shown (n=3).

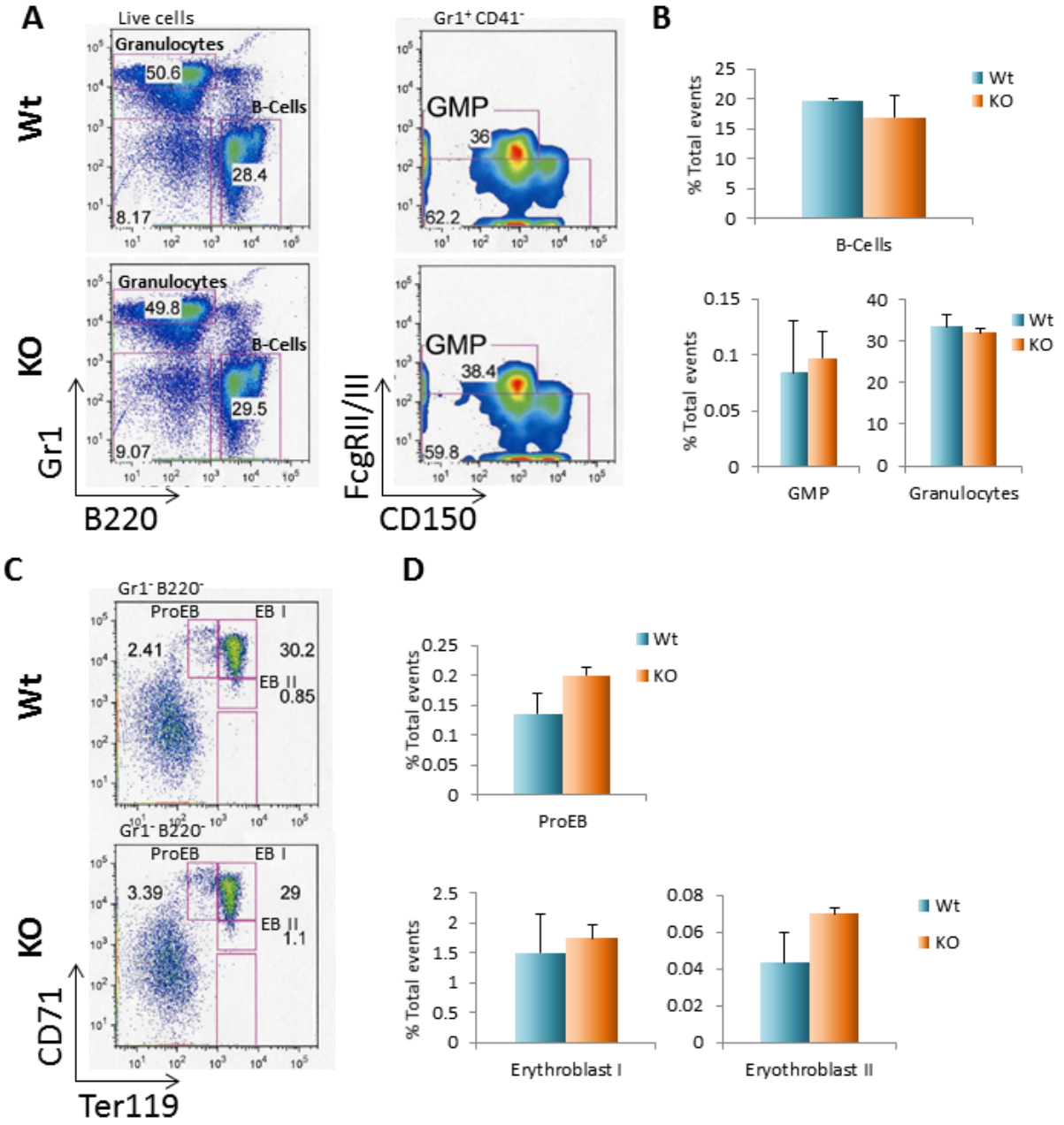

Figure 3.3 No hematopoietic lineage-specific defects observable in the marrow of *Phf8* KO mice. A) Flow analysis of B-cells, granulocytes and granulocyte-macrophage projenitors (GMPs) in bone marrow. B-cells=B220+, Granuloctytes=Gr1+, GMP=Gr1-B220-CD150-, FcgRII/III+. B) Quantification of data shown in A shown as a percentage of total events (wt n=2, KO n=3). C) Flow analysis for erythroid projenitors in bone marrow. ProEB=Gr1- B220- Ter119low CD71hi, EB I=Gr1- B220- Ter119hi CD71hi, EB II=Gr1- B220- Ter119low, CD71low. D) Quantification of C shown as percentage of total events (wt n=2, KO n=3).

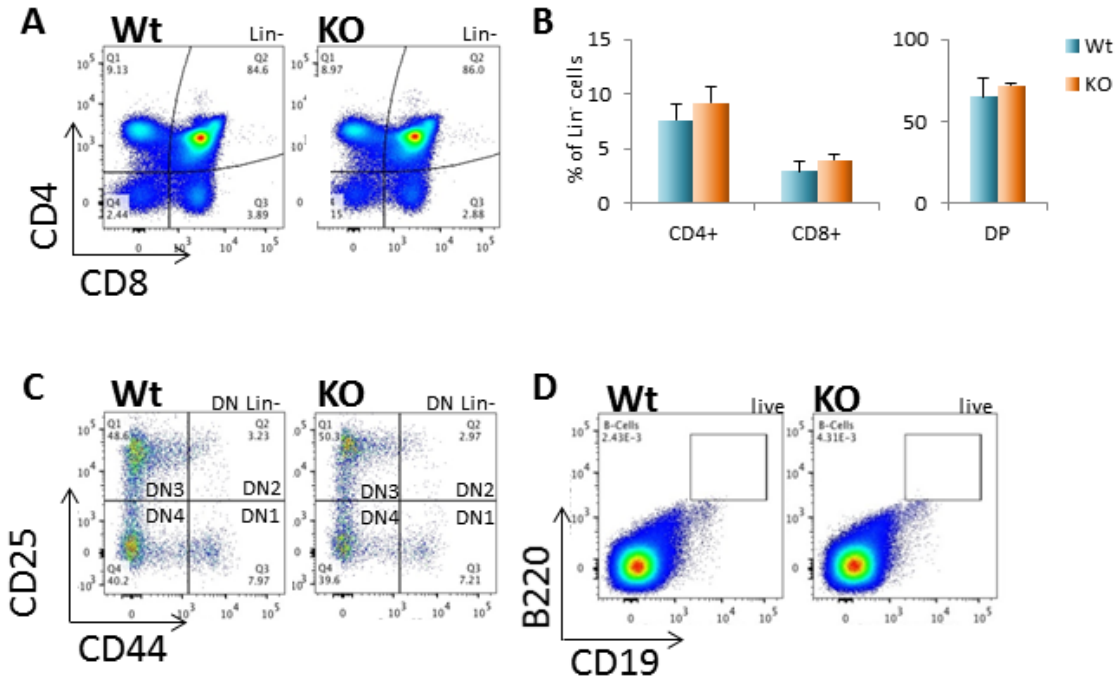

Figure 3.4 T-cell development proceeds as normal during hematopoiesis in the thymus of *Phf8* KO mice. A) Flow analysis of CD4/CD8 stain on lin- cells in the thymus. Double negative (DN) cells give rise to CD4+CD8+ (DP) cells which progress to become either CD4+ or CD8+ single positive cells. Lin=B220, Mac1 & Gr1. B) Quantification of A as percentage of parent gate (lin-) (n=3). C) DN stain of early T-cell development. Cells progress from DN1 to DN2 to DN3 and on to DN4 before becoming DP. DN1=CD4-CD8-CD44+CD25-, DN2=CD4-CD8-CD44+CD25+, DN3=CD4-CD8-CD44-CD25+, DN4=CD4-CD8-CD44-CD25-. D) Quantification of C, shown as percentage of parent, DN lin-. E) B-cell stain on the thymus of *Phf8* wt and KO mice. No B-cells (B220+CD19+) detected.

Additionally, we observed a significant reduction in the ratio of host derived $CD4^+$ and $CD8^+$ peripheral T-cells in the *Phf8* KO mice compared to WT mice at 8 weeks post-transplant (Fig. 3.5c). However, this difference largely disappeared at 16 weeks post-transplant (Fig. 3.5d), with B-cells being unaffected at either time point (Fig. 3.5c&d). This indicates a slight impairment in T-cell development within *Phf8* KO marrow, which is overcome over time. Analysis of the thymus of transplanted mice at 4 months did not indicate any obvious block in T-cell development in *Phf8* KO chimeras, although we did observe a very slight, albeit not statistically significant, trend toward an increase in the DN1 population at the expense of the DN2 population (Fig. 3.5f). As such, these data suggests that, although there is no perceptible difference in hematopoiesis under homeostatic conditions, very subtle defects in the LSK and downstream granulocyte populations, and T-cells can be unmasked in a competitive setting.

Discussion

PHF8 has been proposed to function as an oncogene in a number of cancers including T-ALL. This has primarily been demonstrated through *in vitro* knockdown and xenograft studies performed with cell lines. The primary goal of this study was to determine if a cleaner, genetic null mutation in an *in vivo* setting would behave similarly to these previously published results. To this end, we used the retroviral *NotchΔE* model, as it is well established, rapidly produces tumors in a high percentage of mice and, importantly, is Notch driven. If Phf8 was required to activate Notch signaling in the context of driving T-ALL, then we would expect *Phf8* KO chimeras to be resistant to leukemia formation. However, we observed that *Phf8* KO chimeras developed

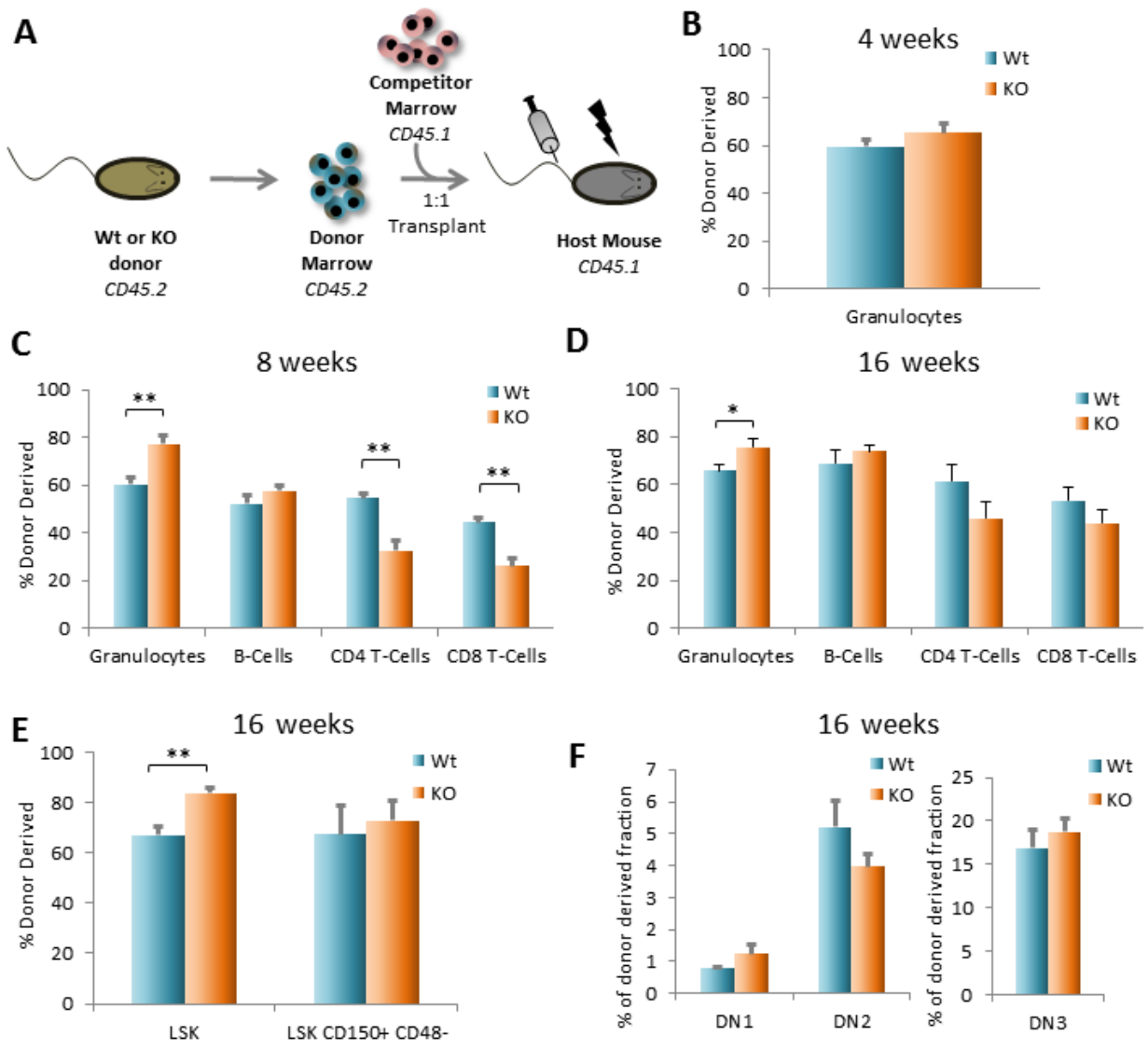

Figure 3.5 Subtle hematopoietic defects observed for *Phf8* KO marrow in a competitive setting. A) Experimental design for competitive transplants (wt n=4, KO n=5). B) Analysis of granulocytes in peripheral blood at 4 weeks post-transplant to confirm equal contribution. Granulocyte=Gr1+Mac1+, Donor=CD45.2+, Host/Competitor=CD45.1+. C) Analysis of peripheral blood at 8 weeks post-transplant. Subtle increases in granulocytes, possible reflecting an HSC phenotype and decreases in T-Cells are observed. B-cells=B220+CD19+, CD4T=CD4+, CD8T=CD8+. D) HSC analysis in the marrow at 16 weeks. E) Stain for splenic granulocytes and lymphocytes at 16 weeks. A subtle difference in granulocytes is observed but the T-cell defect seems to be compensated for. F) Thymic DN analysis at 16 weeks. DN1=CD4-CD8-CD44+CD25-, DN2=CD4-CD8-CD44+CD25+, DN3=CD4-CD8-CD44-CD25+. *=p<0.05, **=p<0.01.

leukemia with the same latency and severity as WT controls. This suggests that Phf8 is not only dispensable for T-ALL, but that it has no bearing on the progression of the disease in this model. There are many possible explanations for the discrepancy between these results and the previously published study. The simplest of these would be off-target effects of the shRNA used in the prior study, as only a single shRNA targeting Phf8 was used. It is further possible that the *in vitro* model did not properly recapitulate tumorigenesis *in vivo*; although the knockdown cell lines were used in a xenograft transplant, this is still a different context from T-ALL. Another possibility is that the acute knockdown of Phf8 in these cell lines caused undue stress that the genetic knockout was able to compensate for given a greater period of time. This possibility could have implications for Phf8 as a drug target in T-ALL, as it may indicate that resistance would be likely to develop after Phf8 inactivation. It is also possible that Phf8's role in T-ALL is highly context dependent. For example, the *NotchΔE* truncation is a very strong driver of T-ALL and it is conceivable that a weaker driver of T-ALL might be more acutely sensitive to the absence of *Phf8*. This raises an interesting possibility, which could be tested experimentally. If infection of *Phf8* KO marrow with a weaker driver of T-ALL, such as the *Notch-P12* mutation (Chiang *et al*. 2008), revealed an improvement in survival rate for the *Phf8* KO over the WT, then it would suggest that Phf8 does indeed play a key role in T-ALL and validate Phf8's potential as a drug target in a subset of mutational backgrounds. Whatever the reason for the inconsistencies, the previous authors presented a considerable amount of molecular characterization that suggested that PHF8 behaves as a coactivator for the ICN1-CSL-MAML complex in the T-ALL lines (Yatim *et al*. 2012). In addition to driving T-ALL, disruption of Notch signaling causes well-documented impairments in T-cell development (Tanigaki & Honjo 2007).

It is therefore possible that part of Phf8's normal function is to mediate Notch signaling during thymocyte development. Although we did not observe any defects during normal homeostasis that would support this idea, we were able to detect subtle defects in a competitive setting. It is likely that, as we saw in the brain, ESCs, and NPCs, loss of Phf8 only leads to very subtle changes in gene expression which are fully compensated for in the thymus during normal homeostasis and only manifest under a condition of extreme stress.

The remainder of the hematopoietic system was similarly unaffected by the loss of *Phf8*, with the only observable defect being a slight increase in the LSK population following a competitive transplant. The fact that we did not observe a similar defect as was reported by Cellot *et al*. (2013) is not entirely surprising considering a number of key differences in the experimental design of our studies. Cellot *et al*. (2013) infected LSK $CD150^{+}$ cells with a Phf8 shRNA during a 5-day *in vitro* culture, followed by a transplant into a sublethally irradiated mouse without competitor marrow. The study found a reduction in chimerism for the Phf8 knockdown cells, however, this was measured only by percentage of GFP+ cells in peripheral blood and no lineage-specific stains were done, making the data difficult to interpret. Furthermore, HSCs expand poorly *in vitro* and it has been demonstrated that their *in vitro* preservation is far more dependent on Notch signaling than their *in vivo* counterparts (Benveniste *et al*. 2014). It is therefore plausible that this *in vitro* culture step may have introduced additional variables.

Methods

Virus production

Platinum-E retroviral packaging cells (Cell Biolabs, Inc) were transfected using *Trans*IT transfection reagent (Mirus Bio) with pCL-Eco and either pMiGr-NotchΔE or pMiGr-empty vector. Media was changed after 12hrs and viral supernatant was collected at 48 and 72 hrs post transfection. Supernatant was concentrated in an ultracentrifuge by spinning an SW32 Ti rotor (Beckman Coulter) at 20,000rpm for 1hr and 30min at 4^{o}C. Virus was resuspended in PBS and stored at -80^{o}C. Virus was titered by infecting lineage depleted bone marrow and running a flow cytometric analysis for GFP.

Mice and transplants

For the T-ALL experiments, whole bone marrow was extracted, filtered and RBC lysis was performed for 7min on ice with ACK buffer (150mM ammonium chloride, 10mM potassium bicarbonate, 1mM EDTA) and quenched with full media (DMEM with 10% FBS). Bone marrow was lineage depleted by incubating in PBS 3% serum for 30min on ice with a 5ul/million cells of a cocktail of biotinylated lineage antibodies (Mac1, Gr1, B220, CD3e & Ter119; eBioscience) diluted 1:20. Cells were washed and incubated with streptavidin-coated Dynabeads (Life Technologies) for 30min on ice. The unbound fraction was washed and prestimulated with cytokines (SCF 50ng/ml, Flt3 50ng/ml, Il-3 10ng/ml and Il-6 10ng/ml) in StemSpan SFEM (Stemcell Technologies) for 48 hours. 1million cells were infected with virus containing either *NotchΔE* or empty vector control. Cells were transduced with virus for an additional 48hrs in

SFEM. Following infection, infected cells were split equally among 6 experimental mice, mixed with 2 x 10^5 unfractionated rescue marrow (CD45.1) and transplanted retro-orbitally into lethally irradiated (2 x 600rads) host mice(CD45.1). Mice were analyzed every 3wks to track progression through retro-orbital bleeds. Mice were allowed to develop leukemia and sacrificed when morbid for the generation of the Kaplan-Meier survival curve. For secondary transplants, bone marrow was extracted, RBC lysed and sorted for GFP on an Aria III (BD Biosciecnes). 5 x 10^4 GFP^+ cells were transplanted into sublethally irradiated (450rads) host mice (CD45.1).
For the competitive transplants, whole bone marrow was extracted from donor mice (CD45.2) and RBC lysed. 1 x 10^6 cells were mixed 1:1 with competitor marrow (CD45.1) and transplanted retro-orbitally into lethally irradiated (2 x 600rads) host mice (CD45.1). Mice were analyzed through retro-orbital bleeds at 4, 8 and 16wks.

Flow Cytometry Analysis

Blood was collected from retro-orbital bleeds and RBCs were lysed in ACK buffer (see above). Cells were pelleted and stained with 1ul of fluorochrome-conjugated antibody per 5 million cells for 1hr on ice in PBS with 3% serum. Cells were washed twice and resuspended in PBS-serum with either DAPI or 7-AAD and filtered through 45 micron mesh for analysis on an LSR-II (BD Biosciences), data was further processed in FloJo. The Gr-1 antibody was purchased from BD Biosciences and Sca-1 from Biolegend, all other antibodies used for flow cytometry were purchased from eBioscience.

Western Blot

Whole cell extract was run on 10% SDS-PAGE gels at 150V until separated and transferred at 4^{o}C for overnight at 20V (Phf8) onto a PVDF membrane. Membranes were blocked in 5% milk PBS-T (1X PBS, 0.1% Tween-20) for 30min at RT then incubated with primary antibodies(Phf8 Abcam ab36068) for 1hr in block at RT. Membranes were washed in PBS-T, and incubated in the appropriate horseradish-peroxidase-conjugated secondary for 45min at RT. Membranes were then washed again and visualized using ECL reagents (Pierce).

Tissue Preparation

Harvested tissues were fixed overnight at 4^{o}C in 10% neutral buffered formalin, then washed in PBS, embedded in paraffin, sectioned and mounted onto slides. Mounted sections were stained with hematoxalin and eosin and imaged on a light microscope.

Chapter 4

Discussion and Future Directions

Summary of thesis work

Phf8 is a recently identified histone demethylase with ties to cancer, craniofacial development and behavior (Laumonnier *et al*. 2005; Abidi *et al*. 2007; Koivisto *et al*. 2007; Bjorkman *et al*. 2012; Yatim *et al*. 2012; Arteaga *et al*. 2013; Sun *et al*.2013; Shen *et al*. 2014). The goal the thesis work presented here was to generate and characterize a knockout mouse model for *Phf8* to assess its role in these processes in a mammalian model system. To this end, we generated a null allele of *Phf8* using conventional gene targeting in ESCs to remove the catalytic *JmjC* domain. Mice null for *Phf8* are not protected from developing T-ALL, however they do display subtle signs of defects in T-cell and hematopoietic progenitor development. We further find that loss of *Phf8* is compatible with mammalian development and is not sufficient to cause clefting in mice. Importantly, we report that *Phf8* KO mice are resilient to anxiety and depression, which has not previously been documented. We propose that the resilient phenotype observed here is likely due to the de-repression of serotonin receptors within the prefrontal cortex, which we have identified as direct targets of Phf8.

Phf8's role in tumorigenesis

Although Phf8 has been implicated as an oncogene in multiple cancers, its role in these tumors had previously not been validated with a genetic knockout model *in vivo*. Here we present the first such study using our *Phf8* knockout mouse and a mouse model for T-ALL driven by a constitutively active form of Notch1. Surprisingly, we observed that loss of *Phf8* had no bearing on the development or progression of T-ALL. This result would suggest that Phf8 is not

a critical regulator of Notch signaling in T-ALL, which contrasts with previous data. It remains possible, however, that Phf8 could still function as an oncogene in the context of other cancers and possibly even if a weaker driver of T-ALL were used as a model. Our knockout mouse might thus be very useful to dissect Phf8's role in additional cancer models, and in alternative T-ALL models. A genetic model of prostate cancer (Wang *et al*. 2003) or the use of a less-potent T-ALL driver mentioned previously (Chiang *et al*. 2008) would be obvious choices in dissecting this role.

Regulation of T-cell development by Phf8

The proposed role for Phf8 in driving T-ALL involved its activity as a co-activator for the Notch pathway (Yatim *et al*. 2012). Several of these Notch target genes are of central importance to T-cell development (Koch & Radtke 2011), therefore we analyzed our *Phf8* KO mice for defects here. Though subtle, we were able to observe a defect in the generation of CD4 and CD8 T-cells in a competitive setting. While it is likely that this is due to Notch activity, further study of our knockout mouse could be helpful in the elucidation of Phf8's role here. Notch is present throughout early T-cell development, with evidence that it is absolutely essential in the DN1 and DN3 stage (Koch & Radtke 2011). While we analyzed *Phf8* knockout mice for signs of a loss of Notch signal – i.e. ectopic B-cell development in the thymus – we were unable to uncover any defects. However, it remains possible that the molecular analysis of the DN1 or DN3 population, perhaps by comparing expression levels of key Notch target genes between *Phf8* KO and WT, could uncover more of Phf8's function in the thymus. Additionally, Phf8's role in Notch signaling has thus far only been demonstrated in transformed

cell lines. It would therefore also be interesting to analyze Notch targets for the presence of Phf8 and its histone methyl-lysine substrates by ChIP in *Phf8* KO and WT mice.

Lack of craniofacial defects in Phf8 *KO mice*

Several reports have indicated that loss of function mutations of *PHF8* in humans contribute to the development of cleft lip and palate (Laumonnier *et al*. 2005; Abidi *et al*. 2007; Koivisto *et al*. 2007), though we detected no evidence of this in our knockout mouse. Although this was unexpected, it is notable that even in the families in which *PHF8* mutations were identified, clefting was not 100% penetrant. This observation and our data suggest that there are likely additional factors, which interact with Phf8 to contribute to cleft lip and palate. Further analysis of our knockout mouse may be able to identify some of these; although, it is not immediately clear what they may be, as multiple signaling pathways have been implicated in the process of clefting including the Tgf-β, Fgf, and Shh signaling pathways. Perhaps some light could be shed on Phf8's role in craniofacial development through the analysis of neural crest stem cells, which are an *in vitro* representation of the cells that will go on to form, among other structures, the palate (Teng & Labosky 2006). RNA-seq and ChIP-seq analyses could be used here to identify target genes of Phf8 specific to the developing neural crest and therefore more likely to contribute to clefting. With likely targets identified, it would be possible to cross the *Phf8* KO mice with additional mouse models of the identified targets to determine if loss of *Phf8* in other mutant backgrounds leads to clefting phenotypes.

Behavioral functions of Phf8

The first published study of Phf8 was a case study linking it to familial intellectual disability (Laumonnier *et al*. 2005). It was therefore surprising that we did not detect signs of this disability in our mice. We probed the *Phf8* knockout mice for signs of defects in working memory through the use of a radial arm maze and learning through contextual fear conditioning. Neither of these assays gave any indication that *Phf8* KO mice have an intellectual deficit on a 129S4/SvJaeJ background. We cannot, however, rule out a defect in memory consolidation nor that loss of *Phf8* may display intellectual disability in a different mouse strain. Subjecting the *Phf8* KO mice to a Morris water maze paradigm (D'Hooge & De Deyn 2001) would allow for the measurement of memory consolidation and it would be highly interesting to see the consequences of *Phf8* loss in this context. Additionally, outcrossing our *Phf8* KO allele to alternate strains of mice and subjecting them to the same behavioral tests could possibly reveal a strain specific effect for *Phf8* loss. Though beyond the scope of what we were able to assess in this study, these would be important next steps in the behavioral analysis of the *Phf8* null mouse.

Temporal requirement for Phf8

We have demonstrated that the loss of *Phf8* in mice leads to resiliency towards anxiety and depression; however, it remains unknown whether it is *Phf8*'s role during development or in the adult that is important in conferring this phenotype. It would therefore be of interest to assess the temporal requirement for *Phf8* with regard to these phenotypes. This could be done by exposing our targeted *Phf8* allele (Fig. 2.1a) to FLPase instead of Cre, which will result in the

removal of the Neomycin-resistance cassette and generation of a conditional knockout allele (*Phf8* cKO). Mice carrying the *Phf8* cKO allele could be crossed to a *Rosa26-Cre*^{ERT2} line, which would allow for the deletion of *Phf8* at multiple time points during development and in the adult via tamoxifen injection.

Allelic similarities between mouse and human

The *Phf8* KO allele which we've generated by deleting the catalytic *jmjC* domain is a model for the *jmjC*-disrupting mutations found in patients. As such, we expect that molecularly it would behave similarly to human alleles; however, it was not possible for us to demonstrate this here. Therefore, it may be interesting to compare the function of our knockout allele to alleles similar to those described in patients and, indeed, to compare the different human mutations to each other. This could be achieved by using CRISPR/Cas to quickly introduce the mutations found in patients (three point mutations and one 12bp deletion) into mouse ESCs. Cells harboring these mutations could then be assayed for growth rates, histone methylation levels, and gene expression and compared to our original KO allele. If differences were observed between our allele and any of those found in patients, mice could be made from one or more of these ESC lines and assessed for cleft palate, resiliency and intellectual disability to demonstrate whether or not allelic differences can account for different phenotypic outcomes. We find this an unlikely scenario, however, given the previously-mentioned predicted similarities in protein products for all of these alleles.

Repressive activity of Phf8

The observation that loss of Phf8 leads to the upregulation of a number of its direct targets is not novel (Fortschegger *et al*. 2010; Wang *et al*. 2014), however the mechanisms are unclear given its substrate specificity for repressive marks. Nevertheless, the data we report here would indicate that gene repression is an important part of Phf8's function in controlling behavior and therefore certainly worth investigating. Among the first of these experiments that should be done is to confirm in cell culture that Phf8 is functionally competent to repress a transgenic reporter construct containing the *Htr1a* promoter upstream of a minimal CMV-driven luciferase cDNA. One caveat here may be the choice of cell type, with NPCs being the closest *in vitro* expandable option, however short term culture of primary cortical neurons is possible and this exists as an option if the regulation of *Htr1a* by Phf8 should require cell-type specific cofactors. Following that, the identification of additional cofactors of Phf8 through immunoprecipitation and subsequent mass-spectrometry in NPCs may help to shed more light on the mechanisms of Phf8's repressive function. Alternatively, human PHF8 has been shown to act with the repressive demethylase LSD1 (Yatim *et al*. 2012), and it is possible that this factor is in part responsible for Phf8-mediated repression. Additional ChIP experiments for Lsd1 in the cortex of *Phf8* KO and WT mice could serve to determine whether Lsd1 co-occupies these repressed promoter targets with Phf8 and if this occupancy is at all dependent upon Phf8.

Linking resiliency and serotonin regulation by Phf8 to humans

Our finding that loss of Phf8 contributes to resiliency to anxiety and depression in mice could have significant implications to the treatment of these disorders. An important question that remains, however, is whether PHF8 may function similarly in contributing to resiliency in

humans. To date, there has not been a study linking *PHF8* to resiliency to an anxiety disorder or depression in humans. However, identifying factors related specifically to resiliency was not the purpose of the majority of the anxiety and depression GWAS studies and would likely have required the use of a "resilient" control group, which experienced a stressful life event, but did not develop an anxiety disorder or depression. Even still, the identification of common variants associated with anxiety disorders or depression has historically been difficult (Flint & Kendler 2014). It should also be considered that a number of factors functionally linked to resiliency have yet to be linked to these disorders in these large scale genetics studies. Given the difficulties of the human genetics in these conditions, it would be interesting to see the expression of PHF8 in the post-mortem tissue from patients with and without depression or anxiety, particularly in cases where both patients were exposed to a significant life stressor.

Here we have further demonstrated a novel role for Phf8 in the regulation of serotonin receptors within the prefrontal cortex. It is currently unknown if Phf8 similarly regulates these receptors in human neurons, though data from human ESCs suggests that PHF8 does at least bind *HTR1A* and *HTR1B* (Ram *et al*. 2011). It is possible to differentiate human cortical neurons *in vitro* from ESCs (Shi *et al*. 2012), which could serve as a good system to study PHF8's function in the relevant human cells. ChIP for Phf8 in these *in vitro* differentiated cortical neurons should reveal whether the serotonin receptors are targets of PHF8 in human cortical neurons. In parallel, knockdown or CRISPR mediated knockout of PHF8 could be used to confirm that these receptors are similarly negatively regulated by PHF8. Together these approaches should be able to determine how our findings in the mouse translate to the human.

Closing Remarks

The histone demethylase Phf8 has been linked to a diverse set of biologic processes; however, these had yet to be functionally assessed *in vivo* in a mammalian genetic system. I have presented here the first characterization of a *Phf8* null mammalian model. Our data and those of others are consistent with a subtle, fine-tuning role of Phf8 in the regulation of gene expression. This activity appears to be primarily redundant *in vivo*; *Phf8*'s loss leads to very few molecular changes the majority of which do not seem to affect the development of the animal. Nevertheless, these subtle changes are sufficient to affect complex behaviors, as was indicated from the human genetics and as we have now shown in the mouse. Though unexpected, our findings, which demonstrate a novel role for Phf8 in the regulation of serotonin signaling and resiliency, could have important implications relevant to the treatment of anxiety and depression, given that Phf8 is a druggable enzyme (Upadhyay *et al*. 2012). Going forward, it will be important to determine the degree to which these findings are generalizable to the human condition.

Chapter 5

References

1. Abidi F, Miano M, Murray J, and Schwartz C. 2007. A novel mutation in the PHF8 gene is associatd with X-linked mental retardation with cleft lip/cleft palate. *Clin Genet* 72(1):19-22.

2. Adamec R, Toth M, Haller J, Halasz J, and Blundell J. 2012. A comparison of activation patterns of cells in selected prefrontal cortical and amygdala areas of rats which are more or less anxious in response to predator exposure or submersion stress. *Physiol Behav*. 105(3):628-38.

3. Albert PR. 2012. Transcriptional regulation of the 5-HT1A receptor: implications for mental illness. *Philos Trans R Soc Lond B BIol Sci*. 367(1601):2402-15.

4. Anguelova M, Benkelfat C, and Turecki G. 2003. A systematic review of association studies investigating genes coding for serotonin receptors and the serotonin transporter: I. affective disorders. *Mol Psychiatry*. 8(6):574-91.

5. Anisman H, Du L, Palkovits M, Faludi G, Kovacs GG, Szontagh-Kishazi P, Merali Z, and Poulter MO. 2008. Serotonin receptor subtype and p11 mRNA expression in stress-relevant brain regions of suicide and control subjects. J Psychiatry Neurosci. 33(2):131-41.

6. Arteaga MF, Mikesch JH, Qui J, Christensen J, Helin K, Kogan SC, Dong S, and So CW. 2013. The histone demethylase PHF8 governs retinoic acid response in acute promyelocytic leukemia. *Cancer Cell*. 23(3):376-89.

7. Austin MC, Whitehead RE, Edgar CL, Janosky JE, and DA Lewis. 2002. Localized decrease in serotonin transporter-immunoreactive axons in the prefrontal cortex of depressed subjects committing suicide. *Neuroscience*. 114(3):807-15.

8. Avgustinovich DF, Kovalenko IL, and Kudryavtseva NN. 2005. A model of anxious depression: persistence of behavioral pathology. *Neurosci Behav Physiol*. 35(9):917-24.

9. Baba A, Ohtake F, Okuno Y, Yokota K, Okada M, Imai Y, Ni M, Meyer CA, Igarashi K, Kanno J, Brown M, and Kato S. 2011. PKA-dependent regulation of the histone lysine demethylase complex PHF2-ARID5B. *Nat Cell Biol*. 13(6):668-75.

10. Bannister AJ, Zegerman P, Partridge JF, Miska EA, Thomas JO, Allshire RC, and Kouzarides T. 2001. Selective recognition of methylated lysine 9 on histone H3 by the HP1 chromo domain. *Nature*. 410(6824):120-4

11. Benveniste P, Serra P, Dervovic D, Herer E, Knowles G, Mohtashami M, and Zuniga-Pflucker JC. 2014. Notch signals are required for *in vitro* but not *in vivo* maintenance of human hematopoietic stem cells and delay the appearance of multipotent progenitors. *Blood*. 123(8):1167-77.

12. Bernstein BE, Mikkelsen TS, Xie X, Kamal M, Huebert DJ, Cuff J, Fry B, Meissner A, Wernig M, Plath K, Jaenisch R, Wagschal A, Feil R, Schreiber SL, and Lander ES. 2006. A bivalent chromatin structure marks key developmental genes in embryonic stem cells. *Cell*. 125(2):315-26.

13. Bianchi P, Ciani E, Guidi S, Trazzi S, Felice D, Grossi G, Fernandez M, Giuliani A, Calzà L, and Bartesaghi R. 2010. Early pharmacotherapy restores neurogenesis and cognitive performance in the Ts65Dn mouse model for Down syndrome. *J Neurosci*. 30(26):8769-79.

14. Bjorkman M, Ostling P, Harma V, Virtanen J, Mpindi JP, Rantala J, Mirtti T, Vesterinen T, Lundin M, Sankila A, Rannikko A, Kaivanto E, Kohonen P, Kallioniemi O, and Nees M.

2012. Systematic knockdown of epigenetic enzymes identifies a novel histone demethylase PHF8 overexpressed in prostate cancer with an impact on cell proliferation, migration and invasion. *Oncogene*. 31(29):3444-56.

15. Blier P, and Ward NM. 2003. Is there a role for 5-HT1A agonists in the treatment of depression? *Biol Psyichiatry*. 53(3):193-203.

16. Bystritsky A. 2006. Treatment-resistant anxiety disorders. *Mol Psychiatry*. 11(9):805-14.

17. Caspi A, Sugden K, Moffitt TE, Taylor A, Craig IW, Harrington HL, McClay J, Mill J, Martin J, Braithwaite A, and Poulton R. 2003. Influence of life stress on depression: moderation by a polymorphism in the 5-HTT gene. *Science*. 301(5631):386-9.

18. Castagne V, Moser P, Roux S, and Porsolt RD. 2011. Rodent models of depression: forced swim and tail suspension behavioral despair tests in rats and mice. *Curr Protoc Neurosci*. Chapter 8: Unit 10A.

19. Cellot S, Hope KJ, Chagraoui J, Sauvageau M, Deneault E, MacRae T, Mayotte N, Wilhelm BT, Landry JR, Ting SB, Krosl J, Humphries K, Thompson A, and Sauvageau G. 2013. RNAi screen identifies Jarid1b as a major regulator of mouse HSC activity. *Blood*. 122(9):1545-55.

20. Chiang MY, Xu, L, Shestova O, Histen G, L'heureux S, Romany C< Childs ME, Gimotty PA, Aster JC, and Pear WS. 2008. Leukemia-associated NOTCH1 alleles are weak tumor initiators but accelerate K-ras-initiated leukemia. *J Clin Invest*. 118(9):3181-94.

21. Cloos PA, Christensen J, Agger K, Maiolica A, Rappsilber J, Antal T, Hansen KH, and Helin K. 2006. The putative oncogene GASC1 demethylates tri- and dimethylated lysine 9 on histone H3. *Nature*. 442(7100):307-11.

22. Covington HE 3rd, Lobo MK, Maze I, Vialou V, Hyman JM, Zaman S, LaPlant Q, Mouzon E, Ghose S, Tamminga CA, Neve RL, Deisseroth K, and Nestler EJ. 2010. Antidepressant effect of optogenetic stimulation of the medial prefrontal cortex. *J Neurosci*. 30(48):16082-90.

23. D'Hooge R, and De Deyn PP. 2001. Applications of the Morris water maze in the study of learning and memory. *Brain Res Rev*. 36(1):60-90.

24. Davis M, Walker DL, Miles L, and Grillon C. 2010. Phasic vs sustained fear in rats and humans: role of the extended amygdala in fear vs anxiety. *Neuropsychopharmacology*. 35(1):105-35.

25. Demas GE, Nelson RJ, Krueger BK, and Yarowsky PJ. 1996. Spatial memory deficits in segmental trisomic Ts65Dn mice. *Behav Brain Res*. 82(1):85-92.

26. Dhalluin C, Carlson JE, Zeng L, He C, Aggarwal AK, and Zhou MM. 1999. Structure and ligand of a histone acetyltransferase bromodomain. *Nature*. 399(6735):491-6.

27. Drevets WC, Frank E, Price JC, Kupfer DJ, Greer PJ, and Mathis C. 2000. Serotonin type-1A receptor imaging in depression. *Nucl Med Biol*. 27:499-507.

28. Fava M. Rankin MA, Wright EC, Alpert JE, Nierenberg AA, Pava J, and Rosenbaum JF. 2000. Anxiety disorders in major depression. *Compr Psychiatry*. 41(2):97-102

29. Feng W, Yonezawa M, Ye J, Jenuwein T, and Grummt I. 2010. PHF8 activates transcription of rRNA genes through H3K4me3 binding and H3K9me1/2 demthylation. *Nat Struct Mol Biol*. 17(4):445-50.

30. Fischle W, Wang Y, Jacobs SA, Kim Y, Allis CD, and Khorasanizadeh S. Molecular basis for the discrimination of repressive methyl-lysine marks in histone H3 by Polycomb and HP1 chromodomains. *Genes Dev*. 17(15):1870-81.

31. Flint J, and Kendler KS. 2014. The genetics of major depression. *Neuron*. 81:484-503.

32. Fortschegger K, de Graaf P, Outchkourov NS, van Schaik FM, Timmers HT, and Shiekhattar R. 2010. PHF8 targets histone methylation and RNA polymerase II to activate transcription. *Mol Cell Biol*. 30(13):3286-98.

33. Francis NJ, Saurin AJ, Shao Z, and Kingston RE. 2001. Reconstitution of a functional core polycomb repressive complex. *Mol Cell*. 8(3):545-56.

34. Furlong RA, Ho L, Walsh C, Rubinsztein JS, Jain S, Paykel ES, Easton DF, and Rubinsztein DC. 1998. Analysis and meta-analysis of two serotonin transporter gene polymorphisms in bipolar and unipolar affective disorders. *Am J Med Genet*. 81(1):58-63.

35. Gatt JM, Burton KLO, Williams LM, and Schofield PR. 2014. Specific and common genes implicated across major mental disorders: a review of meta-analysis studies. *J Psychiatr Res*. 60:1-13.

36. Gorman JM. 1996. Comorbid depression and anxiety spectrum disorders. *Depress Anxiety*. 4(4):160-8.

37. Grabher C, von Boehmer H, and Look AT. 2006. Notch 1 activation in the molecular pathogenesis of T-cell acute lymphoblastic leukaemia. *Nat Rev Cancer.* 6(5):346-59.

38. Gross C, Zhuang X, Stark K, Ramboz S, Oosting R, Kirby L, Santarelli L, Beck S, and Hen R. 2002. Serotonin1A receptor acts during development to establish normal anxiety-like behavior in the adult. *Nature*. 416(6879):396-400.

39. Gyekis JP, Yu W, Dong S, Wang H, Qian J, Kota P, and Yang J. (2013). No association of genetic variants in BDNF with major depression: a meta- and gene-based analysis. *Am J Med Genet B Neuropsychiatr Genet*. 162B: 61–70.

40. Hasenpusch-Theil K, Chadwick BP, Theil T, Heath SK, Wilkinson DG, and Frischauf AM. 1999. PHF2, a novel PHD finger gene located on human chromosome 9q22. *Mamm Genome*. 10(3):294-8.

41. Hassan AH, Awad S, Al-Natour Z, Othman S, Mustafa F, and Rizvi TA. 2007. Selective recognition of acetylated histones by bromodomains in transcriptional co-activators. *Biochem J*. 402(1):125-33.

42. Heim C, and Nemeroff CB. 1999. The impact of early adverse experiences on brain systems involved in the pathophysiology of anxiety and affective disorders. *Biol Psychiatry*. 46(11):1509-22.

43. Heredia L, Torrente M, Colomina MT, and Domingo JL. 2014. Assessing anxiety in C57BL/6J mice: a pharmacological characterization of the open-field and light/dark tests. *J Pharmacol Toxicol Methods*. 69:108-114.

44. Højfeldt JW, Agger K, and Helin K. 2013. Histone lysine demethylases as targets for anticancer therapy. *Nat Rev Drug Discov*. 12(12):917-30.

45. Horton JR, Upadhyay AK, Qi HH, Zhang X, Shi Y, and Cheng X. 2009. Enzymatic and structural insights for substrate specificity of a family of jumonji histone lysine demethylases. *Nat Struct Mol Biol*. 17(1):38-43.

46. Huang C, Xiang Y, Wang Y, Li X, Xu L, Zhu Z, Zhang T, Zhu Q, Zhang K, Jing N, and Chen CD. 2010. Dual-specificity histone demethylase KIAA1718 (KDM7A) regulates neural differentiation through FGF4. *Cell Res*. 20(2):154-65.

47. Jenuwein T, and Allis CD. 2001. Translating the histone code. *Science*. 293:1074-80.

48. Jin C, Xu W, Yuan J, Wang G, and Cheng Z. 2013. Meta-analysis of association between the -1438A/G (rs6311) polymorphism of the serotonin 2A receptor gene and major depressive disorder. *Neurol Res*. 35(1):7-14.

49. Kessler RC, Chiu WT, Demler O, and Walters EE. 2005. Prevalence, severity and comorbidity of 12-month DSM-IV disorders in the national comorbidity survey replication. *Arch Gen Psychiatry*. 62(6):617-627.

50. Kessler RC, McGonagle KA, Zhao S, Nelson CB, Hughes M, S Eshleman, Wittchen HU, and Kendler KS. 1994. Lifetime and 12-month prevalence of DSM-III-R psychiatric disorders in the United States. Results from the national comorbidity survey. *Arch Gen Psychiatry*. 51(1):8-19.

51. King B, Trimarchi T, Reavie L, Xu L, Mullenders J, Ntziachristos P, Aranda-Orgilles B, Perez-Garcia A, Shi J, Vakoc C, Sandy P, Shen SS, Ferrando A, and Aifantis I. 2013. The ubiquitin ligase FBXW7 modulates leukemia-initiating cell activity by regulating MYC stability. *Cell*. 153(7):1552-66.

52. Kishi T, Tsunoka T, Ikeda M, Kawashima K, Okochi T, Kitajima T, Kinoshita Y, Okumura T, Yamanouchi Y, Inada T, Ozaki N, and Iwata N. 2009. Serotonin 1A receptor gene and major depressive disorder: an association study and meta-analysis. *J Hum Genet*. 54(11):629-33.

53. Kishi T, Yoshimura R, Fukuo Y, Okochi T, Matsunaga S, Umene-Nakano W, Nakamura J, Serretti A, Correll CU, Kane JM, and Iwata N. 2013. The serotonin 1A receptor gene confer susceptibility to mood disorders: results from an extended meta-analysis of patients with major depression and bipolar disorder. *Eur Arch Psychiatry Clin Neurosci*. 263(2):105-18.

54. Kleine-Kohlbrecher D, Christensen J, Vandamme J, Abarrategui I, Bak M, Tommerup N, Shi X, Gozani O, Rappsilber J, Salcini AE, and Helin K. 2010. A functional link between histone demethylase PHF8 and transcription factor ZNF711 in X-linked mental retardation. *Mol Cell*. 38(2):165-78.

55. Klose RJ, Yamane K, Bae Y, Zhang D, Erdjument-Bromage H, Tempst P, Wong J, and Zhang Y. 2006. The transcriptional repressor JHDM3A demethylates trimethyl histone H3 lysine 9 and lysine 36. *Nature*. 442(7100):312-6.

56. Koch U, and Radtke F. 2011. Mechanisms of T cell development and transformation. *Ann Rev Cell Dev Biol*. 27:539-62.

57. Koivisto AM, Ala-Mello S, Lemmelä S, Komu HA, Rautio J, and Järvelä I. 2007. Screening of mutations in the PHF8 gene and identification of a novel mutation in a Finnish family with XLMR and cleft lip/cleft palate. Clin Genet. 72(2):145-9.

58. Kopan R, and Ilagan MX. 2009. The canonical Notch signaling pathway: unfolding the activation mechanism. *Cell*. 137(2):216-33.

59. Kooistra SM, and Helin K. 2012. Molecular mechanisms and potential functions of histone demethylases. *Nat Rev Mol Cell Biol*. 13(5)297-311.

60. Kouzarides T. 2007. Chromatin modifications and their function. *Cell*. 128(4):693-705.

61. Krishnan V, Han MH, Graham DL, Berton O, Renthal W, Russo SJ, LaPlant Q, Graham A, Lutter M, Lagace DC, Ghose S, Reister R, Tannous P, Green TA, Neve RL, Chakravarty S, Kumar A, Eisch AJ, Self DW, Lee FS, Tamminga CA, Cooper DC, Gershenfeld HK, and Nestler EJ. 2007. Molecular adaptations underlying susceptibility and resistance to social defeat in brain reward regions. *Cell*. 131:391-404.

62. Kulesskaya N, and Voikar V. 2014. Assessment of mouse anxiety-like behavior in the light-dark box and open-field arena: role of equipment and procedure. *Physiol Behav*. 133:30-38.

63. Kusserow H, Davies B, Hortnagl H, Voigt I, Stroh T, Bert B, Deng DR, Fink H, Veh RW and Theuring F. 2004. Reduced anxiety-related behavior in transgenic mice overexpressing serotonin$_{1A}$ receptors. *Mol Brain Res*. 129:104-16.

64. Lachner M, O'Carroll D, Rea S, Mechtler K, and Jenuwein T. 2001. Methylation of histone H3 lysine 9 creates a binding site for HP1 proteins. *Nature*. 410(6824):116-20.

65. Lasky-Su JA, Faraone SV, Glatt SJ, and Tsuang MT. 2005. Meta-analysis of the association between two polymorphisms in the serotonin transporter gene and affective disorders. *Am J Med Genet B Neuropsychiatr Genet*. 133B(1):110-5.

66. Laumonnier F, Holbert S, Ronce N, Faravelli F, Lenzer S, Schwartz CE, Lespinasse J, Van Esch H, Lacombe D, Goizet C, Phan-Dinh Tuy F, van Bokhoven H, Fryns JP, Chelly J, Ropers HH, Moraine C, Hamel BC, and Briault S. 2005. Mutations in PHF8 are associated with X linked mental retardation and cleft lip/cleft palate. *J Med Genet*. 42(10):780-6.

67. Lee HJ, Lee MS, Kang RH, Kim H, Kim SD, Kee BS, Kim YH, Kim YK, Kim JB, Yeon BK, Oh KS, Oh BH, Yoon JS, Lee C, Jung HY, Chee IS, and Paik IH. 2005. Influence of the serotonin transporter promoter gene polymorphism on susceptibility to posttraumatic stress disorder. *Depress Anxiety*. 21(3):135-9.

68. Li B, Carey M, Workman JL. 2007. The role of chromatin during transcription. *Cell*. 128(4):707-19.

69. Li H, Ilin S, Wang W, Duncan EM, Wysocka J, Allis CD, and Patel DJ. 2006. Molecular basis for site-specific read-out of histone H3K4me3 by the BPTF PHD finger of NURF. *Nature*. 442(7098):91-5.

70. Lira A, Zhou M, Castanon N, Ansorge MS, Gordon JA, Francis JH, Bradley-Moore M, Lira J, Underwood MD, Arango V, Kung HF, Hofer MA, Hen R, and Gingrich JA. 2003. Altered depression-related behaviors and functional changes in the dorsal raphe nucleus of serotonin transporter-deficient mice. *Biol Psychiatry*. 54(10):960-71.

71. Liu W, Tanasa B, Tyurina OV, Zhour TY, Gassmann R, Liu WT, Ohgi KA, Benner C, Garcia-Bassets I, Aggarwal AK, Desai A, Dorrestein PC, Glass CK, and Rosenfeld MG. 2010. PHF8 mediates histone H4 lysine 20 demethylation events involved in cell cycle progression. *Nature*. 466(7305):508-12.

72. Loenarz C, Ge W, Coleman ML, Rose NR, Cooper CD, Klose RJ, Ratcliffe PJ, and Schofield CJ. 2010. PHF8, a gene associated with cleft lip/palate and mental retardation, encodes for an Nepsilon-dimethyl lysine demethylase.

73. Lopez-Figueroa AL, Norton CS, Lopez-Figueroa MO, Armellini-Dodel D, Burke S, Akil H, Lopez JF, and Watson SJ. Serotonin 5-HT1A, 5-HT1B, and 5-HT2A receptor mRNA expression in subjects with major depression, bipolar disorder and schizophrenia. *Biol Psychiatry*. 55(3):225-33.

74. Lopez-Leon S, Janssens AC, Gonzalez-Zuloeta Ladd AM, Del-Favero J, Claes SJ, Oostra BA, and van Duijn CM. 2008. Meta-analyses of genetic studies on major depressive disorder. *MolPsychiatry*. 13(8):772-85.

75. Luger K, Mäder AW, Richmond RK, Sargent DF, and Richmond TJ. 1997. Crystal structure of the nucleosome core particle at 2.8 A resolution. *Nature*. 389(6648):251-60.

76. Ma Q, Chen Z, Jia G, Lu X, Xie X, and Jin W. 2015. The histone demethylase PHF8 promotes prostate cancer cell growth by activating the oncomiR miR-125b. *Onco Targets Ther*. 8:1979-88.

77. Mikkelsen TS, Ku M, Jaffe DB, Issac B, Lieberman E, Giannoukos G, Alvarez P, Brockman W, Kim TK, Koche RP, Lee W, Mendenhall E, O'Donovan A, Presser A, Russ C, Xie X, Meissner A, Wernig M, Jaenisch R, Nusbaum C, Lander ES, and Bernstein BE. 2007. Genome-wide maps of chromatin state in pluripotent and lineage-committed cells. *Nature*. 448(7153):553-60.

78. Mineur YS, Sluyter F, de Wit S, Oostra BA, and Crusio WE. 2002. Behavioral and neuroanatomical characterization of the Fmr1 knockout mouse. *Hippocampus*. 12(1):39-46.

79. Moses-Kolko EL, Wisner KL, Price JC, Berga SL, Drevets WC, Hanusa BH, Loucks TL, and Meltzer CC. 2008 Serotonin 1A receptor reductions in postpartum depression: a positron emission tomography study. *Fertil Steril*. 89:685-692.

80. Moretti P, Levenson JM, Battaglia F, Atkinson R, Teague R, Antalffy B, Armstrong D, Arancio O, Sweatt JD, and Zoghbi HY. 2006. Lerning and memory and synaptic plasticity are impaired in a mouse model of Rett syndrome. *J Neurosci*. 26(1):319-27.

81. Murrough JW, Henry, S, Hu J, Gallezot JD, Planeta-Wilson B, Neumaier JF, and Neumeister A. 2011. Reduced ventral striatal/ventral pallidal serotonin 1B receptor binding potential in major depressive disorder. *Psychopharmacology*. 213:547-53.

82. Mulchahey JJ, Ekhator NN, Zhang H, Kasckow JW, Baker DG, and Geracioti TD Jr. 2001. Cerebrospinal fluid and plasma testosterone levels in post-traumatic stress disorder and tobacco dependence. *Psychoneuroendocrinology*. 26(3):273-85.

83. Neumeister A, Bain E, Nugent AC, Carson RE, Bonne O, Luckenbaugh DA, Eckelman W, Herscovitch P, Charney DS, and Drevets WC. 2004. Reduced serotonin type 1A receptor binding in panic disorder. *J Neurosci*. 24:589-91.

84. Nielsen AL, Oulad-Abdelghani M, Ortiz JA, Remboutsika E, Chambon P, and Losson R. 2001. Heterochromatin formation in mammalian cells: interaction between histones and HP1 proteins. *Moll Cell*. 7(4):729-39.

85. Nottke A, Colaiácovo MP, and Shi Y. 2009. Developmental roles of the histone lysine demethylases. *Development*. 136(6):879-89.

86. Onaivi ES, Bishop-Robinson C, Darmani NA, & Sanders-Bush E. Behavioral effects of 1-(2,5-dimethyoxy-4iodophenyl)-2-aminopropane, (DOI) in the elevated plus-maze test. *Life Sciences*. 57(26):2455-66.

87. Pear Ws, Aster JC, Scott ML, Hasserjian RP, Soffer B, Sklar J and Baltimore D. 1996. Exclusive development of T cell neoplasms in mice transplanted with bone marrow expressing activated Notch alleles. *J Exp Med*. 83(5):2283-91.

88. Pedersen MT, and Helin K. 2010. Histone demethylases in development and disease. *Trends Cell BIol*. 20(11):662-71.

89. Pizzagalli DA, Holmes AJ, Dillon DG, Goetz EL, Birk JL, Bogdan R, Dougherty DD, Iosifescu DV, Rauch SL, and Fava M. 2009. Reduced caudate and nucleus accumbens response to rewards in unmedicated individuals with major depressive disorder. *Am J Psychiatry*. 166(6):702-10.

90. Pray-Grant MH, Daniel JA, Schieltz D, Yates JR 3rd, and Grant PA. 2005. Chd1 chromodomain links histone H3 methylation with SAGA- and SLIK-dependent acetylation. *Nature*. 433:434-8.

91. Qi HH, Sarkissian M, Hu G, Wang Z, Bhattacharjee A, Gordon DB, Gonzales M, Lan F, Ongusaha PP, Huarte M, Yaghi NK, Lim H, Garcia BA, Brizuela L, Zhao K, Roberts TM and Shi Y. 2010. Histone H4K20/H3K9 demethylase PHF8 regulates zebrafish brain and craniofacial development. *Nature*. 466:503-7.

92. Qiu J, Shi G, Jia Y, Li J, Wu M, Li J, Dong S, Wong J. 2010. The X-linked mental retardation gene PHF8 is a histone demethylase involved in neuronal differentiation. *Cell Res.* 20(8):908-18.

93. Ram O, Goren A, Amit I, Shoresh N, Yosef N, Ernst J, Kellis M, Gymrek M, Issner R, Coyne M, Durham T, Zhang X, Donaghey J, Epstein CB, Regev A, and Bernstein BE. 2011. Combinatorial patterning of chromatin regulators uncovered by genome-wide location analysis in human cells. *Cell*. 147(7):1628-39.

94. Ressler KJ and Mayberg HS. 2007. Targting abnormal neural circuits in mood and anxiety disorders: from the laboratory to the clinic. *Nat Neurosci*. 10(9):1116-24.

95. Ressler KJ, and Nemeroff CB. 2000. Role of serotonergic and noradrenergic systems in the pathophysiology of depression and anxiety disorders. *Depress Anxiety*. Suppl 1:2-19.

96. Ripoll JJ, Ferrandiz C, Martinez-Laborda A, and Vera A. 2006. Implication of 5-HT2A subtype receptors in DOI activity in the four-plates test-retest paradigm in mice. *Behav Brain Res*. 166(1):131-9.

97. Ripoll N, Nic Dhonnchadha BA, Sebille V, Bourin M, and Hascoet M. 2005. The four-plates test-retest paradigm to discriminate anxiolytic effects. *Psychopharmacology* 180(1):73-83.

98. Robinson OJ, Cools R, Carlisi CO, Sahakian BJ, and Drevets WC. 2012. Ventral striatum response during reward and punishment reversal learning in unmedicated major depressive disorder. *Am J Psychiatry*. 169(2):152-9.

99. Russo SJ, Murrough JW, Han MH, Charney DS, and Nestler EJ. 2012. Neurobiology of resilience. *Nat Neurosci*. 15(11):1475-84.

100. Rutter M. 2006. Implications of resilience concepts for scientific understanding. *Ann N Y Acad Sci.* 1094:1-12.

101. SAMHSA (Substance Abuse and Mental Health Services Administration), Results from the 2013 National Survey on Drug Use and Health: Summary of National Findings, NSDUH Series H-48, HHS Publication No. (SMA) 14-4863. Rockville, MD: Substance Abuse and Mental Health Services Administration, 2014

102. Savitz JB, and Drevets WC. 2012. Neuroreceptor imaging in depression. *Neurobiol of Disease*. 52:49-65.

103. Shao Z, Raible F, Mollaaghababa R, Guyon JR, Wu CT, Bender W, and Kingston RE. 1999. Stabilization of chromatin structure by PRC1, a Polycomb complex. *Cell*. 98:37-46.

104. Sheline YI, Barch DM, Donnelly JM, Ollinger JM, Snyder AZ, and Mintun MA. Increased amygdala response to masked emotional faces in depressed subjects resolves with antidepressant treatment: an fMRI study. *Biol Psychiatry*. 50(9):651-8.

105. Shen Y, Pan X, and Zhao H. 2014. The histone demethylase PHF8 is an oncogenic protein in human non-small cell lung cancer. *Biochem Biophys Res Commun*. 451(1):119-25.

106. Shi G, Wu M, Fang L, Yu F, Cheng S, Li J, Du JX, and Wong J. 2014. PHD finger protein 2 (PHF2) represses ribosomal RNA gene transcription by antagonizing PHF finger protein 8 (PHF8) and recruiting methyltransferase SUV39H1. J Biol Chem. 289(43):29691-700.

107. Shi Y, Kirwan P, Smith J, Robinson HP, and Livesey FJ. 2012. Human cerebral cortex development from pluripotent stem cells to functional excitatory synapses. *Nat Neurosci*. 15(3):477-86.

108. Shi Y, Lan F, Matson C, Mulligan P, Whetstine JR, Cole PA, Casero RA, and Shi Y. 2004. Histone demethylation mediated by the nuclear amine oxidase homolog LSD1. *Cell*. 119(7):941-53.

109. Shi Y and Whetstine JR. 2007. Dynamic regulation of histone lysine methylation by demethylases. *Mol Cell*. 25:1-14.

110. Siegle GJ, Steinhauer SR, THase ME, Stenger VA, and Carter CS. 2002. Can't shake that feeling: event-related fMRI assessment of sustained amygdala activity in response to emotional information in depressed individuals. *Biol Psychiatry*. 51(9):693-707.

111. Sun X, Qiu JJ, Zhu S, Cao B, Sun L, Li S, Li P, Zhang S, and Dong S. 2013 Oncogenic features of PHF8 histone demethylase in esophageal squamous cell carcinoma. *PLoS One*. 8(10):e77353.

112. Taliaz D, Loya A, Gersner R, Haramati S, Chen A, and Zangen A. 2011. Resilience to chronic stress is mediated by hippocampal brain-derived neurotrophic factor. *J Neurosci*. 31(12):4475-83.

113. Tanaka KF, Samuels BA, and Hen R. 2012. Serotonin receptor expression along the dorsal-ventral axis of mouse hippocampus. *Philos Trans R Soc Lond B Biol Sci.* 367(1601):2395-401.

114. Tanigaki K, and Honjo T. 2007. Regulation of lymphocyte development by Notch signaling. *Nat Immunol*. 8(5):451-6.

115. Teng L, and Labosky PA. 2006. Neural crest stem cells. *Adv Exp Med Biol*. 589:206-12.

116. Tovote P, Fadok JP, and Luthi A. 2015. Neuronal circuits for fear and anxiety. *Nat Rev Neurosci*. 16(6):317-31.

117. Trivedi MH, Rush AJ, Wisniewski SR, Nierenberg AA, Warden D, Ritz L, Norquist G, Howland RH, Lebowitz B, McGrath PJ, Shores-Wilson K, Biggs MM, Balasubramani GK, Fava M, STAR*D Study Team. 2006. Evaluation of outcomes with citalopram for depression using measurement-based care in STAR*D: implications for clinical practice. *Am J Psychiatry*. 163(1):28-40.

118. Trojer P, Li G, Sims RJ 3rd, Vaquero A, Kalakonda N, Boccuni P, Lee D, Erdjument-Bromage H, Tempst P, Nimer SD, Wang YH, and Reinberg D. 2007. L3MBTL1, a histone-methylation-dependent chromatin lock. *Cell*. 129(5):915-28.

119. Tsukada Y, Fang J, Erdjument-Bromage H, Warren ME, Borchers CH, Tempst P, and Zhang Y. 2006. Histone demethylation by a family of JmjC domain-containing proteins. *Nature*. 439(7078):811-6.

120. Upadhyay AK, Rotili D, Han JW, Hu R, Chang Y, Labella D, Zhang X, Yoon YS, Mai A, and Cheng X. 2012. An analog of BIX-01294 selectively inhibits a family of histone H3 lysine 9 Jumonji demethylases. *J Mol Biol*. 416(3):319-27.

121. Vaswani M, Linda FK, and Ramesh S. 2003. Role of selective serotonin reuptake inhibitors in psychiatric disorders: a comprehensive review. *Prog Neuropsychopharmacol Biol Psychiatry*. 27(1):85-102.

122. Verhagen M, van der Meij A, van Deurzen PA, Janzing JG, Arias-Vásquez A, Buitelaar JK, and Franke B. 2010. Meta-analysis of the BDNF Val66Met polymorphism in major depressive disorder: effects of gender and ethnicity. *Mol Psychiatry*. 15(3):260-71.

123. Vialou V, Robison AJ, Laplant QC, Covington HE 3rd, Dietz DM, Ohnishi YN, Mouzon E, Rush AJ 3rd, Watts EL, Wallace DL, Iñiguez SD, Ohnishi YH, Steiner MA, Warren BL, Krishnan V, Bolaños CA, Neve RL, Ghose S, Berton O, Tamminga CA, and Nestler EJ. 2010 DeltaFosB in brain reward circuits mediates resilience to stress and antidepressant responses. *Nat Neurosci*. 13(6):745-52.

124. Vos T, Flaxman AD, Naghavi M, Lozano R, Michaud C, Ezzati M, *et al*. 2012. Years lived with disability (YLDs) for 1160 sequelae of 289 diseases and injuries 1990–2010: a systematic analysis for the Global Burden of Disease Study 2010. *Lancet*. 380(9859)2163-96.

125. Wade PA, Pruss D, and Wolffe AP. 1997. Histone acetylation: chromatin in action. *Trends Biochem Sci*. 22(4):128-32.

126. Walf AA, and Frye CA. 2007. The use of the elevated plus maze as an assay of anxiety-related behavior in rodents. *Nat Prtoco*. 2:322-328.

127. Wang S, Gao J, Lei Q, Rozengurt N, Pritchard C, Jiao J, Thomas GV, Li G, Roy-Burman P, Nelson PS, Liu X, and Wu H. 2003. Prostate-specific deletion of the murine Pten tumor suppressor gene leads to metastatic prostate cancer. *Cancer Cell*. 4(3):209-21.

128. Wang J, Lin X, Wang S, Wang C, Wang Q, Duan X, Lu P, Wang Q, Wang C, Liu XS, and Huang J. 2014. PHF8 and REST/NRSF co-occupy gene promoters to regulate proximal gene expression. 4:5008.

129. Weisstaub NV, Zhou M, Lira A, Lambe E, González-Maeso J, Hornung JP, Sibille E, Underwood M, Itohara S, Dauer WT, Ansorge MS, Morelli E, Mann JJ, Toth M, Aghajanian G, Sealfon SC, Hen R, and Gingrich JA. 2006. Cortical 5-HT2A receptor signaling modulates anxiety-like behaviors in mice. *Science*. 313(5786):536-40.

130. Welstead GG, Creyghton MP, Bilodeau S, Cheng AW, Markoulaki S, Young RA, and Jaenisch R. 2012. X-linked H3K27me3 demethylase Utx is required for embryonic development in a sex-specific manner. *Proc Natl Acad Sci U S A*. 109(32):13004-9.

131. Weng AP, Ferrando AA, Lee W, Morris JP 4th, Silverman LB, Sanchez-Irizarry C, Blacklow SC, Look AT, and Aster JC. 2004. Activating mutations of NOTCH1 in human T cell acute lymphoblastic leukemia. *Science*. 306(5694):269-71.

132. Whetstine JR, Nottke A, Lan F, Huarte M, Smolikov S, Chen Z, Spooner E, Li E, Zhang G, Colaiacovo M, and Shi Y. 2006. Reversal of histone lysine trimethylation by the JMJD2 family of histone demethylases. *Cell*. 125(3):467-81.

133. Wilkinson MB, Dias C, Magida J, Mazei-Robison M, Lobo M, Kennedy P, Dietz D, Covington H 3rd, Russo S, Neve R, Ghose S, Tamminga C, and Nestler EJ. 2011. A novel role of the WNT-dishevelled-GSK3β signaling cascade in the mouse nucleus accumbens in a social defeat model of depression. *J Neurosci*. 31(25):9084-92.

134. Willner P, Scheel-Kruger J, and Belzung C. 2013. The neurobiology of depression and antidepressant action. *Neurosci Biobehav Rev*. 37(10 Pt 1):2331-71.

135. Wilson A, MacDonald HR, and Radtke F. 2001. Notch 1-deficient common lymphoid precursors adopt a B cell fate in the thymus. *J Exp Med*. 194(7):1003-12.

136. Cohen-Woods S, Craig IW, and McGuffin P. 2013. The current state of play on the molecular genetics of depression. *Psychol Med*. 43(4):673-87

137. Yatim A, Benne C, Sobhian B, Laurent-Chabalier S, Deas O, Judde JG, Lelievre JD, Levy Y, and Benkirane M. 2012 NOTCH1 nuclear interactome reveals key regulators of its transcriptional activity and oncogenic function. *Mol Cell*. 48(3):445-58.

138. Yehuda R, Brand SR, Golier JA, and Yang RK. 2006a. Clinical correlates of DHEA associated with post-traumatic stress disorder. *Acta Psychiatr Scand*. 114:187-93.

139. Yehuda R, Brand S, and Yang RK. 2006b. Plasma neuropeptide Y concentrations in combat exposed veterans: relations to trauma exposure, recovery from PTSD and coping. *Biol Psychiatry*. 59(7):660-3.

140. Zhu G, Liu L, She L, Tan H, Wei M, Chen C, Su Z, Huang D, Tian Y, Qiu Y, Liu Y, and Zhang X. 2015. Elevated expression of histone demethylase PHF8 associates with adverse prognosis in patients of laryngeal and hypopharyngeal squamous cell carcinoma. *Epigenomics.* 7(2):143-53.

141. Zhu Z, Wang Y, Li X, Wang Y, Xu L, Wang X, Sun T, Dong X, Chen L, Mao H, Yu Y, Li J, Chen PA, and Chen CD. 2010. PHF8 is a histone H3K9me2 demethylase regulating rRNA synthesis. *Cell Res*. 20(7):794-801.

142. Zhuang X, Gross C, Santarelli L, Compan V, Trillat AC, and Hen R. 1999. Altered emotional states in knockout mice lacking 5-HT1A or 5-HT1B receptors. *Neuropsychopharmacology*. 21:52S-60S.

Appendix

Supplementary Tables & Figures

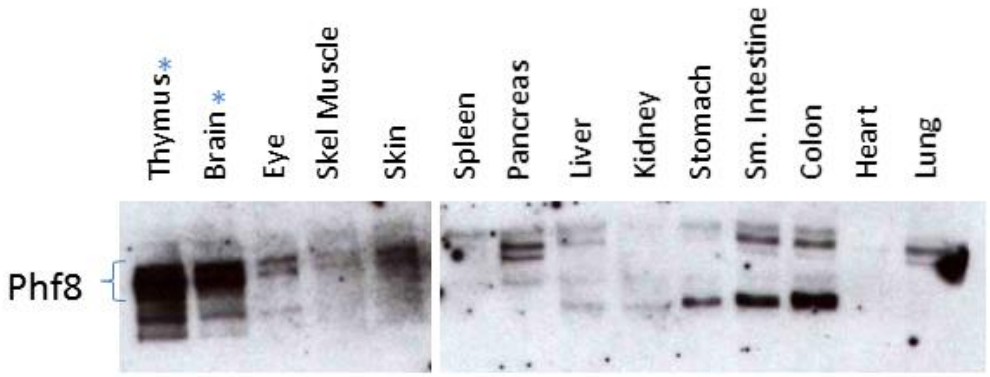

Supplemental figure 1 Expression of Phf8 in multiple adult tissues. Western blot analysis with WCE collected from multiple tissues showing Phf8 expression. In the adult Equal amounts of protein were loaded in each lane. Phf8 appears highly expressed in the thymus and brain of the adult, though it is more weakly expressed in multiple tissues throughout the body.

Supplemental Table 1 Primers used in this thesis. All primers used are shown here as forward (F) and reverse (R) pairs. Numbered pairs are part of the same PCR-reaction.

Primer	Sequence
Avp RT-qPCR 101F	GCTGCCAGGAGGAGAACTAC
Avp RT-qPCR 101R	AAAAACCGTCGTGGCACTC
Htr1a ChIP En 118F	TCTAAATGGCGCTCTGAAGC
Htr1a ChIP En 118R	CATCCCTGTCTCCAGCAACT
Htr1a ChIP Prom 119F	AGGTAAGAGGCGGGGTTTAG
Htr1a ChIP Prom 119R	ACATTCCAGTCCACACCACA
Htr1a RT-qPCR 108F	TGAAGACACTGGGCATCATC
Htr1a RT-qPCR 108R	TTATGGCACCCAACAACTCA
Htr1b ChIP En1 120F	TGAAACTTGGAGTCGCCTTT
Htr1b ChIP En1 120R	AGCGCAAAGACTCAAAGCTC
Htr1b ChIP En2 121F	CCCATCCTCCAGTCTTCAAC
Htr1b ChIP En2 121R	AGCTTCCAGTCCGTTTTCAA
Htr1b ChIP Prom 122F	GGGAGGATTGAATGACAAGC
Htr1b ChIP Prom 122R	GGGGCTTTGAGACATCTTTG
Htr1b RT-qPCR 109F	TCTCCCTGGTGATGCCTATC
Htr1b RT-qPCR 109F	TGTGGAACGCTTGTTTGAAG
Htr2a ChIP En 123F	GGCCTCTTTGGCTGAGAGTA
Htr2a ChIP En 123R	CCCTGCTGGACTGTAGTGCT
Htr2a ChIP Prom 128F	CCTGGACACATCATCACTGG
Htr2a ChIP Prom 128R	GCTGAGGGGTGAAGAATGAG
Htr2a RT-qPCR 110F	ATAGCCGCTTCAACTCCAGA
Htr2a RT-qPCR 110R	TCATCCTGTAGCCCGAAGAC
Otx RT-qPCR 100F	GCCAGGAGGAGAACTACCTG
Otx RT-qPCR 100R	CTCCGAGAAGGCAGACTCAG
Phf8 Ext Probe 7F	TTATCCCCAAGTCCCCCTAT
Phf8 Ext Probe 7R	CAGGAAGGACCATCCAGAGA
Phf8 RT-qPCR 52F	AAAGGAAAAGGCGAACCTGT
Phf8 RT-qPCR 52R	CCACCATGTCCTCATCTGTG
Utf1 ChIP Prom 35F	TCCTGGGTCCCTAAGGAAAG
Utf1 ChIP Prom 35R	CCCTCGCCTACCTAGTTCCT